Published in final edited form as: J. Org. Chem. 2020, 85, 5838−5862.
https://dx.doi.org/10.1021/acs.joc.0c00130?ref=pdf

Imine or Enamine? Insights and Predictive Guidelines from the Electronic Effect of Substituents in H-Bonded Salicylimines

R. Fernando Martínez,* Esther Matamoros, Pedro Cintas, and Juan C. Palacios*

Departamento de Química Orgánica e Inorgánica, Facultad de Ciencias and IACYS-Unidad de Química Verde y Desarrollo Sostenible, Universidad de Extremadura, E-06006 Badajoz, Spain

ABSTRACT: Imine and enamine bonds decorate the skeleton of numerous reagents, catalysts, and organic materials. However, it is difficult to isolate at will a single tautomer, as dynamic equilibria occur easily, even in the solid state, and are sensitive to electronic and steric effect, including π-conjugation and H-bonding. Here, using as model Schiff bases generated from salicylaldehydes and TRIS in a set of linear free energy relationships (LFER), we disclose how the formation of either imines or enamines can be controlled and provide a comprehensive framework that captures the structural underpinning of this prediction. This work highlights the potentiality of tailor-made designs *en route* to compounds with desirable functionality.

INTRODUCTION AND BACKGROUND

Hydrogen bonding is by far the most salient weak interaction playing central roles in chemistry, biology, and materials design.[1,2] The key aspect of the H-bond arises from its directionality, a fact accounting for, among others, molecular packing in crystals or stabilization of the second-order structure of proteins.[1] Besides, formation of intramolecular hydrogen bonds is often responsible for stabilization of particular conformers and tautomers of heterocyclic systems.[3] Not by chance, the nature and strength of intramolecular hydrogen bonds has been thoroughly investigated in recent decades by both theoretical and experimental analyses.[4]

In terms of stabilization energy H-bonds are usually classified as strong (>15 kcal/mol), moderately strong (4-15 kcal/mol), and weak (<4 kcal/mol).[4a] Gilli and co-workers suggested,[5] based on a large collection of neutron and X-ray crystal data, that one of the three classes of really strong H-bonds are resonance-assisted H-bonds,[6] or π-cooperative H-bonds,[1b] where the two oxygen atoms are connected by a π-conjugated system of single and double bonds. The team introduced in the late 1980s the concept of *resonance-assisted hydrogen bonds* (RAHBs), whereby the synergistic interplay between hydrogen bond and heteroconjugated systems can strengthen significantly the hydrogen bond itself.[6]

Intramolecular RAHBs have been generally invoked in six-membered rings created by typical covalent bonds and one H-bond interaction as enaminone-iminoenol resonant fragment.[7] Experimental support

largely comes from NMR data as the strong hydrogen bonds have unusual downfield proton shifts (δ_H = 16-20 ppm).[6]

The strongest nonconventional hydrogen bonds (RAHB) have been rationalized in terms of the extra stabilization associated to the partial delocalization of the π-electrons through the entire conjugated system of single and doble bonds. Some authors have however criticized this original concept of RAHB; the characteristics of the σ-skeleton, not the π-electron delocalization, would rather be behind the stability of this interaction.[8] Without explicitly denying the existence of π-effects, these researchers attribute the additional stabilization of RAHBs to a shorter distance between the hydrogen donor and the acceptor. Said that, numerous papers witness a direct relationship between the π-electron skeleton and the structural parameters involved in RAHB.[9] The π-electronic effects could then favor the stabilization caused by hydrogen bonding and, in addition, the quasi-ring formed through the H-bridge can partially adopt the role of a typical aromatic ring. Accordingly, the concept of aromaticity can be extended to pseudo-aromatic rings (or quasi-aromatic rings), for which π-electron delocalization mediated by hydrogen bonding can be evaluated through indices based on geometrical considerations.[10,11] Application of the NBO theory reveals that the π-component of the electron density within the resonant spacer determines the dominant characteristics of hydrogen bonding while σ-skeleta only reflect the π-polarization.[12]

Recently, we have studied in detail the tautomeric and conformational equilibria of mono- [Ar^1-NH-CH=CAr^2-CH=O] and di-azaderivatives [Ar^1-NH-CH=CAr^2-CH=N-Ar^1] of malondialdehydes, namely acrolein and vinamidines structures with extended conjugation.[13] The major stabilizing effect favoring a given tautomer or conformer is provided by intramolecular hydrogen bonding (O-H···N and N-H···N bonds), which contributes to further electron delocalization.

The search for evidences in imines derived from salicylaldehyde constitutes a major challenge, because the structure in solution may be different from that in the solid state.[7,14] They can be regarded as phenoliminic (**1**), ketoaminic (**2**) or zwitterionic (**3**) tautomers. Average bond distances values (from the Cambridge Structural Database, CSD) for characteristic bond lengths in enol-imino and keto-amino tautomers are shown in Scheme 1 (see this scheme for numbering of aromatic carbons along the manuscript).[15]

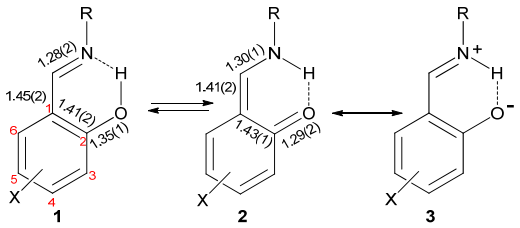

Scheme 1

More than 90% of *N*-substituted salycilaldimines derived from aliphatic and aromatic amines, registered during the last fifty years in the CSD, exist predominately in enolimine form (**1**) in crystaline state.[15,16] Nevertheless, literature search from 1970 to the present, shows that some of such derivatives adopt an enamine structure (**2**) in the lattice. Some come from aliphatic amines[16a,16d] and others from aromatic amines.[16c,17] In a few cases, previously misassigned structures have been corrected,[18] notably cases in which the imine is described with a zwitterion structure (**3**).[16b,19] Similar results emerge from ^{15}N and ^{13}C

NMR spectra in the solid state.[20] Furthermore, the structural elucidation is complex indeed as these Schiff bases are sensitive to heat and light leading to thermochromism and photochromism, respectively.[21] In general, the imine form is more stable than its enamine counterpart and changing populations of both tautomers with temperature causes the thermochromism phenomenon.

While the imine form predominates in gas phase or in solution, the enamine form in crystalline state adopts essentially a zwitterionic structure, stabilized by electrostatic interactions and intermolecular hydrogen bonds. Thus, DFT calculations modeling the crystal lattice in the derivative of *tris*(hydroxymethyl)aminomethane (TRIS) and 5-bromosalicylaldehyde show that in solid state the enamine is more stable than the iminic form, in total agreement with data obtained by X-ray diffraction.[22]. The opposite occurs with *N*-(2-*t*-butylphenyl)salicylaldimine.[22a]

A priori, it remains uncertain to predict whether a particular salicylamine will present either imine or enamine structures in the solid state or in solution. To a significant extent, substituents on the salicyl aromatic core may bias the structural outcome. For example, derivatives of 2,3-dihydroxybenzaldehyde show both imine[23] and enamine[24] structures in crystals. When the hydroxyl group at C-3 is alkylated, the resulting compound adopts a phenoliminic disposition,[25] although ketoamine structures have been detected as well.[26] Likewise, two compounds derived from 2,4-dihydroxybenzaldehyde presenting enamine structures in the solid state have been reported.[20,27] More complex structures are formed when more than one *o*-hydroxyarylaldehyde moiety are involved.[28] Thus, stable keto-enamine forms are described for diimines of 3,6-diformylcatechol[28a], triimines of 2,4,6-triformylphloroglucinol (mixtures of regioisomers),[28e] and tetraimines of tetraformylresorcin[4]arene.[29] Although this behavior seems to be capricious, it appears that various factors, most likely electronic and steric, do affect the tautomeric equilibria of salicyl imine/enamine structures. It is worth pointing out that this rapid equilibrium also influences reactivity as disclosed recently by a mild deuteration method of aromatic compounds, whic is facilitated by a keto-enamine tautomeric intermediate.[30]

It has been claimed that the position of proton in the intramolecular hydrogen bond is strongly determined by substituents at salicylaldehyde and by substituents on the imine nitrogen atom (X and R, respectively in Scheme 1). Substituents at the aromatic ring increasing acidity of the OH proton (i.e. electron withdrawing group, EWG) promote proton transfer from oxygen to nitrogen. The same effect can be obtained by increasing the basicity of the imine nitrogen atom by appropriate substitution patterns (electron donating group, EDG).[20]

However, on the basis of previous literature, the prediction of enol-imine *versus* ketoenamine forms is far from being straightforward. There are no experimental quantitative studies on the electronic effect of substituents on the tautomeric equilibrium in salycilimine derivatives, the purpose of the present paper is to bridge this gap, looking for predictive rules, from which the major or unique structure adopted in the solid state or solution could be inferred. Accordingly, we shall consider the influence of substituents on the N-H···O bonding of heteronuclear RAHBs in enaminone-iminoenol equilibria. This investigation is also motivated by the fact that Schiff bases have received considerable attention owing to their potentiality in so diverse areas such as liquid crystals,[31] organic dyes,[32] catalysts,[33] and intermediates in organic synthesis.[34] Moreover, numerous Schiff bases exhibit a broad range of biological activities;[35]

salicylideneaniline derivatives for instance were found to be effective against *Mycobacterium tuberculosis* H37Rv.[36]

RESULTS AND DISCUSSION

The electronic structure of aromatic Schiff bases and their conformation are interlocked issues. Introduction of substituents at the aromatic ring modifies the properties of Schiff bases by changing their electronic structure and conformation.[37] Thus, the anomalous substituent effects observed for benzylideneanilines were explained by changes in the molecular conformation induced by substituents.[38] Likewise, the correlation between ^{13}C chemical shifts and the Hammett parameters evidenced a twisted conformation of salicylideneanilines.[39] To remove the conformational complexity, we chose Schiff bases derived from salicylaldehydes and TRIS. The geometry of the *tris*(hydroxymethyl)methyl group eliminates interference of possible conformations and electronic changes that they can cause. To this end, the influence of substituents at the aromatic ring on the tautomeric ketoamine-phenolimine equilibrium was investigated.

Synthesis of Salicyliden Derivatives of TRIS. A wide series of Schiff bases **4**-**33** could easily be obtained by reaction of TRIS whith both monosubstituted and polysubstituted salicylaldehydes (see SI).

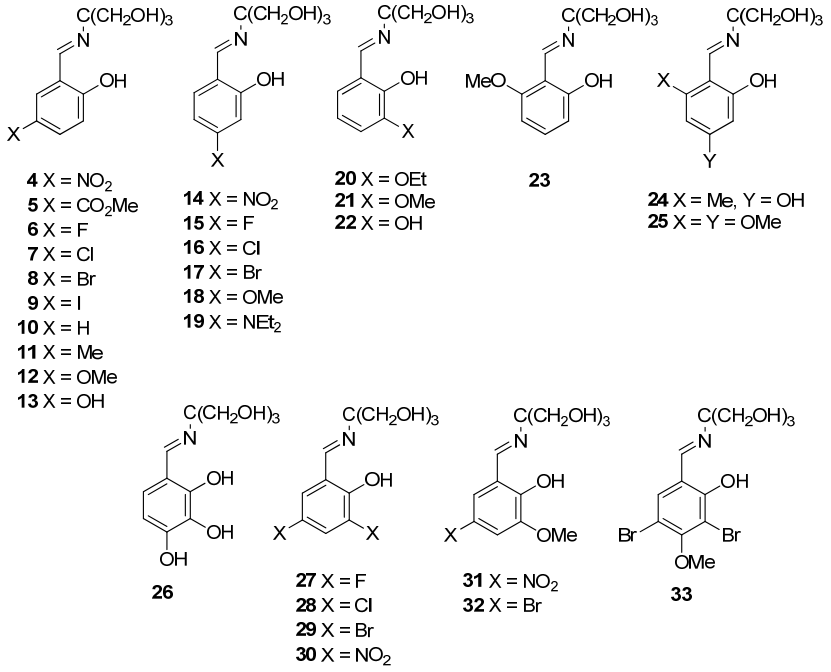

Structure and Tautomeric Equilibrium in the Solid State. In the absence of single-crystal data, accurate structural elucidation is not always obvious from other techniques. FT-IR spectroscopy is a valuable tool, nevertheless. The streching vibrations of the C=N (imine) and C=O (enamine) bonds usually overlap; however, the intensity of the latter is much higher than the less polar C=N bond (in fact the carbonyl absorption becomes the most intense band). This comparative assessment should be taken with caution as diagnostic criterium in assigning the predominant tautomer in the solid state. Table 1S lists the most significant IR absorptions of all Schiff bases synthesized. The existence of multiple

hydrogen bonds, both inter- and intramolecular, is reflected by the broad absorption of OHs and NHs streching vibrations, almost covering the entire 3500-2000 cm^{-1} region. In general, and as mentioned above, the more intense absorption appears at 1650-1625 cm^{-1} ($\bar{\nu}_{C=O}$) and, frequently, it has a similar intensity as the band at 1610-1590 cm^{-1} ($\bar{\nu}_{NC=C}$), often overlapped. The intensity of both absorptions, typical of intramolecularly linked NH-C=C-CO enaminic systems, allow to conclude that in solid state at room temperature all have enaminic structure (**34**-**63**). This conclusion is supported by the background on the solid state structure of Schiff bases derived from TRIS, as some salicylaldehyde derivatives have been previously prepared and their solid state structures studied by X-ray diffractometry (see SI).[22b,40,41]

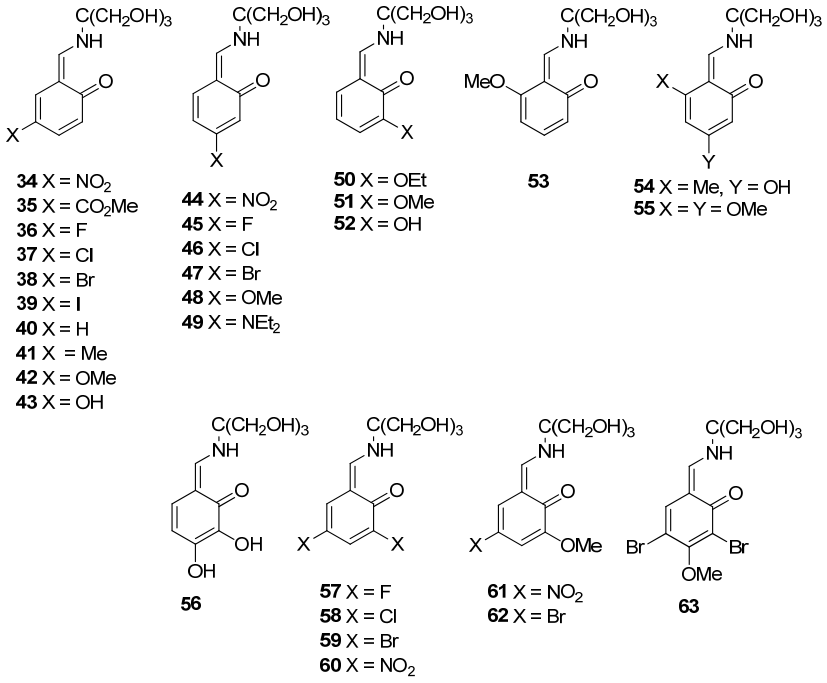

In summary, all imines derived from salicylaldehydes and TRIS determined by X-ray diffraction, both by ourselves[42] (**38**[22b], **48**,[42] **53**,[42] **57**[42] and **64**[22b]) and other teams (**34**,[40e,g] **37**,[40c,40h] **38**,[40e] **40**,[40a-40d] **50**,[40g], **51**,[40d] **52**,[40d] **66**, and **67**,[26,40f,40i] **68**,[40j] **69**,[41a] **70**[41b,41c] **71**,[41d] **72**,[41e] **73**,[41e] **74**,[41e] **75**,[41a] **76**,[41c] **77**,[41f] **78**[40f]) show either enaminic or zwitterionic structure, which applies to **65** as well.[22b] Therefore, it is plausible to conclude that all Schiff bases derived from TRIS synthesized in this work (**4**-**33**) should have solid state enamine structures (**34**-**63**). Interestingly, another group,[40f] based on IR data alone, conjectured that Schiff bases **79** (Y = F, Cl, Br, I, Et, NO_2, Ac) should most likely be enamine tautomers in solid state.

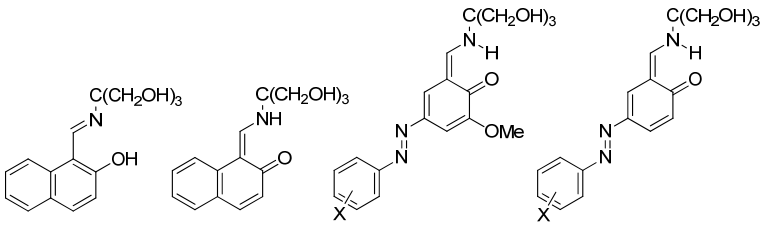

64 **65**

66 X = 2-Cl
67 X = 3-Cl
68 X = 2-Me
69 X = 4-Me
70 X = 3-CF_3
71 X = 4-*n*Bu
72 X = 2,6-Cl_2
73 X = 4-MeO
74 X = 3-MeO

75 X = 2-Cl
76 X = 3-Cl
77 X = 4-Et
78 X = H
79 X = 4-Y

Structure and Tautomeric Equilibrium in Solution. As noted above, compounds **4**-**33** may exhibit in solution a tautomeric behavior different to that adopted in the solid state. The imine form can be inferred from the presence of two singlet signals in ^{1}H NMR spectra, one shifted downfield (~13-15 ppm) for the phenolic proton bound intramolecularly, and the other for the imino proton (~8.5-9.5 ppm). Conversely, an enamine structure will show two doublet signals that are coupled each other, one corresponding to the intramolecularly bound NH group (~14-16 ppm), along with the ethylene proton (~8.5-10 ppm). Since chemical shifts are similar in both structures, only the multiplicity of signals matters as diagnostic element.[43-45] Besides, there are also significant differences in ^{13}C NMR spectra, because the phenolic carbon of imines appears at a higher field than the carbonyl signal of enamines (~155-160 ppm *versus* ~170-181 ppm),[45,46] and ^{15}N NMR spectra, where the iminic nitrogen appears at a higher field than the enaminic nitrogen (~ -63 ppm *versus* ~ -247 ppm).[43,47] In addition, one cannot forget that, like in the solid state, the structure in solution often varies with temperature.[47,48]

Table 2S collects both ^{1}H and ^{13}C NMR data of Schiff bases **4**-**33**. Although in the solid state at room temperature all have enamine structures (**34**-**63**); half of them in DMSO-d_6 solution adopt an imine structure ($J_{H,NH}$ = 0 Hz). In contrast, Schiff bases **4**, **5**, **14**, **15**, **18**, **20**, **21**, **23**-**25** and **28**-**33** appear to exhibit enamine structures, consistent with non-zero appreciable couplings ($J_{H,NH} \neq 0$ Hz). Nevertheless, the unequivocal assignment is not as simple as thought due to a rapid equilibrium between the two tautomeric forms. The observed chemical shifts (δ_{exp}) are an average of those corresponding to the "pure" imine and enamine forms (δ_i and δ_e, respectively). In other words: $\delta_{exp} = n_i\delta_i + n_e\delta_e$, where n_i and n_e are the populations of molecules with imine and enamine structures, respectively. The same happens with the coupling constants (varying between 0 and 14.6 Hz), which for the tautomeric equilibrium can be represented by equation $J_{exp} = n_iJ_i + n_eJ_e$ (Obviously, $n_i + n_e = 1$). This explains why even if **20** and **21** have coupling constants $J_{H,NH} \neq 0$ Hz, which would indicate an enamine structure, chemical shifts of C-2 (~159 ppm) are typical of an imine structure. That is, in the imine-enamine equilibrium the population of molecules with imine structure is predominant, although the existence of residual coupling suggests the coexistence with enamine tautomers.

Substituent Effects on the Tautomeric Equilibrium: Predominant Structures in Solution. The presence of a strong intramolecular hydrogen bond (~10-20 kcal/mol),[3] consistent with a chelate ring, is a

valuable motif that can be harnessed in structural elucidation. The position of the hydrogen atom, covalently linked to oxygen in phenolimines or to nitrogen in ketoenamines, obviously depends on the relative basicity of both atoms: hydrogen will bind to the most basic atom. In this sense the proton transfer process can be interpreted as an intramolecular acid-base reaction between a donor (D) and an acceptor (:A):

$$R\text{-}D\text{-}H\cdots{:}A\text{-}R^1 \rightleftharpoons R\text{-}D{:}\cdots H\text{-}A\text{-}R^1$$

Moreover, this hydrogen bonding will be stronger as the difference of basicity in solution (ΔpK_a) or proton affinity in the gas phase (ΔPA) decrease, which is known as the "pKa/PA equalization principle" (ΔpK_a or $\Delta PA \approx 0$).[49] A conspicuous example of this principle is provided by malondialdehyde, in which the transfer of the intramolecularly bound proton of the cyclic enolic form and the delocalization lead to a structure identical to the initial one. It is obvious that $\Delta pK_a = 0$ and a very strong hydrogen bond is formed (15-25 kcal/mol). On the other hand, between an alcohol and a ketone, $R^1O\text{-}H\cdots O{=}CR_2$, $\Delta pKa \approx$ 21-25 and the resulting bond is very weak indeed (4-5 kcal/mol).[49a] In our case both ends basic centers are not equal and $\Delta pK_a \neq 0$, so the hydrogen bridge is not as strong (2-15 kcal/mol) as that of malondialdehyde.

It is therefore pertinent to ascertain how the electronic character of the substituents affects the basicity of the oxygen and nitrogen atoms involved in the tautomeric equilibrium. Their basicity depends in turn on the electron density of each atom, which is otherwise reflected by the chemical shift of the proton, the nitrogen atom, and the iminic and phenolic carbons in their NMR spectra. Although previous investigations address the effect of the substituents on the chemical shift of the iminic hydrogen and carbon atoms in simple imines,[50] it is surprising to note that little or no experimental studies have been conducted to evaluate their influence on the imine-enamine structures of Schiff bases from salicylaldehydes, thus making it impossible to predict the prevalent tautomer in solution.

In our study, for simplicity, only the substituents at the aromatic rings were taken as variables. Scheme 2 illustrates the whole phenolimine-ketoenamine tautomeric equilibrium.

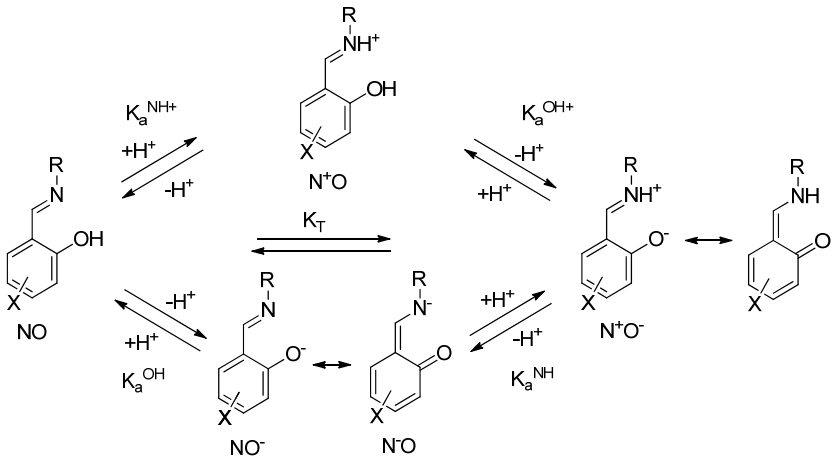

Scheme 2

The acid dissociation constants are defined by the following equations:

$$K_a^{OH} = \frac{[NO^-][H^+]}{[NO]} \quad , \quad K_a^{NH} = \frac{[NO^-][H^+]}{[N^+O^-]} \quad ,$$

$$K_a^{NH+} = \frac{[NO][H^+]}{[N^+O]} \quad , \quad K_a^{OH+} = \frac{[N^+O^-][H^+]}{[N^+O]} \qquad [1]$$

The pK_a values, measured experimentally for some salicylimines, lie within ~7.8-10.[51] Acordingly, the tautomeric equilibrium constant K_T can be expressed as:

$$K_T = \frac{[N^+O^-]}{[NO]} = \frac{K_a^{OH}}{K_a^{NH}} = \frac{K_a^{OH+}}{K_a^{NH+}} \qquad [2]$$

By considering the electronic effects exerted by the substituents on the phenolic hydroxyl and the iminic nitrogen, and assuming independent behavior of both groups, the substituent effect on the former can be described by the Hammett equation [3]:

$$\log K_a^{OH} = \rho^{OH} \sigma_x^{OH} + a \qquad [3]$$

In a similar way, the effect on the imine functionality can be described by equation [4]:

$$\log K_a^{NH} = \rho^{NH} \sigma_x^{NH} + b \qquad [4]$$

Where $\sigma_x^{OH} = \sigma_{para}^{x}$ if the substituent is placed at C-5 and $\sigma_x^{OH} = \sigma_{meta}^{x}$ if it is at C-4. Analogously, $\sigma_x^{NH} = \sigma_{para}^{x}$ when the substituent is located at C-4 and $\sigma_x^{NH} = \sigma_{meta}^{x}$ when it is at C-5.

Conversion of both equations into the logarithmic form of equation [2] leads to [5], where c = a-b.

$$\log K_T = \log K_a^{OH} - \log K_a^{NH} = \rho^{OH} \sigma_x^{OH} - \rho^{NH} \sigma_x^{NH} + c \qquad [5]$$

In strict sense, however, the imino and phenolic groups do not act independently, since they are connected through a spacer that allows a continuous delocalization between them and, in addition, united to each other by the hydrogen bonding. Gilli *et al.*[49d] have suggested that Schiff bases derived from salicylaldehydes are a fine example of synergy between the strength of the hydrogen bond and the degree of π-delocalization, whereas Krygowski *et al.*[52] state that the most important factor affecting the delocalization of π-electrons through the linker is the effect of groups attached to the ring, one of whose bonds is part of the spacer itself. In addition, Solà *et al.*[9n] indicate that the effect of the substituents and the effect of the mesomeric assistance on the hydrogen bond are mutually cooperative, and both effects can then be treated as components of the same phenomenon. In this way, any electronic alteration is transmitted along the spacer and the hydrogen bond, which results in leveling of the electronic density and matches the pK_a of both termini. The argument merely reinforces the principle of equalization of pK_a values ($\Delta pK_a \approx 0$).

Since the effect of two different substituents (X and Y) on a chemical function attached to an aromatic ring can be represented by the same value of ρ, thereby making effects additive in Hammett's equation, $\log K_{xy} = \rho_x\sigma_x+\rho_y\sigma_y = \rho(\sigma_x+\sigma_y) = \rho\Sigma\sigma_{xy,}$ where $\rho_x = \rho_y = \rho$, $\Sigma\sigma_{xy} = \sigma_x+\sigma_y$; similarly, in the case of salicylidene derivatives one can accept the hypothesis that $\rho^{OH} = \rho^{NH} = \rho$, thus simplifying equation [5] to [6]:

$$\log K_T = \rho\,(\sigma_x^{OH} - \sigma_x^{NH}) + c = \rho\,\sigma_{ef} + c \qquad [6]$$

The difference $\sigma_{ef} = \sigma_x^{OH} - \sigma_x^{NH}$, represents the net or effective effect that a given substituent X exerts on the delocalized cyclic tautomeric system, while *c* is a constant, which should in principle be different from zero, due to the different termini of the tautomeric skeleton. However, as we shall see later, for TRIS derivatives $c \approx 0$ ($c = 0.04$).

It is well known that the electronic effect of a substituent in *meta*-position is essentially inductive, whereas in *para*-substitution it is composed of inductive and resonance effect. Hence it is evident that σ_{ef} largely represents the mesomeric effect of a substituent on the tautomeric system. With the adopted definition of K_T the values of σ_{ef} have a parallel interpretation to those of σ; that is, a negative value of σ_{ef} indicates a positive mesomeric or electron-releasing effect, while a positive one implies a negative mesomeric or electron-withdrawing effect.

Accepting that $c = 0$, if $\sigma_x^{OH} = \sigma_x^{NH}$, then $\sigma_{ef} = 0$ and $K_T = 1$; that is, both forms, imine and enamine, are in equilibrium in identical proportions. If $\sigma_x^{OH} \leq \sigma_x^{NH}$, then $\sigma_{ef} \leq 0$, $K_T < 1$ and the imine structure predominates; on the other hand, if $\sigma_x^{OH} \geq \sigma_x^{NH}$, then $\sigma_{ef} \geq 0$, $K_T > 1$ and the enamine structure is the prevalent form. Table 1 shows the values of σ_{ef} for various salicylidene derivatives monosubstituted at C-3 and C-5 positions, which are related to their structures in solid state and solution.

Table 1. Hammett constants obtained for monosubstituted salicyl derivatives of TRIS and correlations with tautomeric preferences in solid state and solution.

Compound	X	σ_{OH}[a]	σ_{NH}[a]	σ_{ef}[b]	σ^-_{OH}[c]	σ^+_{NH}[d]	$\sigma_{ef}^{\pm}$[e]	Solution[h]	Solid state[i]
4	5-NO_2	0.81	0.71	0.10	1.23	0.71	0.52	enamine	enamine
5	5-CO_2Me	0.44	0.35	0.09	0.74	0.35	0.39	enamine	
6	5-F	0.15	0.34	-0.19	0.15	0.34	-0.19	imine	
7	5-Cl	0.24	0.37	-0.13	0.24	0.37	-0.13	imine	enamine
8	5-Br	0.26	0.37	-0.11	0.26	0.37	-0.11	imine	enamine
9	5-I	0.18	0.34	-0.16	0.18	0.34	-0.16	imine	enamine
10	H	0.00	0.00	0.00	0.00	0.00	0.00	imine	enamine
11	5-Me	-0.14	-0.06	-0.08	-0.14	-0.16	-0.08	imine	
12	5-OMe	-0.28	0.10	-0.38	-0.28	0.10	-0.38	imine	enamine
13	5-OH	-0.38	0.13	-0.51	-0.38	0.13	-0.51	imine	enamine
14	4-NO_2	0.71	0.81	-0.10	0.71	0.81	-0.10	imine	
15	4-F	0.34	0.15	0.19	0.34	-0.07	0.41	enamine	enamine
16	4-Cl	0.37	0.24	0.13	0.37	0.11	0.26	enamine	

17	4-Br	0.37	0.26	0.11	0.37	0.15	0.22	enamine	
18	4-OMe	0.10	-0.28	0.38	0.10	-0.78	0.88	enamine	enamine
19	4-NEt_2	-0.23	-0.72	0.49	-0.23	-1.70[f]	1.47	enamine	enamine
67[g]	5-PhN_2	0.39	0.32	0.07	0.39	0.32	0.07	enamine	enamine

[a]Reference 53a. [b]σ_{OH} - σ_{NH}. [c]Reference 53b. [d]Reference 53c. [e]$\sigma^{-}_{OH} - \sigma^{+}_{NH}$. [f]$\sigma$ (4-NMe_2). [g]References 26,40f; [h]In DMSO-d_6. [i]From X-ray data.

It can be seen that all substituents having $\sigma_{ef} \leq 0$ values, which are fundamentally substituents at the C-5 position, afford imine structures in solution. In stark contrast, for values of $\sigma_{ef} \geq 0$, largely substituents at C-4, an enamine structure is prevalent in solution. Obviously, for $\sigma_{ef} \sim 0$ values there is ambiguity in the assignment of either imine or enamine structure as the predominant species. Examples of calculated σ_{ef} values are shown in Figure 1. As expected, there is no correlation between the effect of the substituents and the resulting solid state structure, as packing forces in the crystal can reverse the structure observed in solution.

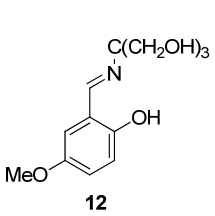

12

$\sigma_{ef}^{OMe} = \sigma_{para}^{OMe} - \sigma_{meta}^{OMe} =$

$= -0.28-0.10= -0.38$

Imine: δ_{C2} 156.6 ppm, $J_{CH,NH}$ 0.0 Hz

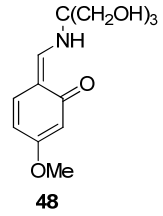

48

$\sigma_{ef}^{OMe} = \sigma_{meta}^{OMe} - \sigma_{para}^{OMe} =$

$= 0.10-(-0.28)= 0.38$

Enamine: δ_{C2} 174.2 ppm, $J_{CH,NH}$ 6.0 Hz

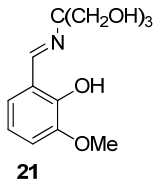

21

$\sigma_{ef}^{OMe} = \sigma_{orto}^{OMe} - \sigma_{meta}^{OMe} =$

$= 0.00-0.10= -0.10$

Imine: δ_{C2} 158.8 ppm, $J_{CH,NH}$ 4.0 Hz

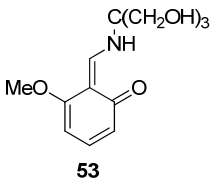

53

$\sigma_{ef}^{OMe} = \sigma_{meta}^{OMe} - \sigma_{para}^{OMe} =$

$= 0.10-(-0.28)= 0.38$

Enamine: δ_{C2} 170.8 ppm, $J_{CH,NH}$ 6.4 Hz

Figure 1. Calculated Hammett constants (OMe substitution) and preferential tautomer composition in solution from proton NMR data.

For either imine or phenol functionality, the electronic effect supplied by a substituent depends on their relative positions. As shown in Scheme 3, for imine **80** a nitro group (strong EWG), positioned *para* to the hydroxyl may increase the acidity of the latter by both inductive (-I) and mesomeric (-M) effects. When the same group is placed *meta* with respect to the imine group, it exerts an inductive effect (-I) only; however the basicity associated with the lone pair on nitrogen (located in the nodal plane of the π system) is not substantially altered by mesomeric effects.

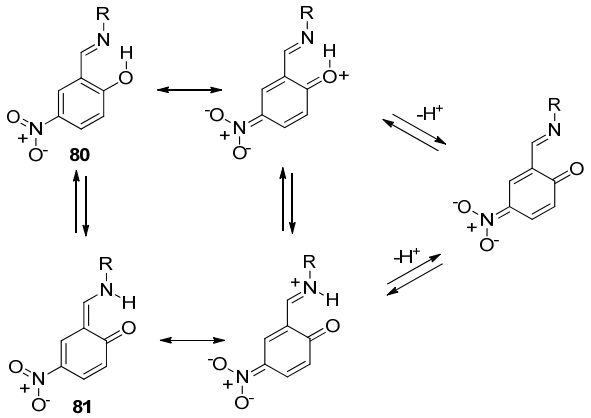

Scheme 3

Although the nitro group at C-5 increases the acidity of both the OH of phenol form (**80**) and the NH of **81**, the first effect predominates as evidenced by the value $\sigma_{ef}^{NO_2} = \sigma_{NO2}^{OH} - \sigma_{NO2}^{NH} = \sigma_{para}^{NO_2} - \sigma_{meta}^{NO_2} = 0.81\text{-}0.71 = 0.10$. Therefore, the preferential structure adopted in solution corresponds to enamine (**34**, $J_{CH,NH} = 8.8$ Hz, $\delta_{C2} = 180.2$ ppm). It is relevant to note that this result is not a consequence of how powerful the electronic effect of the substituent is, but rather of the difference $\sigma_{ef} = \sigma_x^{OH} - \sigma_x^{NH}$. Therefore, the methoxycarbonyl group placed at the same position, even being more moderate attractor than the nitro group, does actually exert the same effect, since the value of σ_{ef} is essentially the same: $\sigma_{CO2Me}^{OH} - \sigma_{CO2Me}^{NH} = 0.44\text{-}0.35 = 0.09$ (**35**, $J_{CH,NH}$ 9.2 Hz, δ_{C2} 176.7 ppm).

When the EWG is in the *meta*-position to the hydroxyl (**82**), its acidity increases by (–I) effect and concomitantly decreases the basicity of the nitrogen by (–M) effect. The resulting effects are similar on the enamine structure (**83**), the NH acidity increases while basicity of the carbonyl oxygen decreases (Scheme 4).

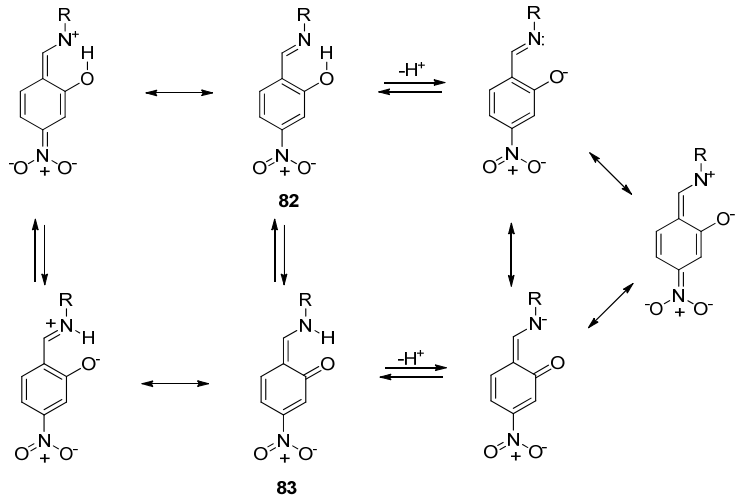

Scheme 4

Again, the value of σ_{ef} is going to dictate which effect predominates; now $\sigma_{ef}^{NO_2} = \sigma_{NO2}^{OH} - \sigma_{NO2}^{NH} = \sigma_{meta}^{NO_2} - \sigma_{para}^{NO_2} = -(\sigma_{para}^{NO_2} - \sigma_{meta}^{NO_2}) = 0.71\text{-}0.81 = -0.10$ and the equilibrium is shifted

towards the imine form (**14**/**44**, $J_{CH,NH}$ 5.6 Hz, δ_{C2} 168.6 ppm). In fact, the value of δ_{C2} is very close to the value it adopts when $K_T = 1$ (δ_{C2} 167.7 ppm, see later), which indicates a slight excess of the enamine form in solution. The above examples emphasize that the effect exerted by a substituent in one position is reversed by passing to the other, because it will always be true that $(\sigma_{para}^{X} - \sigma_{meta}^{X}) = -(\sigma_{meta}^{X} - \sigma_{para}^{X})$; that is, $\sigma_{ef}^{5\text{-}X} = -\sigma_{ef}^{4\text{-}X}$.

An EDG with lone electron pairs on *para*-position relative to the hydroxyl will have a different effect to the nitro group. The OH acidity will be decreasing by destabilizing the phenoxide ion (effect +M > -I), while the basicity of the nitrogen decreases as well by inductive effect (-I). Both effects are opposed and the former predominates over the second. Something similar happens for the enamine tautomer (Scheme 1S). A clear-cut example is provided by the methoxy group, for which $\sigma_{ef}^{MeO} = \sigma_{MeO}^{OH} - \sigma_{MeO}^{NH} = \sigma_{para}^{MeO} - \sigma_{meta}^{MeO} = -0.28\text{-}0.10 = -0.38$ and the preferential structure of **12** in solution is iminic ($J_{CH,NH}$ 0.0 Hz, δ_{C2} 156.6 ppm) (Figure 1).

Scheme 2S illustrates the remaining case when the EDG with lone pairs is placed at the *meta*-position to the hydroxyl, as the latter increases its acidity (effect -I) and the substituent effect increases the basicity of nitrogen too (+M effect). The effect is now reversed because $\sigma_{ef}^{MeO} = \sigma_{MeO}^{OH} - \sigma_{MeO}^{NH} = \sigma_{meta}^{MeO} - \sigma_{para}^{MeO} = 0.10\text{-}(-0.28) = 0.38$; that is, $\sigma_{ef}^{4\text{-}X} = -\sigma_{ef}^{5\text{-}X}$, and the structure of **18** in solution is enamine ($J_{CH,NH}$ 6.0 Hz, δ_{C2} 174.2 ppm) (Fig. 1). Similar conclusions can be reached when EDG and EWG devoid of lone pairs are present (*e.g.*, methyl or trifluoromethyl, respectively), whose influences hinge on hyperconjugation. Table 1 also collects the values of $\sigma^{-}_{OH} = \sigma^{-}_{5X}$ and $\sigma^{+}_{NH} = \sigma^{+}_{4X}$, as well as the values of $\sigma_{ef}^{\pm}$ ($= \sigma^{-}_{OH} - \sigma^{+}_{NH}$). In most cases the absolute values of $\sigma_{ef}^{\pm}$ are greater than or equal to the absolute values of σ_{ef} ($|\sigma_{ef}^{\pm}| \geq |\sigma_{ef}|$). However, the results and conclusions reached remain unaffected.

Steric Effects on Tautomeric Equilibria. For substituents at C-3, position adjacent to the hydroxyl, the corresponding σ_{OH} values are not usually tabulated because they are contaminated by steric effects. For relatively small groups, such as oxygen-containing functions, the values of σ_{OH} at the *para*-position have been taken; that is, it has been assumed that the effect exerted on C-3 is virtually identical to that exerted on C-5. Similarly, the values for substituents at C-6, adjacent to the iminic group, have been equated to those located at C-4. Bulkier groups such as Cl, Br or I can add significant alterations by approaching the phenolic group to the imino group, thereby increasing the strength of the hydrogen bridge (as the distance between oxygen and nitrogen atoms becomes shorter).[49] As expected, substituents such as the nitro group or the methoxycarbonyl would hinder their delocalization on the aromatic ring due to the lack of coplanarity. Remarkably, predictions on the structure in solution for these compounds, reached by equating the values σ_{OH} and σ_{NH} of substituents at C-3 and C-6 to those of C-5 and C-4, respectively, are coincidental with the tautomers found experimentally. The use of the σ_{ortho} constants reported by Barlin and Perrin[54] for *ortho*-substituents on phenols does not introduce any variation in the results obtained for 3-substituted salicylidenimines (Table 2): $\sigma_{ef}^{\ ortho} = \sigma_{x\ ortho}^{OH} - \sigma_{x\ meta}^{NH}$. No σ_{ortho} values have been communicated for substituents contiguous to the imine group; we chose the use of σ_{para} values for such specific cases.

Table 2. Hammett constants for 3-substituted salicylidenimines and correlations with tautomeric preferences in solid state and solution.

Compound	X	σ_{OH}[a]	σ_{NH}[a]	σ_{ef}[b]	σ_{ef}^{ortho}[c]	σ^{-}_{OH}[d]	σ^{+}_{NH}[e]	$\sigma_{ef}^{\pm}$[f]	Solution[f]	Solid structure
20	3-OEt	-0.24	0.10	-0.34	-0.10	-0.24	0.10	-0.34	imine	enamine
21	3-OMe	-0.28	0.10	-0.38	-0.10	-0.28	0.10	-0.38	imine	enamine
22	3-OH	-0.38	0.13	-0.51	-0.51	-0.38	0.13	-0.51	imine	enamine
23	6-OMe	0.10	-0.28	0.38	0.38	0.10	-0.78	0.88	enamine	enamine

[a]Reference 53a. [b]$\sigma_{OH} - \sigma_{NH}$. [c]$\sigma_{ef}^{ortho}$ calculated with the values σ_{ortho} ($\sigma_{ortho}^{OMe} = \sigma_{ortho}^{OEt} = 0.0$), reference 54. [d]Reference 53b. [e]Reference 53c. [f]$\sigma^{-}_{OH} - \sigma^{+}_{NH}$. [f]In DMSO-$d_6$.

Newly owing to the different performance of substituent at different positions, the values of σ_{ef} at C-3 and C-5 are reversed by moving to positions C-4 and C-6, with consequent variation in the structure adopted in solution. This is illustrated by the drastic effect caused by some substituents; for example, the methoxy group at position C-5 (**12**) or C-3 (**21**) leads preferentially to imine structures, but at C-4 (**18**) or C-6 (**23**) the enamine tautomer is generated (Figure 1).

Electronic Effects on Polysubstituted Schiff Bases. The preceding Hammett-type analysis can be extended to polysubstituted salicylaldehydes. Thus, for several substituents X, Y, ... one can write:

$$\log K_T = \rho\,(\sigma_x^{OH} - \sigma_x^{NH}) + \rho\,(\sigma_y^{OH} - \sigma_y^{NH}) + \ldots\ldots + c = \rho\,\Sigma(\sigma_i^{OH} - \sigma_i^{NH}) + c \qquad [7]$$

$$\log K_T = \rho\,\sigma_{ef}^{x} + \rho\,\sigma_{ef}^{y} + \ldots\ldots + c = \rho\,\Sigma\sigma_{ef}^{i} + c = \rho\,\sigma_{ef}^{T} + c \qquad [8]$$

$$\log K_T = \rho\,\Sigma(\sigma_i^{OH} - \sigma_i^{NH}) + c = \rho\,(\Sigma\sigma_i^{OH} - \Sigma\sigma_i^{NH}) + c \qquad [9]$$

and equations [8] and [9] are transformed into [10]:

$$\log K_T = \rho\,(\Sigma\sigma_i^{OH} - \Sigma\sigma_i^{NH}) + c = \rho\,\sigma_{ef}^{T} + c \qquad [10]$$

where now $\sigma_{ef}^{T} = \Sigma\sigma_{ef}^{i} = \Sigma\sigma_i^{OH} - \Sigma\sigma_i^{NH}$ and c is a constant.

Since $c \approx 0$ for TRIS derivatives, if $\Sigma\sigma_x^{OH} \leq \Sigma\sigma_x^{NH}$, then $\sigma_{ef} \leq 0$, $K_T < 1$ and the imine structure predominates; on the other hand, if $\Sigma\sigma_x^{OH} \geq \Sigma\sigma_x^{NH}$, then $\sigma_{ef} \geq 0$, $K_T > 1$ and the enamine tautomer is favored. Table 3 collects data for various polysubstituted compounds.

Table 3. Hammett constants for polysubstituted TRIS-derived salicylimines and correlations with tautomeric preferences in solid state and solution.

Comp.	X	$\Sigma\sigma_{OH}$[a]	$\Sigma\sigma_{NH}$[a]	σ_{ef}[b]	σ_{ef}^{ortho}[c]	$\Sigma\sigma^{-}_{OH}$[d]	$\Sigma\sigma^{+}_{NH}$[e]	$\sigma_{ef}^{\pm}$[f]	Solution[g]	Solid state
24	4-OH-6-Me	0.07	-0.52	0.59		0.07	-1.23	1.30	enamine	enamine
25	4,6-$(OMe)_2$	0.20	-0.56	0.76		0.20	-1.56	1.76	enamine	
26	3,4-$(OH)_2$	-0.25	-0.25	0.00	0.00	-0.25	-0.79	0.54	imine	enamine
27	3,5-F_2	0.30	0.68	-0.38	0.01	0.30	0.68	-0.38	imine	enamine
28	3,5-Cl_2	0.48	0.74	-0.26	0.18	0.48	0.74	-0.26	enamine	
29	3,5-Br_2	0.52	0.74	-0.22	0.22	0.52	0.74	-0.22	enamine	

30	3,5-$(NO_2)_2$	1.62	1.42	0.20	0.63	2.46	1.42	1.04	enamine
31	5-NO_2-3-OMe	0.53	0.81	-0.28	0.00	0.95	0.81	0.14	enamine
32	5-Br-3-OMe	-0.02	0.47	-0.49	-0.21	-0.02	0.47	-0.49	imine
33	3,5-Br_2-4-OMe	0.62	0.46	0.16	0.60	0.62	-0.04	0.66	enamine

[a]Reference 53a. [b]$\sigma_{OH} - \sigma_{NH}$. [c]$\sigma_{ef}$ calculated with the values σ_{ortho}, reference 54. [d]Reference 53b. [e]Reference 53c. [f]$\sigma^{-}_{OH} - \sigma^{+}_{NH}$. [g]In DMSO-$d_6$.

For compounds **27**-**29** and **31,** both σ_{ef} and $\sigma_{ef}^{\pm}$ values are < 0, which points to imine structures. This prediction, however, disagrees with the actual enamine structure in solution of dihaloderivatives **28** and **29**, probably due to the steric effects created by bulky Cl and Br atoms at C-3. By employing the σ_{ortho} values of Barlin and Perrin,[54] then $\sigma_{ef}^{ortho} > 0$ (0.18 and 0.22, respectively), consistent with the formation of enamine tautomers in solution. The values of $\sigma_{ef}^{ortho} \sim 0$ shown by **27** and **31** prevent their predictive structure in solution; in fact compound **27** is imine ($\sigma_{ef}^{ortho} \sim 0$) whereas **31** is an enaminic derivative ($\sigma_{ef}^{ortho} = 0.00$).

Structural Predictions in Schiff Bases: Reliability, Scope and Limitations. In order to prove how reliable the above treatment is to predict the structure of unknown and known Schiff bases in solution, further explorations were undertaken. Thus, compounds **13** and **84**-**86** (Table 4) illustrate how the arrangement of phenolic hydroxyls can dictate their preferred structure in solution. While **13** is imine (σ_{ef} = -0.51), **84** (σ_{ef} = 0.51) and **86** (σ_{ef} = 1.02) would be enamines. By moving the OH group from C-6 (**86**) to C-5 in **85** (σ_{ef} = 0), the tendency to form an enamine tautomer is virtually removed. Although **84** has not yet been synthesized, its analogue **24** has enamine structure as predicted for **84** (the methyl group at C-6 does not cause any appreciable alteration since its σ_{ef} = 0.08). Predictions can be extended to external factors capable of governing the tautomeric equilibrium such as the acidity or basicity. Transformation of phenols **13**, **22** or **84** into their conjugate bases **87**-**89** would still maintain the imine or enamine character they already possess.

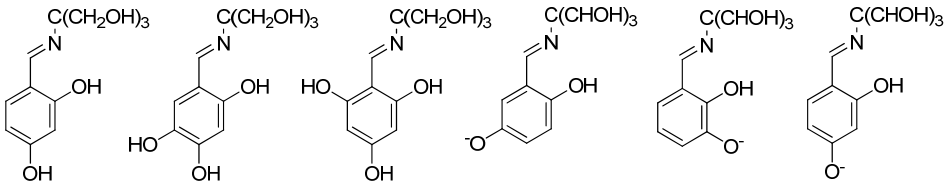

Table 4. Substituent constants for polyhydroxylated Schiff bases and predicted structure in solution.

Comp.	X	σ_{OH}[a]	σ_{NH}[a]	σ_{ef}[b]	σ^{-}_{OH}[c]	σ^{+}_{NH}[d]	$\sigma_{ef}^{\pm}$[e]	Predicted structure
84	4-OH	0.13	-0.38	0.51	0.13	-0.38	0.51	enamine
85	4,5-$(OH)_2$	-0.25	-0.25	0.00	-0.25	-0.79	0.54	?
86	4,6-$(OH)_2$	0.26	-0.76	1.02	0.26	-1.84	2.10	enamine
87	5-O^-	-0.81	-0.47	-0.34	-0.81	-0.47	-0.34	imine

88	3-O$^-$	-0.81	-0.47	-0.34	-0.81	-0.47	-0.34	imine
89	4-O$^-$	-0.47	-0.81	0.34	-0.47	-0.81	0.34	enamine

[a]Reference 53a. [b]$\sigma_{OH} - \sigma_{NH}$. [c]Reference 53b. [d]Reference 53c. [e]$\sigma^-_{OH} - \sigma^+_{NH}$.

Salicylimines derived from anilines also obey equation [5], although the constant term (*c*) can now be different from zero ($c \neq 0$). The enamine structure described for Schiff bases **66-79**,[26,40f] is in agreement with the positive value of σ_{ef} calculated for compound **78** (Table 1). Also, imines derived from 2,3-dihydroxybenzene-1,4-dicarbaldehyde (**90**) and 2,5-dihydroxybenzene-1,4-dicarbaldehyde (**91**) have in solution imine structures, which correlate well with the magnitude of σ_{ef} (< 0), while those from 2,4-dihydroxybenzene-1,3-dicarbaldehyde (**92**) and 2,4,6-trihydroxybenzene-1,3,5-tricarbaldehyde (**93**) exhibit on the contrary an enamine structure (σ_{ef} > 0) (Table 5).[28] The latter is clearly prone to form enamines (**96**, **97**, Scheme 5),[28d,55] which agrees with the arrangement of the three hydroxyl groups, like **86**.

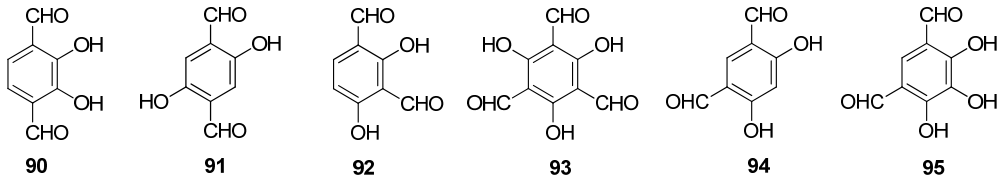

Table 5. Predictions and reported tautomers for *N*-phenylamines derived from aldehydes **90**-**95**.

Imines of[a]	$\sum\sigma_{OH}$	$\sum\sigma_{NH}$	σ_{ef}[b]	Predicted structure	Solution	Solid state
90	-0.03	0.55	-0.58	imine	imine	imine
91	-0.03	0.55	-0.58	imine	imine	
92	0.55	-0.03	0.58	enamine	enamine	enamine
93	1.10	-0.06	1.16	enamine	enamine	enamine
94	0.55	-0.03	0.58	enamine	imine	
95	0.17	0.10	0.07	enamine	imine	

[a] Referred to *N*-phenylimines. [b] For CH=NPh, $\sigma_p = 0.42$ and $\sigma_m = 0.35$ (ref. 53a).

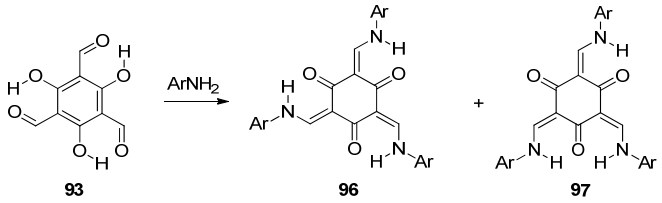

Scheme 5

A curious case involves the Schiff bases derived from 2,4-dihydroxybenzene-1,5-dicarbaldehyde (**94**) and 2,3,4-trihydroxybenzene-1,5-dicarbaldehyde (**95**), as they show an imine structure in solution (**98**, **99**).[28c,28d] While there is some ambiguity for the latter, because $\sigma_{ef} \sim 0$, the former with $\sigma_{ef} = 0.58$

should correspond to the enaminic tautomer. However, in both cases the paradox is solved if one assumes that in order to form a dienaminic structure, diradical species (**100**, **101**), whose formation would otherwise be energetically unfavorable, are required.

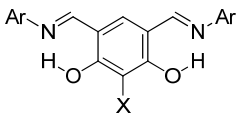

98 X=H
99 X=OH

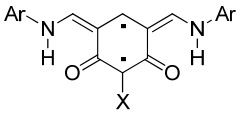

100 X=H
101 X=OH

Previous theoretical calculations have been used to predict the structure of some Schiff bases, not yet synthesized, derived from anilines and other polysubstituted salicylaldehydes like **102**-**107**[28c,28d]. Results fully agree with our predictions gathered in Table 6, even if some uncertainty occurs for the imines derived from **103**, **105** and **107**, since $\sigma_{ef} = 0$. For the two latter ones, the calculations suggest the imine and enamine, respectively, to be the most stable tautomers. Like the cases of **98** and **99**, the dienamine structure of **106** would lead to a diradical species.

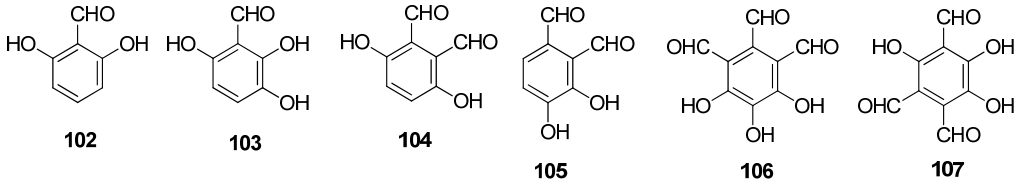

102 **103** **104** **105** **106** **107**

Table 6. Predictions and reported tautomers for *N*-phenylamines derived from aldehydes **102**-**108** and **112**.

Imines of[a]	$\sum\sigma_{OH}$	$\sum\sigma_{NH}$	σ_{ef}	Predicted structure[b]	Predicted structure[c]
102	0.13	-0.38	0.51		enamine
103	-0.25	-0.25	0.00		?
104	-0.03	0.55	-0.58	imine	imine
105	-0.03	0.55	-0.58	imine	imine
106	0.52	0.52	0.00	imine	imine
107	0.52	0.52	0.00	enamine	?
108[d]	-0.86	-0.26	-0.60		imine
112	-0.15	-0.50	0.35		enamine

[a]Referred to *N*-phenylimines. [b]At the B3LYP/6-31G* level, reference 28c. [c]This work, based on σ_{ef}. [d]R = ^{t}Bu.

Application to imine/enamine cavitands serve to illustrate the scope further. Thus, campestarenes, a family of stable, novel shape-persistent conjugated Schiff base macrocycles with 5-fold symmetry mediated by 3-center hydrogen bonding (**109**, R = alkyl),[56] can be obtained from aminosalicylaldehydes (**108**). These compounds, like the macrocycle with 3-fold symmetry **110**,[28b,28c] have an imine structure, as the starting salicylaldehydes, such as **108** (R = ^{t}Bu) and **90**, have negative values of σ_{ef}. In contrast, primary aliphatic and aromatic imines of tetraformylresorcin[4]arenes exist

exclusively as keto-enamine tautomers (**111**),[29] in agreement with positive σ_{ef} values for **102** and **112** (Tables 5 and 6).

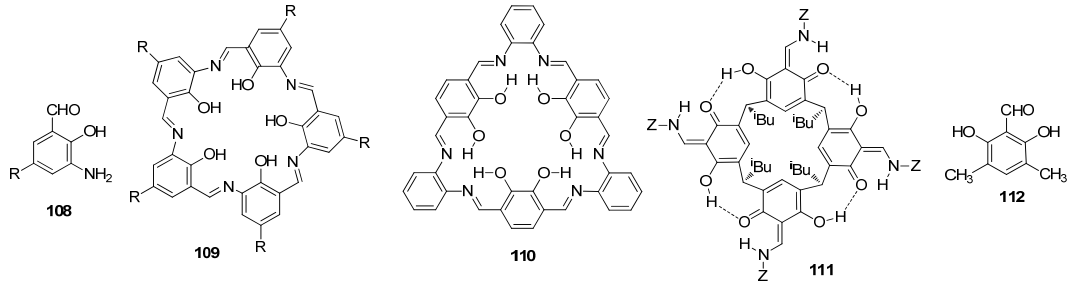

The most important conclusion to be drawn from all of the above is that not only the electronic character of the substituents is responsible for the imine or enamine structure of salicylidene derivatives (in the gaseous phase or solution), but also, and equally important, the position they occupy with respect to the tautomeric system. This predictive analysis appears to be general, only limited by the knowledge of σ values for specific chemical groups. Clearly, the availability of σ_{ortho} data introduces another limitation. It is important to stress again that the rule hinges on the substituent at the imino nitrogen as well, and variations are sensitive to the independent term (*c*) in equations [6] and [9]. As repeteadly mentioned, for *tris*(hydroxymethyl)methyl, $C(CH_2OH)_3$, $c \approx 0$; but the rationale could in principle be applicable to either aliphatic or aromatic substituent. Examples are provided by Schiff bases **113** (X = H, F, Cl, Br, NO_2, CH_3, OCH_3, CN)[30a], which exhibit imine structures in Cl_3CD solution (σ_{ef} = -0.10) or **114** (σ_{ef} = -0.20) and **115** (σ_{ef} = -0.13), both imines in isopentane at room temperature.[21a]

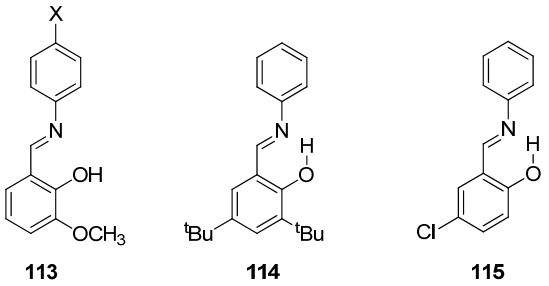

Finally, the inability to form unstable species such as diradicals derived from **98**, **99** and **106** may also invalidate predictions based on the magnitude of σ_{ef}. Obviously, solid state structures, for which crystal's forces rather than electronic effects, play a dominant role, often deviate from this trend. Condensates derived from TRIS have all an enamine structure in solid state. In solution, the favorable structure of compounds **6**-**13**, **20**-**22**, **27** and **32** is largely the imine tautomer. However, adducts **4**, **5**, **14**, **15**, **18**, **20**, **21**, **23**-**25**, **28**-**33** showed $J_{CH,NH} \neq 0$ values indicating that, in general, an enamine structure may also be the predominating form (**34**, **35**, **44**, **45**, **48**, **50**, **51**, **53**-**55**, **58**-**63**).

Electronic Effects of Substituents on Chemical Shifts. As customary in assessing the electronic influence of substituents in delocalized systems by NMR spectroscopy, correlations between the chemical shift of the azomethine carbon with both Hammett and Taft substituent parameters allow to elucidate the

mode of transmission of the electronic effect, as well as the influence of substitution on the conformation and polarity of the C=N bond.[37,38,50,57]

As pointed out in previous remarks, the basicity of the oxygen and nitrogen atoms involved in the tautomeric equilibrium depends on the electron density of each atom, which is collectively well understood by shift of the proton, the nitrogen atom, and the imino and phenolic carbons. Table 3S summarizes the NMR data for the carbon of iminic Schiff bases bearing substituents at C-3 and C-5 (**6**-**9**, **11**-**13**, **20**-**22**, **27** and **32**), which lead to a poor linear plot with σ_{NH} (regression coefficient, $r = 0.798$; Fig. 1S). The low correlation is largely due to the influence of steric effects that contaminate the σ_{NH} values at the positions adjacent to the phenolic hydroxyl. In fact, by removing such points, a good relationship is obtained ($r = 0.966$; Fig. 2).

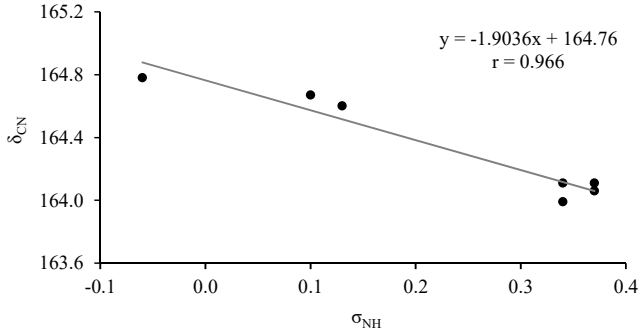

Figure 2. Linear relationship between carbon resonances of iminic signals ($\delta_{C=N}$) and σ_{NH} values (*ortho*-substituents were deliberately omitted).

On the other hand, Hammett's representation for the enamines lacking steric effects, i.e. without substituents at C-3 and C-6: **4**, **5**, **14**-**19**, and **78** is linear, fitting well both the values of σ_{NH} and those of σ_{NH}^{+} (Table 4S, Fig. 3).

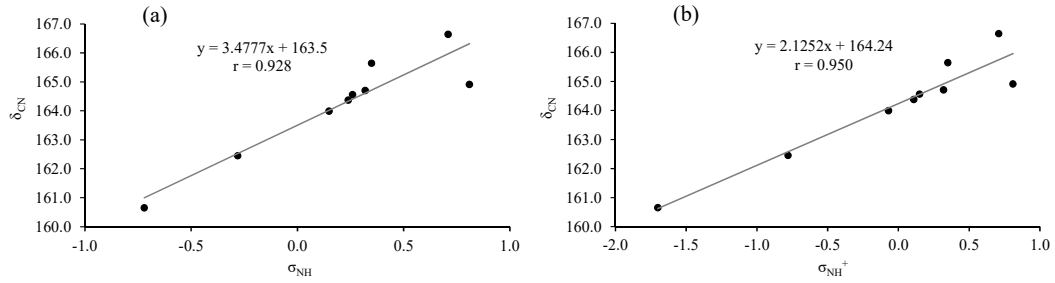

Figure 3. Linear relationship between iminic chemical shifts ($\delta_{C=N}$) and σ_{NH} (a) and σ^{+}_{NH} parameters for compounds **4**, **5**, **14**-**19**, and **78**.

Also, data for enamines **26**, **28**-**31** and **33**, substituted at C-3, position contiguous to the phenolic hydroxyl, lead to fairly good linear plots with both σ ($r = 0.957$) and σ^{+} ($r = 0.940$), although the fit is better against the former (Table 4S, Fig. 2S). When the representation is carried out for imines as function of σ_{ef}, a pretty good linear relationship is obtained again (if one omits the divergent case of compound **11**) (Fig. 4).

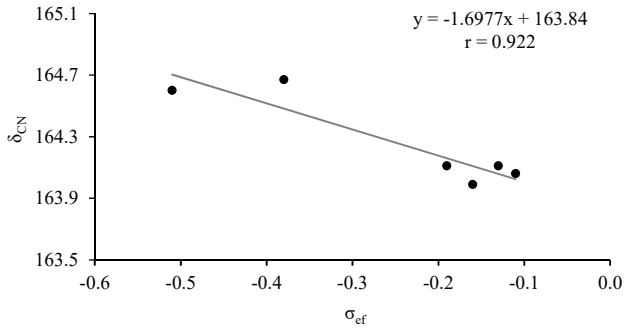

Figure 4. Linear relationship between chemical shifts ($\delta_{C=N}$) and σ_{ef} for iminic structures.

For plots against σ_{OH}, only a modest correlation could be obtained for the chemical shifts at C-2 for imines **6**-**13**, which becomes acceptable (r = 0.935) by removing the deviation caused by **6** (Table 5S, Fig. 5).

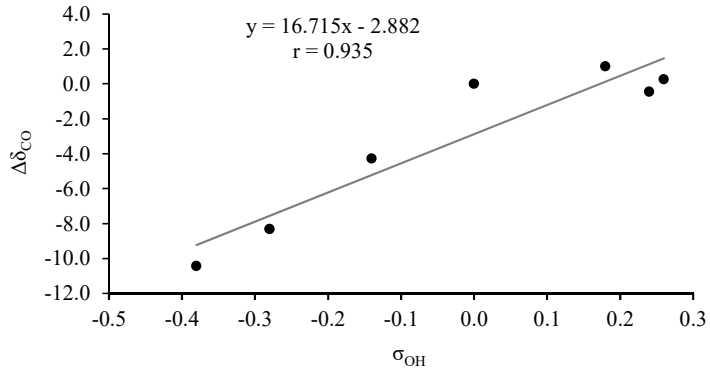

Figure 5. Linear relationship between chemical shifts (δ_{CO}) and σ_{OH} for **7**-**13**.

Finally, the representation of the chemical shifts for phenolic or NH protons leads to a linear graph, with both imines (r = 0.952) and enamines (r = 0.950) (Table 6S, Fig. 3S). In fact, the chemical shifts of the phenolic proton of imines and the NH proton of enamines (**5**-**19** and **78**) can be plotted at the same time, although the fit is a little worse (r = 0.944) (Fig 6). As shown, the O–H/N–H shifts increase as σ_{OH} increases. This trend demonstrates that the H-bond becomes stronger as we move from electron-donating to electron-withdrawing groups.

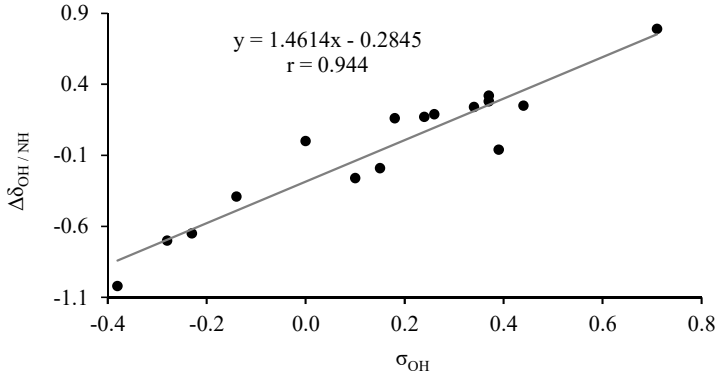

Figure 6. Hammett-type correlation between the OH/NH chemical shifts and σ_{OH} for **5**-**19** and **78**.

Overall, these results prove that both carbons, iminic and phenolic, and OH/NH of the tautomeric system are subject to the same effects and support the hypothesis that this system responds globally to the effect of the substituents, thus justifying the approximation $\rho^{OH} \approx \rho^{NH} \approx \rho$ to derive equations [6] and [10].

Electronic Effect of the Substituents on the Tautomeric Equilibrium. Some research teams have used ^{13}C chemical shifts to estimate K_T,[37,43] although it has been noted that the corresponding ^{15}N shifts of the iminic nitrogen lead to more accurate results, because their variation between imine and enamine structures is ten times greater than that shown by the corresponding ^{13}C atoms. The values of the coupling constants ^{15}N-H, ^{13}C-^{13}C and ^{13}C-^{15}N have also been used for identical purposes.[37,47,58,59] We have attempted to quantify the influence of the substituents on the tautomeric equilibrium using ^{13}C chemical shifts. Equations [11] and [12] can be used to calculate the populations of each tautomer, provided that we have adequate δ_i/δ_e and J_i/J_e values:

$$n_i = (\delta_e - \delta_{exp})/(\delta_e - \delta_i) = (J_e - J_{exp})/(J_e - J_i) \qquad [11]$$

and analogously,

$$n_e = (\delta_{exp} - \delta_i)/(\delta_e - \delta_i) = (J_{exp} - J_i)/(J_e - J_i) \qquad [12]$$

For the imine-enamine balance, the equilibrium constant $K_T = n_e/n_i$ is expressed by:

$$K_T = n_e/n_i = (\delta_{exp} - \delta_i)/(\delta_e - \delta_{exp}) = (J_{exp} - J_i)/(J_e - J_{exp}) \qquad [13]$$

The tautomerization constants (K_T) of **4-33** have been calculated on the basis of equation [13]. The values δ_i = 154.45 ppm from imine **13** and δ_e = 180.18 ppm from enamine **34** were arbitrarily chosen, because they are the lowest and highest ones, respectively, and could then reflect "pure" imine and enamine tautomers. The final equation [14] is similar to the one obtained by other authors,[43] and the resulting data are shown in Table 7S. Such results can be employed for a Hammett plot by representing the logarithmic expression [15], which affords rather modest free-energy relationships (LFER) with both σ_{ef} (r = 0.789) and $\sigma_{ef}^{\pm}$ (r = 0.781) values (Fig. 4S).

$$K_T = (\delta_{C2} - 154.45)/(180.18 - \delta_{C2}) \qquad [14]$$

$$\log K_T = \log [(\delta_{C2} - 154.45)/(180.18 - \delta_{C2})] = \rho\, \sigma_{ef} + c \qquad [15]$$

Figure 7 shows the same representations for derivatives substituted at C-4 and C-5 positions only, in order to avoid the influence of steric effects at C-3 and C-6. The regression coefficients are improved, especially when the deviations caused by **18** and **19** (gray line) are not taken into account.

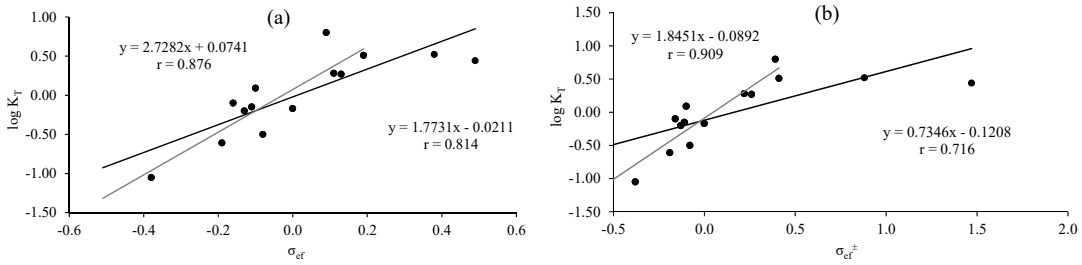

Figure 7. Representations of log K_T *vs* σ_{ef} (a) and $\sigma_{ef}^{\pm}$ (b).

Finally, a plot of log K_T for the TRIS-salicylimines **4**-**33** *versus* the corresponding δ_{C2} values yields an excelent linear relationship between these two variables (Fig. 5S):

$$\log K_T = 0.0845 \times \delta_{C2} - 14.143 \quad (r = 0.988) \qquad [16]$$

The calculation of K_T through equation [14] has a serious drawback when the values of δ_{C2} approach those of δ_e or δ_i: when $\delta_{C2} \rightarrow \delta_e$ (180.18) then K_T and log $K_T \rightarrow \infty$ and when $\delta_{C2} \rightarrow \delta_i$ (154.45) then $K_T \rightarrow 0$ and log $K_T \rightarrow -\infty$. In other words, for values of δ_{C2} close to δ_e and δ_i, small experimental errors in the determination of δ_{C2} are magnified. Equation [16] can be used to calculate the values of K_T and log K_T in the extreme zones. Thus, for **12** and **34** the values of 0.08 and 12.1 are obtained for K_T, respectively, which indicate that the imine form of **12** and enamine of **34** are either prevalent or exclusive in solution and are more realistic than those obtained by equation [14].

In addition, when the proportions of the imine and enamine tautomers are equal, $K_T = 1$ and log $K_T = 0$, δ_{C2} becomes 167.4 ppm (almost coincidental with the arithmetic mean of δ_e and δ_i, 167.6 ppm). Since δ_{C2} is actually an experimental average between δ_e and δ_i ($\delta_{exp} = n_i\delta_i + n_e\delta_e$, with $n_i + n_e = 1$), δ_{C2} values lower than the latter indicate a predominance of the imine form, whereas at higher ones the enamine tautomer predominates. Therefore, the carbon shift of 167.5 ppm can be used as an approximate boundary to define the predominance of one form or another in solution. On applying this conclusion to the δ_{C2} values shown in Table 2S, it is found that compounds **20**, **21** and **32**, even though they have δ_{C2} values less than 167.5 ppm, show significant $J_{NH,CH}$ couplings. In addition, compounds **28** and **29**, with values almost identical to 167.5 ppm, possess high values of $J_{NH,CH}$ (11.6 Hz), very close to those shown by compounds with a clear predominance of the enamine structure (*e.g.*, **64**, 179.8 ppm, $J_{NH,CH}$ =12.4 Hz).

Although the issue of quasi-aromaticity will be treated later, in the present context it should also be mentioned that new σ_p^+ constants can be obtained from the regression of the aromaticity descriptors HOMA (geometry-based, $\sigma^+_{p(H)}$) and magnetic index NICS[60] ($\sigma^+_{p(N)}$) (Table 8S). When these new values of σ_p^+ are plotted against log K_T, fine correlations could be obtained as shown in Figure 8. Likewise, good correlations with the chemical shifts at C-2 are depicted in Fig. 9.

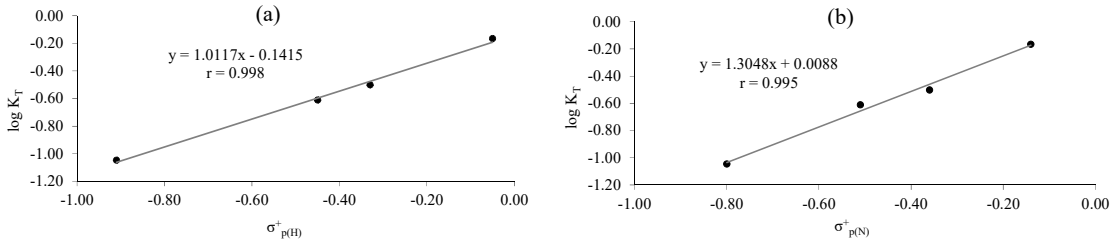

Figure 8. Linear relationships of log K_T *vs* σ_p^+ constants calculated from HOMA (a) and NICS (b) indexes.

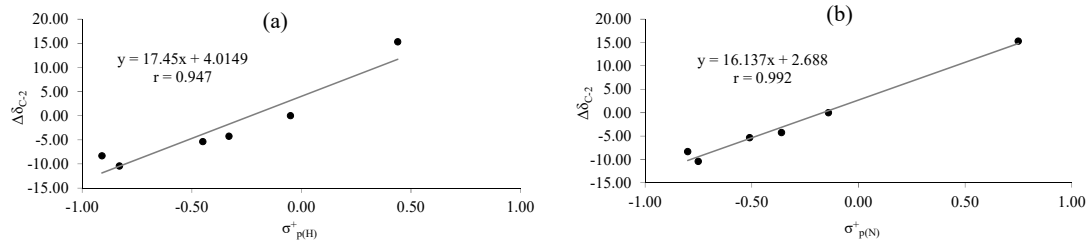

Figure 9. Linear representations of δ_{C-2} *vs* σ_p^+ constants derived from HOMA (a) and NICS (b) indexes.

Analysis of Substituent Effects on Examples Drawn from Literature. It is obvious that either thumb rule claiming generality should not only have predictive capability, but also justify results from previous literature. As preliminary examples we chose the salicylamines derived from methylamine (**116**-**126**) described by Hansen *et al*.[45e], for which we calculated the tautomerization equilibrium constants using equation [14], with δ_e = 176.71 and δ_i = 152.19, which are the extreme values of **126** and **120**, respectively. These imines are not included in the representation because their log K_T are unknown. To overcome this limitation, the values δ_e = 180.18 (from enamine **34**) and δ_i = 152.00 (from imines derived from 4-methoxysalicylaldehyde and 4-methoxyaniline)[60] were employed, which correspond to the maximum and minimum shifts reported for salicilimines. Results are shown in Table 10S.

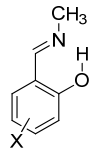

116 X = H
117 X = 5-Br
118 X = 5-Me
119 X = 5-Cl
120 X = 3-OMe
121 X = 3,5-Cl_2
122 X = 3,5-Br_2
123 X = 3,4,5,6-Cl_4
124 X = 5-OMe
125 X = 4-OMe
126 X = 4,6-$(OMe)_2$

The representation of log K_T versus σ_{ef} gives rise to good fits (Figure 10). The correlation of Fig. 10b improves by removing structure **120** (r = 0.9550).

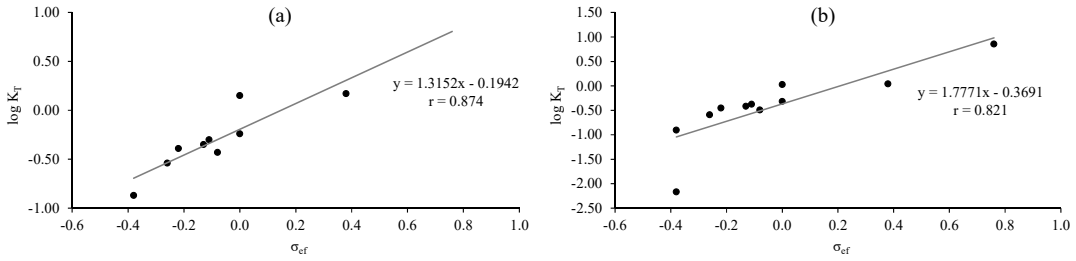

Figure 10. Linear representations of log K_T *vs* σ_{ef} data for structures **116-126**: a) equation [13]: δ_e = 176.71 ppm, δ_i = 152.19 ppm; b) equation [13]: δ_e = 180.18 ppm, δ_i = 152.00 ppm.

Moreover, the linear relationships improve further by removing structures with substituents at C-3 and C-6, which include steric effects not contemplated in the values of σ. Thus, using the data for only **116-119**, **124**, and **125**, an excellent correlation could be obtained with log K_T (r = 0.960) (Figure 11).

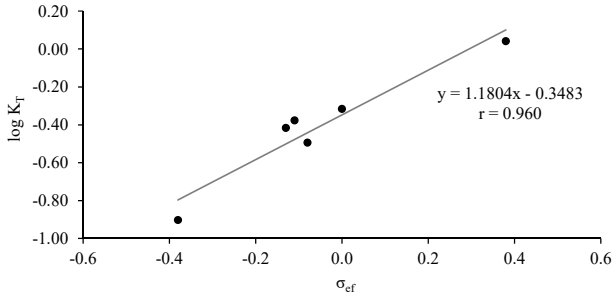

Figure 11. Linear representations of log K_T *vs* σ_{ef} data for structures **116-119**, **124**, and **125** (equation [13]: δ_e = 180.18 ppm, δ_i = 152.00 ppm).

In addition, the plot of chemical shifts δ_{C2} *versus* σ_{ef} generates good fitting (r = 0.954, Figure 12a), further improved if substitutions at C-3 and C-5 are not taken into account (r = 0.983, Figure 12b).

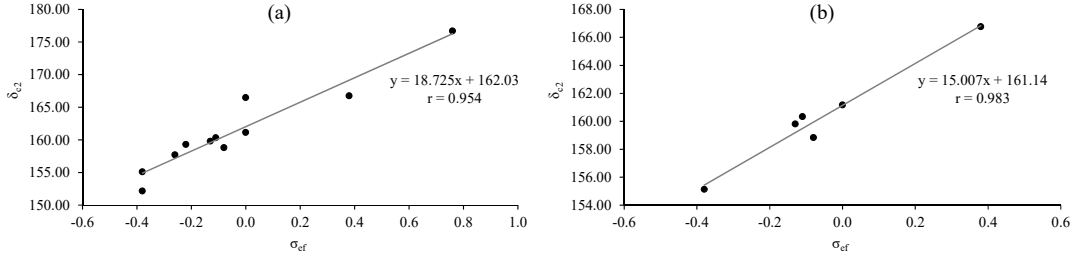

Figure 12. Linear correlations of δ_{C2} *vs* σ_{ef} data for structures **116-126**.

A similar analysis has been performed by using ^{15}N chemical shifts for compounds **119-122** and **124-126**, measured by Schilf *et al.* in $CDCl_3$[48b] and in solid state[48a], plotted against different σ parameters

(Tables 7 and 11S, Figures 8S-13S). Although such δ^{15}_N measurements ($CDCl_3$) were recorded at several temperatures, good linear relationships could be obtained nevertheless.

Table 7. Hammett correlations of iminic nitrogen chemical shift of **119-122** and **124-126**.[a]

Hammett equation[a]	r	T (K)
$\delta\ ^{15}_N = -101.25\sigma_{ef} - 131.61$	0.925	266
$\delta\ ^{15}_N = -118.84\sigma_{ef} - 141.36$	0.947	217
$\delta\ ^{15}_N = -117.97\sigma_{ef} - 147.43$	0.926	205.5
$\delta\ ^{15}_N = -95.71\sigma_{ef}^{ortho} - 120.63$	0.876	266
$\delta\ ^{15}_N = -112.60\sigma_{ef}^{ortho} - 128.45$	0.899	217
$\delta\ ^{15}_N = -117.43\sigma_{ef}^{ortho} - 134.16$	0.923	205.5
$\delta\ ^{15}_N = -54.88\sigma_{ef}^{\pm} - 118.33$	0.949	266
$\delta\ ^{15}_N = -63.82\sigma_{ef}^{\pm} - 125.88$	0.962	217
$\delta\ ^{15}_N = -63.04\sigma_{ef}^{\pm} - 132.12$	0.936	205.5
$\delta\ ^{15}_N = -57.48\sigma_{ef}^{\pm ortho} - 114.08$	0.965	266
$\delta\ ^{15}_N = -66.91\sigma_{ef}^{\pm ortho} - 120.92$	0.980	217
$\delta\ ^{15}_N = -67.18\sigma_{ef}^{\pm ortho} - 126.96$	0.968	205.5
$\delta\ ^{15}_N = -109.76\sigma_{ef} - 173.16$[b]	0.675	297
$\delta\ ^{15}_N = -14.92\sigma_{OH}^{ortho} - 125.22$	0.142	266

[a] In $CDCl_3$ at 50.68 MHz. [b]In solid state at 50.68 MHz.

However, δ^{15}_N values measured in the solid state led to representations with worse regression coefficients (Figure 14S), thereby evidencing the dominant role of intermolecular interactions in the crystalline lattice as prime factor in tautomer's stability.[22]

Good representations were also obtained not only for δ_{OH} and δ^{15}_N, but also for δ_{OD} and δ_{OT} of the respective deuterated and tritiated forms of **124-126**[47c] (Tables 8 and 12S, Figures 15S-23S).

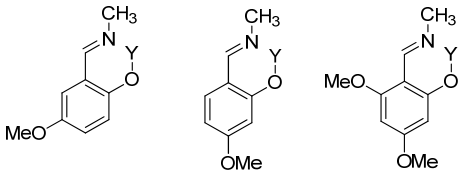

124 Y=H,D,T **125** Y=H,D,T **126** Y=H,D,T

Table 8. Hammett correlations for NMR data of **124-126**.[a]

Hammett equation[a]	r	T (K)
$\delta_{OH} = 1.11\sigma_{ef} + 13.30$	0.983	303
$\delta_{OD} = 0.87\sigma_{ef} + 12.98$	0.970	303
$\delta\ ^{15}_N = -98.56\sigma_{ef} - 116.62$	0.931	303
$\delta_{OH} = 2.57\sigma_{OH} + 13.56$	0.999	303
$\delta_{OD} = 2.04\sigma_{OH} + 13.18$	0.994	303
$\delta\ ^{15}_N = -211.94\sigma_{OH} - 140.17$	0.873	303
$\delta_{OH} = 0.58\sigma_{ef}^{\pm} + 13.14$	0.963	303
$\delta_{OD} = 0.46\sigma_{ef}^{\pm} + 12.85$	0.945	303
$\delta\ ^{15}_N = -54.82\sigma_{ef}^{\pm} - 100.29$	0.959	303
$\delta_{OH} = 1.03\sigma_{ef} + 13.39$	0.968	298
$\delta_{OT} = 0.79\sigma_{ef} + 12.92$	0.956	298

$\delta_{OH} = 2.41\sigma_{OH} + 13.63$	0.993	298
$\delta_{OT} = 1.87\sigma_{OH} + 13.11$	0.987	298
$\delta_{OH} = 0.54\sigma_{ef}^{\pm} + 13.24$	0.942	298
$\delta_{OT} = 0.41\sigma_{ef}^{\pm} + 12.81$	0.927	298
$\delta\ ^{15}_{N} = -129.33\sigma_{ef} - 134.41$	0.983	223
$\delta\ ^{15}_{N} = -286.32\sigma_{OH} - 165.26$	0.949	223
$\delta\ ^{15}_{N} = -70.67\sigma_{ef}^{\pm} - 113.93$	0.995	223

[a]In $CDCl_3$ at 500.13 (^{1}H) and 50.68 (^{15}N) MHz.

Our analysis can be successfully extended to another family of structurally related substances, namely *N*-benzylsalicylimines **127**-**130**[47f] (Table 9 with linear regressions gathered in Figures 24S-26S), as well as **131**-**134** (Tables 10 and 13S, Figures 27S-29S).

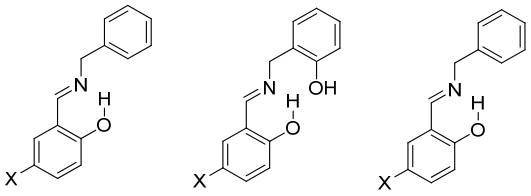

127 X = H
128 X = 5-NO_2
129 X = 5-OMe
130 X = 5-Br

131 X = H
132 X = 5-NO_2
133 X = 5-OMe
134 X = 5-Br

135 X = 5-Cl
136 X = 5-OH

Table 9. Hammett correlations for NMR data of **127**-**130**.[a]

Hammett equation[a]	r	T (K)
$\delta_{OH} = 3.00\sigma_{ef} + 13.84$	0.881	266
$\delta_{C2} = 36.43\sigma_{ef} + 166.58$	0.841	266
$\delta\ ^{15}_{N} = -127.16\sigma_{ef} - 114.52$	0.666	266
$\delta_{OH} = 1.84\sigma_{ef}^{\pm} + 13.54$	0.984	266
$\delta_{C2} = 23.54\sigma_{ef}^{\pm} + 162.85$	0.990	266
$\delta\ ^{15}_{N} = -96.54\sigma_{ef}^{\pm} - 101.40$	0.922	266

[a]In DMSO-d_6 at 500.13 (^{1}H), 125.77 (^{13}C) and 50.68 (^{15}N) MHz.

Table 10. Hammett correlations for NMR data of **131**-**134**.[a]

Hammett equation[a]	r	T (K)
$\delta_{OH} = 4.30\sigma_{ef} + 14.42$	0.838	266
$\delta_{C2} = 39.83\sigma_{ef} + 167.76$	0.833	266
$\delta\ ^{15}_{N} = -156.95\sigma_{ef} - 125.73$	0.675	266
$\delta_{OH} = 2.77\sigma_{ef}^{\pm} + 13.98$	0.984	266
$\delta_{C2} = 25.90\sigma_{ef}^{\pm} + 163.68$	0.988	266
$\delta\ ^{15}_{N} = -118.21\sigma_{ef}^{\pm} - 109.54$	0.926	266

[a]In DMSO-d_6 at 500.13 (^{1}H), 125.77 (^{13}C) and 50.68 (^{15}N) MHz.

Besides, like in above-mentioned correlations, good fitting could be established between the electronic effect of the substituents and the pK_a values of Schiff bases **127**-**130**, **135** and **136**[51], as shown in Tables 11 and 14S, and Figures 30S and 31S.

Table 11. Hammett correlations for pK_a of **127-130**, **135,** and **136**.[a]

Hammett equation[a]	r	T (K)
$pK_a = -2.43\sigma_{ef} + 8.28$	0.896	296.15
$pK_a = -1.60\sigma_{ef}^{\pm} + 8.54$	0.915	296.15

$pK_a = -1.30\sigma_{OH} + 8.84$	0.895	296.15
$pK_a = -0.95\sigma_{OH^-} + 8.87$	0.878	296.15

[a]In CD_3OD at 296.15 ± 1 K.

In summary, the quality of all linear correlations allow us to demonstrate the utility and broad scope of this analysis to quantify the electronic effects of the substituents involved in the tautomeric equilibrium of salicylimine derivatives.

Imine/Enamine-Oxazolidine Equilibria. When DMSO-d_6 solutions of the Schiff bases derived from TRIS are kept at room temperature, partial isomerization (~5%) to a cyclic oxazolidine occurs (see SI).

Imine-Enamine Tautomerizations. The experimentally-measured C=O and C-N bond lengths for **18** ($d_{C=O}$ 1.288 Å, d_{C-N} 1.306 Å) and **23** ($d_{C=O}$ 1.310 Å, d_{C-N} 1.300 Å)[42] are midway between the calculated at M06-2X/6-311G++(d,p) level for the structures of imine (~1.335 and ~1.282 Å for C-O and C=N, respectively) and enamine (~1.255 and 1.322 Å for C=O and C-N, respectively) tautomers (**48** and **53**). These results suggest the coexistence of imine and enamine structures in a fast equilibrium within the crystal lattice (see SI for the calculation methodology).

To investigate further the feasibility of such imine-enamine transformations, DFT calculations at the aforementioned level were undertaken, both in gas phase and with bulk solvation using the SMD method. The mono-substituted derivatives **34**, **36-38**, **40**, **42-48**, **51**, **53**, **84** and other disubstituted ones, namely **54**, **57**, **60** and **61**, all of which exhibit enamine structures in solid state, were chosen as models, albeit **36-38**, **40**, **42, 43**, **46**, **47**, **51** and **57** adopt a predominant imine structure in solution. The relative stability of imine (**138**) and enamine (**140**) forms, and the corresponding transition state (**139**) were calculated in the gas phase (Scheme 6), with data gathered in Table 15S. Results indicate that the imine form is more stable than the enaminic one, which contrasts with the situation encountered in the solid state favoring the formation of enamine tautomers (**140**). It is obvious that the strong divergence between gas phase and solid state structures should reasonably be ascribed to the intermolecular interactions generated in the crystal lattice.[22]

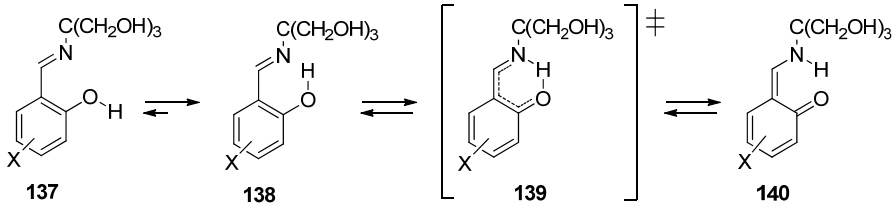

Scheme 6

As this transformation takes place intramolecularly without the participation of solvent's molecules, one should assume that the energies calculated in gas phase for the transition structures will be similar to those present in the solid. The activation energy for the interconversion imine→enamine is sufficiently low, so that it proceeds easily at room temperature ($\Delta G_i^{\ddagger} = \Delta G_{TS}^{\ddagger} - \Delta G_{imine} \leq 7.5$ kcal/mol). The activation energies are, in general, negative for the enamine→imine transformation ($-1.5 \leq \Delta G_e^{\ddagger} = \Delta G_{TS}^{\ddagger} - \Delta G_{enamine} < 1.4$ kcal/mol) (Calculations made on **124-126** lead to similar results, see table 16S).

Analogous results were obtained by including solvent effects (DMSO, Table 17S), although solvation decreases the tautomerization barriers; for imine→enamine: $\Delta G_i^{\ddagger} \leq 5.2$ kcal/mol and for enamine→imine: $-1.0 \leq \Delta G_e^{\ddagger} < 0.9$ kcal/mol. The corresponding transition structures are not only characterized by a low energy barrier but also by their high imaginary frequency (~800-1000 cm^{-1}), the latter listed in Tables 15S-17S for all imines studied. This behavior has been recently found in mono- and di-azaderivatives of malondialdehydes[13,62] and in heterocyclic hydrazones of gossypol,[63] featuring strong intramolecular H-bonding as well.

Table 17S shows that in solution the enaminic forms **60** and **61** are more stable than their iminic counterparts **30** and **31**, unlike the rest of Schiff bases. Interestingly, in the first case the activation energy is negative for imine→enamine tautomerization ($\Delta G_i^{\ddagger}$ = -1.0 kcal/mol) and positive for enamine→imine tautomerization ($\Delta G_e^{\ddagger}$ ~1.5 kcal/mol), while in the second both are positive ($\Delta G_i^{\ddagger}$, $\Delta G_e^{\ddagger} < 1.0$ kcal/mol). A plot of the electronic energy profiles extracted from Tables 15S and 17S is shown in Figure 13a, and reveals the lack of symmetry in the tautomerization of salicylidene derivatives from TRIS. The saddle points show an almost identical energy to the enaminic tautomers **140**, and therefore their structure must be similar. Figure 13b shows a similar picture for the intramolecular hydrogen transfer between tautomers **138** and **140** based on the $\Delta G^{\ddagger}$ values, which might suggest a more complex reaction path involving at least another relative local minimum and an additional saddle point sandwiched between the transition structure drawn and tautomer **140**.

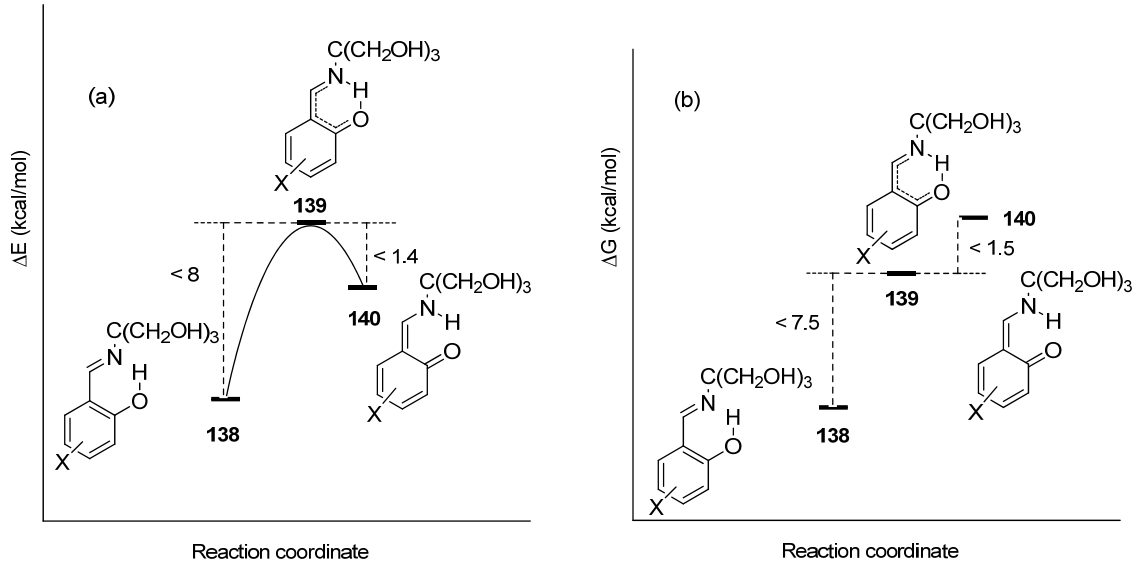

Figure 13. Schematic diagram showing the relative energy profiles for the tautomerization of **138** and **140**; (a) electronic energies; (b) free energies.

Furthermore, the internal reaction coordinate (IRC) for the transition structure $\mathbf{TS_{10/40}}$ in DMSO, corresponding to the tautomerization of simpler Schiff bases (**10** into **40**) was calculated (Table 18S). The IRC obtained evidenced that $\mathbf{TS_{10/40}}$ (Figs. 10S and 11S) is actually the true saddle point. This prototropy is characterized by a low energy barrier (< 6 kcal/mol) and a high imaginary frecuency ~1000 cm^{-1}, which

cause a sharp drop in the zero point energy (ZPE) as shown in Figure 14 using thermochemical data for each structure along the reaction path (Table 19S).

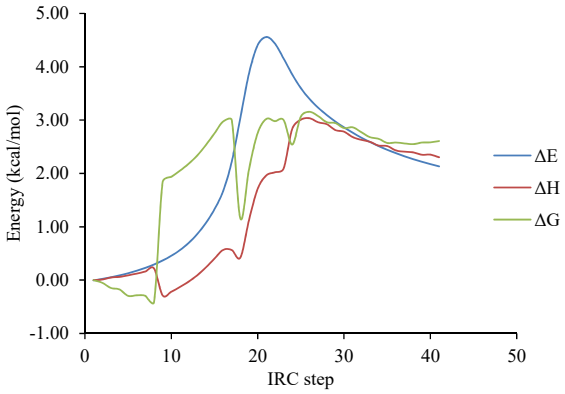

Figure 14. Variations of enthalpy (ΔH), electronic (ΔE) and free energy (ΔG) calculated at 298.15 K (in kcal/mol) near the saddle point for **10**/**40**.

Addition of thermal corrections, including the ZPE correction, to the electronic energy does justify a marked decrease in the internal energy and hence, of the enthalpy and free energy at the saddle point, thus leading to negative values for $\Delta H^{\ddagger}$ and $\Delta G^{\ddagger}$. This particular behavior is responsible for a variational effect that displaces the maximum values of $\Delta H^{\ddagger}$ and $\Delta G^{\ddagger}$ with respect to the saddle point. The necessary correction could then be formulated in terms of the Marcus theory.[64]

Hydrogen Bonding Analysis. The OH/NH group forms an intramolecular hydrogen bond, almost coplanar with the aromatic ring. As pointed out earlier, the strong hydrogen bond between O-H and N or N-H and O atoms, is evidenced by the observation of a large downfield shift of the proton peak for **4-33**/**34-63** in DMSO-d_6 (Table 2S). Their hydrogen bonding energy (E_{HB} in kcal/mol) can be calculated by means of the Schaefer's correlation:[65] $\Delta\delta = (-0.4 \pm 0.2) - E_{HB}$, where $\Delta\delta$ is given in ppm for the chemical shift difference between the O-H signal of **4-33**/**34-63** (δ_{exp}) and that in phenol (δ 4.29). Since $\Delta\delta = \delta_{exp} - 4.29$, equation [17] can be employed here:

$$E_{HB} = -\delta_{exp} + 3.89 \pm 0.2 \qquad [17]$$

The hydrogen-bonding energy is collected in Table 2S and estimated to be -11.5 to -9.5 kcal/mol for **4-33**/**34-63** in DMSO-d_6. These values are expected for a strong hydrogen bond. Emsley[66] defined a weak or normal hydrogen bond as one whose strength is less than 50 kJ/mol (12 kcal/mol). Current figures suggest a weak hydrogen bond shows a strength of 4 kcal/mol at most, one strong 4-15 kcal/mol, and one very strong 15-40 kcal/mol.[1c,4a,67]

However, Kleinpeter *et al.*[68] have shown that ring current effects on resonance-assisted and intramolecularly bridged hydrogen bond protons contribute significantly to the chemical shift of the latter, making it questionable to use δ(OH)/ppm for estimating intramolecular hydrogen bond strength (the difference is usually less than 1 ppm). Thus, for imine structures the strength of the hydrogen bridge can be estimated by DFT calculations as the difference in stability between the open (**137**) and closed (**138**)

forms (Scheme 6). To this end, a rotation of 180º around the C-OH bond was carried out with further optimization of **137**. The energy difference between the initial and final structures can be regarded as measurement of the hydrogen bond strength ($\Delta\Delta G_r = -E_{HB}$) (Tables 15S and 17S). The value found for imines in DMSO [M06-2X/6-311++G(d,p)] lies in general in the range from -11.6 to -9.0 kcal/mol, in total agreement with that determined by equation [17]. This protocol is not applicable to enamines, and the hydrogen bonding energy (E_{HB} in kcal/mol) in **34**, **36-38**, **40**, **42-48**, **51**, **53**, **54**, **57**, **60**, **61**, and **84** was estimated by another empirical relationship, equation [18],[69] developed for intramolecular hydrogen bonding in enol-aldehydes and enol-imines derived from malonaldehyde and salicylaldehyde.

$$E_{HB}\,(\text{kcal/mol}) = -5.554 \times 10^5 \exp(-4.12 d_{D\ldots A}) \qquad [18]$$

where $d_{D\ldots A}$ denotes either an experimentally measured or theoretically calculated distance (in Å) between donor (D) and acceptor (A) atoms involved in that non-covalent interaction. In general, in the gas phase the apparent hydrogen bond energy (E_{HB}) lie within -14 to -10 kcal/mol for imines (Table 20S) and 16.5-13 kcal/mol for enamines (Table 21S), slightly higher than those obtained by previous calculations. However, in presence of DMSO the H-bonding energies are -13 to -12 kcal/mol for imines (Table 22S) and -11 to -10 kcal/mol for enamines (Table 23S), which points to a leveling effect of the strength between both tautomers caused by solvation. It is also noteworthy that electron-withdrawing groups (NO_2) lead to the strongest hydrogen bonds in imine structures (~ 14 kcal/mol for **4** and **31**, ~ 17 kcal/mol for **30**) and the weakest in enamine tautomers (~ 10 kcal/mol for **34** and **61**, ~ 9 kcal/mol for **60**).

Pseudo-Aromaticity in H-bonded Tautomeric Salicylimines. The intramolecular hydrogen bonding in Schiff bases derived from salicylaldehydes, for which the concept of resonance-assisted hydrogen bonds (RAHB) can be invoked,[5-7] and despite the cautionary elements formulated by other authors,[8] invites clearly to explore whether or not there is some delocalization of the π-electrons through single and double bonds. If true, such strong hydrogen bonds may have a significant covalent character beyond their electrostatic nature.[5] This delocalization can be evaluated for pseudo-heterocyclic tautomers of Schiff bases derived from salicylaldehydes in terms of geometrical considerations.[10,70,71] These include a series of well-established aromaticity indexes such as the Harmonic Oscillator Model of Aromaticity (HOMA).[71,72] The calculated HOMA values of pseudo-heterocyclic and carbocyclic rings for tautomers **138** and **140**, and their transition structures **139** (Scheme 6), corresponding to the intramolecular proton transfer in gas phase of salicylimines substituted at C-4 and C-5, are collected in Tables 12 and 32S (see also Tables 24S-31S).

Table 12. HOMA values for pseudo-heterocyclic rings.[a]

X	137	138	139	140	Σ_{HOMA}[b]
5-NO_2	0.11	0.36	0.66	0.62	0.98
5-F	0.06	0.32	0.74	0.69	1.01
5-Cl	0.08	0.34	0.73	0.69	1.03
5-Br	0.08	0.34	0.73	0.69	1.03
5-OMe	0.03	0.29	0.74	0.72	1.01
5-OH	0.04	0.30	0.75	0.72	1.02
H	0.10	0.35	0.73	0.68	1.03

4-NO_2	0.08	0.33	0.71	0.70	1.03
4-F	0.13	0.38	0.71	0.64	1.02
4-Cl	0.12	0.37	0.73	0.67	1.04
4-Br	0.12	0.36	0.73	0.68	1.04
4-OMe	0.14	0.38	0.69	0.64	1.02
4-OH	0.15	0.40	0.70	0.62	1.02

[a]At M06-2X/6-311G(d,p) level in gas phase. [b]Σ_{HOMA} = HOMA(**138**) + HOMA(**140**).

Data in Table 12 show a significant increase of the electronic delocalization in pseudo-heterocyclic rings from imine (~0.3-0.4) to enamine (~0.6-0.7) tautomers. The hydrogen bond is essential for this delocalization to occur, because in open imines lacking hydrogen bridge the HOMA value is practically zero (~0.1). The HOMA indices for enamines are only slightly lower than those reached in the transition state. Moreover, the sum of the HOMAs of the cyclic imine and its tautomeric enamine remains essentially constant (*ca*. 1.0, eq. [19]) for all cases studied (Table 12, last column).

$$\Sigma_{\text{HOMA pseudoheterocycle}} = \text{HOMA}_{\text{closed im (}\mathbf{138}\text{)}} + \text{HOMA}_{\text{enam (}\mathbf{140}\text{)}} = 1.0 \qquad [19]$$

This finding is appealing indeed, as it proves the inter-relationship between imine and enamine structures, or in other words, *the aromaticity lost by the imine is concomitantly gained, at the same extent, by the enamine form irrespective of the electronic character of the substituent.*

Something similar happens with the carbocyclic ring, as the sum of the HOMA indices of the benzene ring in the imine structures and the corresponding 2,4-cyclohexadienone ring in the enamine tautomers is approximately constant (*ca*. 1.45, Table 32S, last column). By considering the equilibrium shown in Scheme 6 and data of Table 12, one sees that the enamine pseudo-ring is more aromatic (greater HOMA) than the iminic one, because the former loses the aromaticity of the benzenic ring (quinonoid structure instead of Kekulé-type benzene) while gaining the pseudo ring with hydrogen bonding. In this context, it has already been indicated that for some substituted phenols (like salicylaldehydes), the transfer of aromaticity from the benzenic ring to the H-bonded ring takes place via the effect of electron delocalization.[73]

Structural variations associated with the electronic effect of the substituents, as they alter the strength of the hydrogen bond, can in addition be inferred from changes in bond lengths and bond angles involved in that bonding. Table 33S lists the geometric parameters associated with the hydrogen bonds calculated for several imines (**138**) and enamines (**140**), and we were able to found some useful correlations. Thus, for the imine structures of **4**, **6-8**, **10**, **12-18**, and **84**, pretty good linear relationships were obtained between the length of the OH bond and the distances O···N (r = 0.941) and H···N (r = 0.967) (Figure 15).

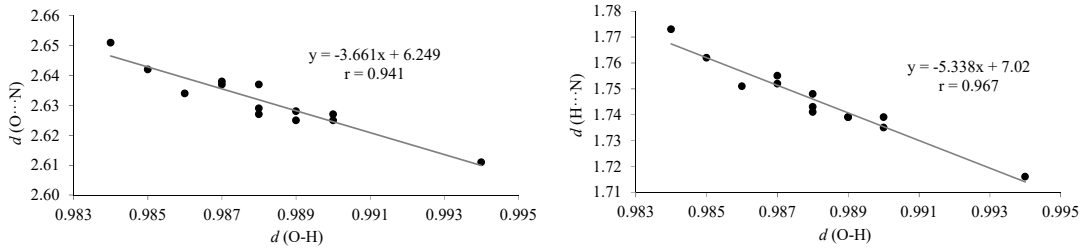

Figure 15. Linear plots involving bond distances in imines **4**, **6-8**, **10**, **12-18**, and **84**.

Also, for the enamine structures of **34**, **36-38**, **40**, **42-48**, and **38S** (enamine form of **84**) similar linear representations could be obtained between the length of the NH bond and the distances N···O (r = 0.959) and H···O (r = 0.989) (Figure 16).

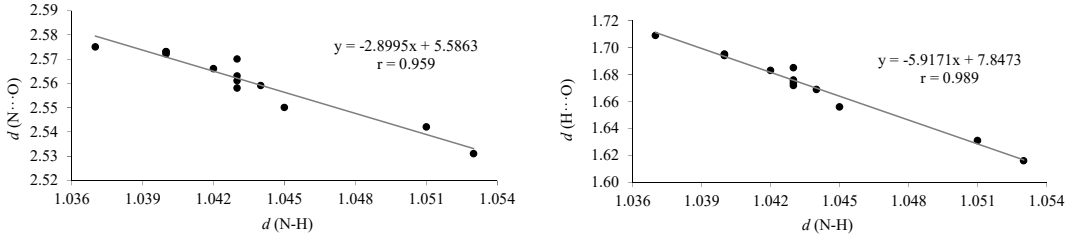

Figure 16. Linear plots involving bond distances in enamines **34**, **36-38**, **40**, **42-48**, and **38S**.

Figures 15 and 16 show that the longer the length of the OH or NH bond, the stronger the hydrogen bridge bond is, which translates into shorter distances O···N, H···O, and H···N. In addition, for imines **4**, **6-8**, **10**, **12-18**, and **84** there exists another correlation between Hammett's parameters (σ_{OH}) with distances H···N ($d_{H\cdots N} = -0.037\sigma_{OH} + 1.754$; r = 0.884, Fig. 12S), O···N ($d_{O\cdots N} = -0.026\sigma_{OH} + 2.637$; r = 0.893, Fig. 13S), and O-H ($d_{O\text{-}H} = 0.066\sigma_{OH} + 0.9866$; r = 0.875, Fig. 17) showing that the electron-attracting groups intensify the strength of hydrogen bonding, which parallels with shorter distances between the hydroxy and nitrogen atoms. These linear relationships unveil how the electronic effect of the substituents modulates the geometry, and accordingly the strength of the hydrogen bonds. Surprisingly, such representations for enamine structures **34**, **40**, **42**, **44**, **45**, **47**, and **48** (as function of σ_{OH}) lead to poor correlations.

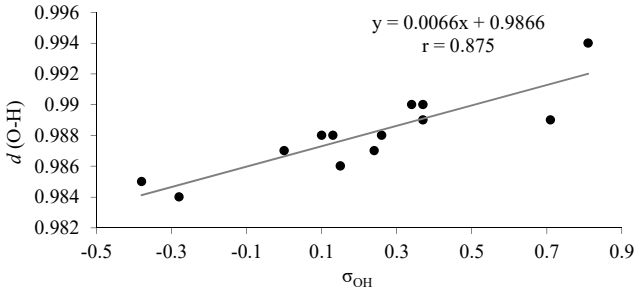

Figure 17. Linear plot between d(O-H) distances and σ_{OH} values for imines **4**, **6-8**, **10**, **12-18** and **84**.

CONCLUSIONS

Through this comprehensive study, we have shown that tautomeric preferences for imine and enamine structures can be controlled by a judicious choice of substituents. Using as model Schiff bases derived from salicylaldehydes and TRIS, the solid state is invariably composed of an enamine structure, whereas

there is a rapid equilibrium in solution between imine and enamine tautomers. This balance is governed, among other factors, by the electronic effect of the substituents present in the salicylaldehyde ring. For the first time it was possible to quantify the influence of that electronic effect on the tautomeric equilibrium through a linear free energy relationship (LFER): log $K_T = \rho\sigma_{ef}$, where $\sigma_{ef} = \sigma_{para}^{X} - \sigma_{meta}^{X}$. When $\sigma_{ef} < 0$, the Schiff base adopts an imine structure, and conversely an enamine form if $\sigma_{ef} > 0$. The parameter σ_{ef} fundamentally measures the mesomeric effect of the substituents on the tautomeric system. The scope and limitations of these predictions have been rationalized in detail, which can be extended to other Schiff bases described in the literature or hitherto unknown. Accordingly, these results allow the *de novo* design of novel salicylimines in which the predominant or exclusive structure can be fine-tuned by the electronic character of the substituents, thereby modifying the reactivity and physical properties of the compound in question, as either imine or enamine motifs are present for instance in materials and drugs.

Good to excellent correlations have been obtained for the chemical shifts of the OH/NH protons and the iminic (C=N), enamine (NC=) or phenolic (C2) carbons with the Hammett σ constants, showing the profound effect that substituents exert on the entire tautomeric system. The free activation energies of the imine → enamine tautomerization are very small ($\Delta G^{\ddagger} < 5$ kcal/mol, in DMSO), whereas the reversed path proceeds generally with negative values ($\Delta G^{\ddagger} < 0$ kcal/mol, in DMSO).

All imines/enamines exhibit a strong intramolecular hydrogen bridge (9-11 kcal/mol, in DMSO), whose analysis agrees with the RAHB model. Moreover, good linear correlations could be obtained between some structural parameters of the hydrogen bridge and Hammett's σ-constants. In addition, the sum of the HOMA delocalization indices of the pseudo-heterocyclic ring, generated by hydrogen bonding in the imine (HOMA ~ 0.35) and enamine (HOMA ~ 0.65) structures, remains approximately constant ($\Sigma_{HOMA} \sim 1.0$), indicating that when an imine converts into enamine, the electron delocalization lost by the iminic moiety is automatically gained by rapid equilibration with the enamine form. Needless to say, the hydrogen bond accounts for the existence of delocalization in the pseudo-ring; its absence leads to essentially null HOMA indices.

EXPERIMENTAL SECTION

General. Melting points were determined on Gallenkamp and Electrothermal IA 9000 apparatuses and are uncorrected. FT-IR spectra were recorded in the range of 4000-600 cm^{-1} on a THERMO spectrophotometer. Solid samples were recorded on KBr (Merck) pellets. NMR spectra were recorded on a Bruker 400 AC/PC instrument, in DMSO-d_6. Assignments were confirmed by homo- and hetero-nuclear double resonance, isotopic exchange after addition of D_2O, and DEPT (distortionless enhancement by polarization transfer) experiments. All *J* values are given in hertz. Microanalyses were determined on a Leco CHNS-932 analyzer.

Computational Details. The computational DFT study has been performed using the M06-2X[74] hybrid density functional in conjunction with the 6-311++G(d,p) basis set[75] as implemented in the Gaussian09 package.[76] The M06-2X method was chosen on the basis of previous studies showing its accuracy in estimating conformational energies related to non-covalent interactions.[77] In all cases, frequency

calculations were also carried out to confirm the existence of true stationary points on the potential energy surface. All thermal corrections were calculated at the standard values of 1 atm at 298.15 K. Solvent effects were modeled through the method of density-based, self-consistent reaction field (SCRF) theory of bulk electrostatics, namely, the solvation model density (SMD) method[78] as implemented in the Gaussian09 suite of programs. This solvation method accounts for long-range electrostatic polarization (bulk solvent)[79] as well as for short-range effects associated with cavitation, dispersion, and solvent structural effects.[80]

Synthesis of Starting Materials. Aldehydes **6S**, **11S**, and **13S** were synthesized. By iodination with iodine monochloride, salicylaldehyde **6S** was obtained in high yield (85%),[81] whereas the nitro derivative **11S** was prepared by demethylation of the precursor 2-methoxy-4-nitrobenzaldehyde with boron tribromide in dichloromethane (70%).[82] Finally, treatment of 3-chlorophenol with two moles of ethylmagnesium chloride and subsequent formylation with paraformaldehyde produced the 4-chloroderivative **13S** (69%) (Scheme 5S).[83]

5-Iodosalicylaldehyde (6S):[81] A 1*M* solution of iodine monochloride in dichloromethane (100 mL, 0.10 mol) was added to a solution of salicylaldehyde (10.7 mL, 0.10 mol) in dichloromethane (37 mL) at 0 °C. The resulting solution was heated to room temperature and allowed to stir overnight. The colored solution was treated with a saturated aqueous solution of Na_2SO_3 (25 mL) and the organic phase was separated, washed with water, dried with $MgSO_4$, filtered and concentrated to dryness, yielding a yellowish solid (21.12 g, 85%).

4-Nitrosalicylaldehyde (11S):[82] To a solution of 2-methoxy-4-nitrobenzaldehyde (0.5 g, 2.8 mmol) in anhydrous dichloromethane (4.3 mL) and under an inert atmosphere, a 1*M* solution of BBr_3 in CH_2Cl_2 (6.11 mL, 6.1 mmol) was added at 0 °C. After 24 hours of stirring at room temperature, the reaction flask was placed in an ice-water bath and 1*N* HCl (12.0 mL) and water (17 mL) were added. The aqueous phase was extracted with CH_2Cl_2 (3 x 10 mL) and the resulting organic phase was washed with a saturated NaCl solution (2 x 15 mL). After drying the organic phase with anhydrous $MgSO_4$, the solvent was removed (0.32 g, 70%).

4-Chlorosalicylaldehyde (13S):[83] To a solution of 3-chlorophenol (13.0 g, 0.10 mol) in toluene (100 mL) at 10 °C was added dropwise a 2*M* solution of ethylmagnesium chloride in ethyl ether (50 mL). The ether was removed under reduced pressure and the reaction mixture was cooled to room temperature, after which paraformaldehyde (7.5 g) was added. The mixture was heated at 70 °C for 18 hours, cooled to 10 °C, and a concentrated HCl solution (10 mL) in 50 g of ice was added followed by 200 mL of hexane. The organic phase was separated and washed twice with 50 mL of water, dried with anhydrous $MgSO_4$ and the solvent was removed (11.1 g, 69%).

Synthesis of Schiff bases. General synthetic procedure. To a solution of α,α,α-tris (hydroxymethyl)-methylamine (2.0 g, 16.5 mmol) in water (16 mL), a suitable aromatic aldehyde solution (16.5 mmol) in methanol (5 mL) was slowly added. When the title compound did not precipitate, the mixture was evaporated under vacuum and gave rise to a solid on standing or on cooling. The resulting product was

collected by filtration, washed successively with cold water, ethanol, and diethyl ether, and recrystallized from ethanol or methanol.

(*Z*)-6-({[1,3-Dihydroxy-2-(hydroxymethyl)propan-2-yl]amino}methylene)-4-nitrocyclohexa-2,4-dienone (34): (3.79 g, 85%); m.p. 232-233 ºC; IR (KBr) $\bar{\nu}_{max}$/cm^{-1} 3500-3100 (OH), 1651 (C=O), 1613 (C=C). ^{1}H NMR (400 MHz, DMSO-d_6) δ 14.33 (1H, d, $J_{NH,CH}$ = 8.8 Hz, NH), 8.74 (1H, d, $J_{CH,NH}$ = 8.8 Hz, CH=), 8.55 (1H, d, J = 2.8 Hz, H-arom), 8.00 (1H, dd, J = 3.2 Hz, J = 9.6 Hz, H-arom), 6.51 (1H, d, J = 9.6 Hz, H-arom), 5.27 (3H, s, OH), 3.67 (6H, s, CH_2). ^{13}C NMR (100 MHz, DMSO-d_6): 180.2 (C=O), 166.6 (*C*H=C), 134.4, 133.3, 129.9, 124.1, 113.5 (C-arom), 66.9 (C-N), 60.6 (3C, CH_2). Anal. calcd. for $C_{11}H_{14}N_2O_6 \cdot H_2O$ (288.25): C, 45.83, H, 5.59, N, 9.72. Found: C, 45.53; H, 5.74, N, 9.66. See reference 40e for crystal structure, described as a hydrate.

(*Z*)-6-({[1,3-Dihydroxy-2-(hydroxymethyl)propan-2-yl]amino}methylene)-4-methoxycarbonylcyclohexa-2,4-dienone (35): (2.34 g, 50%); m.p. 200-201 ºC; IR (KBr) $\bar{\nu}_{max}$/cm^{-1} 3500-3100 (OH), 1701 (C=O ester), 1635 (C=O). ^{1}H NMR (400 MHz, DMSO-d_6) δ 14.78 (1H, d, $J_{NH,CH}$ = 9.2 Hz, NH), 8.60 (1H, d, $J_{CH,NH}$ = 9.2 Hz, CH=), 8.09 (1H, s, H-arom), 7.74 (1H, ddd, J = 1.2 Hz, J = 2.0 Hz, J = 9.2 Hz, H-arom), 6.57 (1H, d, J = 9.2 Hz, H-arom), 5.04 (3H, t, J = 4.8 Hz, OH), 3.78 (3H, s, CH_3), 3.64 (6H, d, J = 4.8 Hz, CH_2). ^{13}C NMR (100 MHz, DMSO-d_6): 176.7 (C=O), 166.4 (C=O ester), 165.6 (*C*H=C), 138.1, 134.9, 122.4, 115.5, 114.3 (C-arom), 66.7 (C-N), 61.0 (3C, CH_2), 51.9 (CH_3). Anal. calcd. for $C_{13}H_{17}NO_6$ (283.28): C, 55.12; H, 6.05; N, 4.94. Found: C, 55.01; H, 6.24, N, 4.60.

(*Z*)-6-({[1,3-Dihydroxy-2-(hydroxymethyl)propan-2-yl]amino}methylene)-4-fluorocyclohexa-2,4-dienone (36): (2.89 g, 72%); m.p. 115-116 ºC; IR (KBr) $\bar{\nu}_{max}$/cm^{-1} 3400-3200 (OH), 1644 (C=N), 1537, 1495 (C=C). ^{1}H NMR (400 MHz, DMSO-d_6) δ 14.34 (1H, s, OH), 8.56 (1H, s, CH=N), 7.34 (1H, dd, J = 3.2 Hz, J = 8.8 Hz, H-arom), 7.16 (1H, dt, J = 3.2 Hz, J = 8.8 Hz, H-arom), 6.80 (1H, dd, J = 4.4 Hz, J = 9.2 Hz, H-arom), 4.76 (3H, t, J = 5.2 Hz, OH), 3.60 (6H, d, J = 4.8 Hz, CH_2). ^{13}C NMR (100 MHz, DMSO-d_6): 164.1 (d, J = 2.7 Hz, C=N), 159.5, 155.6, 153.3, 119.8 (d, J = 23.3 Hz), 118.8 (d, J = 7.4 Hz), 117.2 (d, J = 22.9 Hz) (C-arom), 67.9 (C-N), 61.7 (3C, CH_2). Anal. calcd. for $C_{11}H_{14}FNO_4$ (243.23): C, 54.32, H, 5.80, N, 5.76. Found: C, 54.16; H, 5.85, N, 5.68.

(*Z*)-6-({[1,3-Dihydroxy-2-(hydroxymethyl)propan-2-yl]amino}methylene)-4-chlorocyclohexa-2,4-dienone (37): (2.53 g, 59%); m.p. 143-145 ºC; IR (KBr) $\bar{\nu}_{max}$/cm^{-1} 3300-3100 (OH), 1640 (C=N), 1521, 1489 (C=C). ^{1}H NMR (400 MHz, DMSO-d_6) δ 14.70 (1H, s, OH-arom), 8.54 (1H, s, CH=N), 7.52 (1H, d, J = 2.8 Hz, H-arom), 7.28 (1H, dd, J = 2.6 Hz, J = 9.0 Hz, H-arom), 6.77 (1H, d, J = 8.8 Hz, H-arom), 4.83 (3H, t, J = 5.0 Hz, OH), 3.62 (6H, d, J = 4.8 Hz, CH_2). ^{13}C NMR (100 MHz, DMSO-d_6): 164.4 (C-arom), 164.1 (C=N), 132.9, 131.6, 120.6, 120.0, 119.2 (C-arom), 67.6 (C-N), 61.5 (3C, CH_2). Anal. calcd. for $C_{11}H_{14}ClNO_4$ (259.69): C, 50.88; H, 5.43; N, 5.39. Found: C, 50.97; H, 5.44; N, 5.38.

(*Z*)-6-({[1,3-Dihydroxy-2-(hydroxymethyl)propan-2-yl]amino}methylene)-4-bromocyclohexa-2,4-dienone (38): (2.81 g, 56%); m.p. 151-152 ºC; IR (KBr) $\bar{\nu}_{max}$/cm^{-1} 3300-3100 (OH), 1638 (C=N), 1600 (C=C). ^{1}H NMR (400 MHz, DMSO-d_6) δ 14.72 (1H, bs, OH), 8.54 (1H, s, CH=N), 7.63 (1H, d, J = 2.8 Hz, H-arom), 7.38 (1H, dd, J = 2.6 Hz, J = 9.0 Hz, H-arom), 6.71 (1H, d, J = 8.8 Hz, H-arom), 4.82 (3H,

t, J = 5.0 Hz, OH), 3.62 (6H, d, J = 4.8 Hz, CH_2). ^{13}C NMR (100 MHz, DMSO-d_6): 165.2 (C-arom), 164.1 (C=N), 135.7, 134.6, 121.3, 119.8, 107.0 (C-arom), 67.5 (C-N), 61.6 (3C, CH_2). Anal. calcd. for $C_{11}H_{14}BrNO_4$ (304.14): C, 43.44, H, 4.64, N, 4.61. Found: C, 43.41; H, 4.86, N, 4.63.

(*Z*)-6-({[1,3-Dihydroxy-2-(hydroxymethyl)propan-2-yl]amino}methylene)-4-iodocyclohexa-2,4-dienone (39): (5.39 g, 93%); m.p. 177-178 ºC; IR (KBr) $\bar{\nu}_{max}$/cm^{-1} 3400-3200 (OH), 1636 (C=N), 1593, 1516 (C=C). ^{1}H NMR (400 MHz, DMSO-d_6) δ 14.69 (1H, s, OH), 8.51 (1H, s, CH=N), 7.76 (1H, s, H-arom), 7.50 (1H, d, J = 8.8 Hz, H-arom), 6.58 (1H, d, J = 8.8 Hz, H-arom), 4.81 (3H, s, OH), 3.60 (6H, d, J = 4.4 Hz, CH_2). ^{13}C NMR (100 MHz, DMSO-d_6): 165.9 (C-arom), 164.0 (C=N), 141.2, 140.8, 121.8, 120.7, 76.9 (C-arom), 67.4 (C-N), 61.5 (3C, CH_2). Anal. calcd. for $C_{11}H_{14}INO_4$ (351.14): C, 37.63, H, 4.02, N, 3.99. Found: C, 37.57; H, 4.09, N, 4.06.

(*Z*)-6-({[1,3-Dihydroxy-2-(hydroxymethyl)propan-2-yl]amino}methylene)cyclohexa-2,4-dienone (40): (3.12 g, 84%); m.p. 161-163ºC; IR (KBr) $\bar{\nu}_{max}$/cm^{-1} 3300-3100 (OH), 1636 (C=O), 1607, 1534, 1484 (C=C); ^{1}H-NMR (400 MHz, DMSO-d_6) δ 14.53 (1H, s.a, OH-arom), 8.56 (1H, s, CH=N), 7.41 (1H, dd, J = 1.8 Hz, J = 7.8 Hz, H-Arom), 7.27 (1H, m, H-Arom), 6.79 (2H, m, H-Arom), 4.74 (3H, t, J = 5.2 Hz, OH), 3.61 (6H, d, J = 5.2 Hz, CH_2). ^{13}C-NMR (100 MHz, DMSO-d_6): 164.9 (C-arom), 163.7 (C=N), 132.8, 132.6, 119.0, 117.8, 117.6 (C-arom), 67.5 (C-N), 61.8 (3C, CH_2). Anal. calcd. for $C_{11}H_{15}NO_4$ (225.24): C, 58.66, H, 6.71, N, 6.22. Found: C, 58.57; H, 6.87, N, 6.27.

(*Z*)-6-({[1,3-Dihydroxy-2-(hydroxymethyl)propan-2-yl]amino}methylene)-4-methylcyclohexa-2,4-dienone (41): (2.41 g, 61%); m.p. 157-158 ºC; IR (KBr) $\bar{\nu}_{max}$/cm^{-1} 3500-3200 (OH), 1657 (C=N), 1620, 1529 (C=C). ^{1}H NMR (400 MHz, DMSO-d_6) δ 14.14 (1H, s, OH), 8.51 (1H, s, CH=N), 7.21 (1H, d, J = 2.0 Hz, H-arom), 7.10 (1H, dd, J = 2.0 Hz, J = 8.4 Hz, H-arom), 6.70 (1H, d, J = 8.4 Hz, H-arom), 4.70 (3H, t, J = 5.4 Hz, OH), 3.60 (6H, d, J = 5.2 Hz, CH_2), 2.23 (3H, s, CH_3). ^{13}C NMR (100 MHz, DMSO-d_6): 164.8 (C=N), 160.6, 133.3, 132.3, 126.4, 118.8, 117.3 (C-arom), 67.6 (C-N), 61.9 (3C, CH_2), 20.4 (CH_3). Anal. calcd. for $C_{12}H_{17}NO_4$ (239.27): C, 60.24, H, 7.16, N, 5.85. Found: C, 60.01; H, 7.19, N, 5.82.

(*Z*)-6-({[1,3-Dihydroxy-2-(hydroxymethyl)propan-2-yl]amino}methylene)-4-methoxycyclohexa-2,4-dienone (42): (1.81 g, 43%); m.p. 68-69 ºC; IR (KBr) $\bar{\nu}_{max}$/cm^{-1} 3500-3200 (OH), 1638 (C=N), 1536, 1503, 1464 (C=C). ^{1}H NMR (400 MHz, DMSO-d_6) δ 13.83 (1H, s, OH), 8.56 (1H, s, CH=N), 7.04 (1H, d, J = 3.2 Hz, H-arom), 6.92 (1H, dd, J = 3.2 Hz, J = 8.8 Hz, H-arom), 6.76 (1H, d, J = 8.8 Hz, H-arom), 4.71 (3H, s, OH), 3.72 (3H, s, CH_3), 3.62 (6H, d, J = 4.0 Hz, CH_2). ^{13}C NMR (100 MHz, DMSO-d_6): 164.7 (C=N), 156.6, 151.4, 120.0, 118.9, 118.1, 115.3 (C-arom), 67.74 (C-N), 61.90 (3C, CH_2), 55.99 (CH_3). Anal. calcd. for $C_{12}H_{17}NO_5$·(255.27): C, 56.46; H, 6.71; N, 5.49. Found: C, 56.59; H, 6.52, N, 5.40.

(*Z*)-6-({[1,3-Dihydroxy-2-(hydroxymethyl)propan-2-yl]amino}methylene)-4-hydroxycyclohexa-2,4-dienone (43): (1.43 g, 36%); m.p. 160-161 ºC; IR (KBr) $\bar{\nu}_{max}$/cm^{-1} 3500-3100 (OH), 1646 (C=N), 1533 (C=C). ^{1}H NMR (400 MHz, DMSO-d_6) δ 13.51 (1H, s, OH), 8.47 (1H, s, CH=N), 6.79 (1H, d, J = 3.2 Hz, H-arom), 6.75 (1H, dd, J = 3.2 Hz, J = 8.8 Hz, H-arom), 6.66 (1H, d, J = 8.8 Hz, H-arom), 4.70 (3H,

s, OH), 3.60 (6H, s, CH_2). ^{13}C NMR (100 MHz, DMSO-d_6): 164.6 (C=N), 154.5, 149.3, 120.0, 119.3, 117.4, 117.2 (C-arom), 67.8 (C-N), 62.0 (3C, CH_2). Anal. calcd. for $C_{11}H_{15}NO_5$ (241.24): C, 54.77; H, 6.27; N, 5.81. Found: C, 54.39; H, 6.17, N, 5.68.

(*Z*)-6-({[1,3-Dihydroxy-2-(hydroxymethyl)propan-2-yl]amino}methylene)-3-nitrocyclohexa-2,4-dienone (44): (2.45 g, 55%); m.p. 108-109 ºC; IR (KBr) $\bar{\nu}_{max}/cm^{-1}$ 3400-3100 (OH), 1648 (C=N), 1554, 1467 (C=C). ^1H NMR (400 MHz, DMSO-d_6) δ 15.32 (1H, d, $J_{NH,CH}$ = 5.6 Hz, NH), 8.47 (1H, d, $J_{CH,NH}$ = 4.8 Hz, CH=), 7.70 (1H, d, J = 8.8 Hz, H-arom), 7.38 (2H, m, H-arom), 4.99 (3H, s, OH), 3.64 (6H, d, J = 3.2 Hz, CH_2). ^{13}C NMR (100 MHz, DMSO-d_6): 168.6 (C-arom), 164.9 (C=N), 151.1, 134.8, 121.9, 114.2, 109.1 (C-arom), 67.8 (C-N), 61.2 (3C, CH_2). Anal. calcd. for $C_{11}H_{14}N_2O_6$ (270.24): C, 48.89; H, 5.22; N, 10.37. Found: C, 48.74; H, 5.33; N, 10.19.

(*Z*)-6-({[1,3-Dihydroxy-2-(hydroxymethyl)propan-2-yl]amino}methylene)-3-fluorocyclohexa-2,4-dienone (45): (3.37 g, 84%); m.p. 180-181 ºC; IR (KBr) $\bar{\nu}_{max}/cm^{-1}$ 3300-3100 (OH), 1633 (C=O), 1533 (C=C). ^1H NMR (400 MHz, DMSO-d_6) δ 14.77 (1H, d, $J_{NH,CH}$ = 6.4 Hz, NH), 8.43 (1H, d, $J_{CH,NH}$ = 6.0 Hz, CH=), 7.39 (1H, t, J = 8.0 Hz, H-arom), 6.34 (2H, m, H-arom), 5.01 (3H, t, J = 5.2 Hz, OH), 3.60 (6H, d, J = 4.8 Hz, CH_2). ^{13}C NMR (100 MHz, DMSO-d_6): 174.1 (d, J = 14.5 Hz, C=O), 167.4 (d, J = 250.9 Hz, C-F), 164.0 (*C*H=C), 136.4 (d, J = 13.5 Hz), 114.3, 105.8 (d, J = 17.3 Hz), 103.2 (d, J = 24.3 Hz) (C-arom), 66.3 (C-N), 61.2 (3C, CH_2). Anal. calcd. for $C_{11}H_{14}FNO_4$ (243.23): C, 54.32, H, 5.80, N, 5.76. Found: C, 54.08; H, 5.69, N, 5.71.

(*Z*)-6-({[1,3-Dihydroxy-2-(hydroxymethyl)propan-2-yl]amino}methylene)-3-chlorocyclohexa-2,4-dienone (46): (3.09 g, 72%); m.p. 360 ºC (desc.); IR (KBr) $\bar{\nu}_{max}/cm^{-1}$ 3500-3100 (OH), 1647 (C=O), 1592 (C=C). ^1H NMR (400 MHz, DMSO-d_6) δ 14.85 (1H, s, NH), 8.48 (1H, s, CH=), 7.37 (1H, d, J = 8.4 Hz, H-arom), 6.66 (1H, d, J = 2.0 Hz, H-arom), 6.55 (1H, dd, J = 2.0 Hz, J = 8.4 Hz, H-arom), 4.98 (3H, s, OH), 3.61 (6H, s, CH_2). ^{13}C NMR (100 MHz, DMSO-d_6): 171.2 (C=O), 164.4 (*C*H=C), 139.5, 135.2, 120.0, 115.9, 115.0 (C-arom), 66.7 (C-N), 61.2 (3C, CH_2). Anal. calcd. for $C_{11}H_{14}ClNO_4$ (259.69): C, 50.88, H, 5.43, N, 5.39. Found: C, 50.79; H, 5.41, N, 5.45.

(*Z*)-6-({[1,3-Dihydroxy-2-(hydroxymethyl)propan-2-yl]amino}methylene)-3-bromocyclohexa-2,4-dienone (47): (4.57 g, 91%); m.p. 116-117 ºC; IR (KBr) $\bar{\nu}_{max}/cm^{-1}$ 3500-3100 (OH), 1641 (C=O), 1596 (C=C). ^1H NMR (400 MHz, DMSO-d_6) δ 14.81 (1H, s, NH), 8.47 (1H, s, CH=), 7.29 (1H, d, J = 8.4 Hz, H-arom), 6.82 (1H, d, J = 2.0 Hz, H-arom), 6.98 (1H, dd, J = 1.6 Hz, J = 8.4 Hz, H-arom), 4.97 (3H, t, J = 5.0 Hz, OH), 3.60 (6H, d, J = 5.2 Hz, CH_2). ^{13}C NMR (100 MHz, DMSO-d_6): 171.3 (C=O), 164.6 (*C*H=C), 135.3, 128.9, 123.3, 117.7, 116.0 (C-arom), 66.8 (C-N), 61.2 (3C, CH_2). Anal. calcd. for $C_{11}H_{14}BrNO_4$ (304.14): C, 43.44, H, 4.64, N, 4.61. Found: C, 43.54; H, 4.74, N, 4.46.

(*Z*)-6-({[1,3-Dihydroxy-2-(hydroxymethyl)propan-2-yl]amino}methylene)-3-methoxycyclohexa-2,4-dienone (48): (2.11 g, 50%); m.p. 156-157 ºC; IR (KBr) $\bar{\nu}_{max}/cm^{-1}$ 3300-3100 (OH), 1632 (C=O), 1612 (C=C). ^1H NMR (400 MHz, DMSO-d_6) δ 14.27 (1H, d, $J_{NH,CH}$ = 6.0 Hz, NH), 8.27 (1H, d, $J_{CH,NH}$ = 5.6 Hz, CH=), 7.16 (1H, d, J = 8.8 Hz, H-arom), 6.11 (1H, d, J = 8.8 Hz, H-arom), 6.05 (1H, s, H-arom), 4.93 (3H, s, OH), 3.71 (3H, s, OCH_3), 3.60 (6H, s, CH_2). ^{13}C NMR (100 MHz, DMSO-d_6): 174.2 (C=O), 165.3

(C-arom), 162.5 (*C*H=C), 134.9, 111.5, 105.3, 102.3 (C-arom), 65.6 (C-N), 61.5 (3C, CH_2), 55.4 (OCH_3). Anal. calcd. for $C_{12}H_{17}NO_5$ (255.27): C, 56.46, H, 6.71, N, 5.49. Found: C, 56.29; H, 6.58, N, 5.49.

(*Z*)-6-({[1,3-Dihydroxy-2-(hydroxymethyl)propan-2-yl]amino}methylene)-3-diethylaminocyclohexa-2,4-dienone (49): (3.42 g, 70%); m.p. 180-181 ºC; IR (KBr) $\bar{\nu}_{max}$/cm^{-1} 3500-3300 (OH), 1630 (C=O), 1600 (C=C). ^{1}H NMR (400 MHz, DMSO-d_6) δ 13.88 (1H, bs, NH), 8.08 (1H, s, CH=), 6.99 (1H, d, J = 9.2 Hz, H-arom), 6.05 (1H, d, J = 8.8 Hz, H-arom), 5.66 (1H, d, J = 1.6 Hz, H-arom) 4.94 (3H, s, OH), 3.58 (6H, s, CH_2), 3.32 (4H, c, J = 7.0 Hz, N-CH_2), 1.09 (6H, t, J = 7.0 Hz, CH_3). ^{13}C NMR (100 MHz, DMSO-d_6): 173.3 (C=O), 160.7 (*C*H=C), 152.7, 134.9, 108.5, 102.6, 99.1 (C-arom), 65.0 (C-N), 61.7 (3C, CH_2), 44.3 (2C, N-CH_2), 13.2 (2C, CH_3). Anal. calcd. for $C_{15}H_{24}N_2O_4$ (296.36): C, 60.79, H, 8.16, N, 9.45. Found: C, 60.57, H, 8.01, N, 9.35.

(*Z*)-6-({[1,3-Dihydroxy-2-(hydroxymethyl)propan-2-yl]amino}methylene)-2-ethoxycyclohexa-2,4-dienone (50): (3.87 g, 87%); m.p. 165-167ºC; IR (KBr) $\bar{\nu}_{max}$/cm^{-1} 3400-3100 (OH), 1629 (C=N), 1608, 1503 (C=C). ^{1}H NMR (400 MHz, DMSO-d_6) δ 14.75 (1H, d, $J_{NH,CH}$ = 4.4 Hz, NH), 8.48 (1H, d, $J_{CH,NH}$ = 4.8 Hz, CH=), 6.95 (1H, dd, J = 1.2 Hz, J = 8.0 Hz, H-arom), 6.89 (1H, dd, J = 1.4 Hz, J = 7.8 Hz, H-arom), 6.58 (1H, t, J = 7.8 Hz, H-arom), 4.81 (3H, t, J = 5.4 Hz, OH), 3.99 (2H, c, J = 7.1 Hz, CH_2), 3.61 (6H, d, J = 5.2 Hz, CH_2), 1.30 (3H, t, J = 7.0 Hz, CH_3). ^{13}C NMR (100 MHz, DMSO-d_6): 164.6 (C=N), 158.5, 148.9, 124.8, 117.9, 116.5, 115.5 (C-arom), 66.9 (C-N), 64.3 (CH_2), 61.6 (3C, CH_2), 15.4 (CH_3). Anal. calcd. for $C_{13}H_{19}NO_5$ (269.29): C, 57.98, H, 7.11, N, 5.20. Found: C, 57.80; H, 7.22, N, 5.27.

(*Z*)-6-({[1,3-Dihydroxy-2-(hydroxymethyl)propan-2-yl]amino}methylene)-2-methoxycyclohexa-2,4-dienone (51): (2.70 g, 64%); m.p. 182-183 ºC; IR (KBr) $\bar{\nu}_{max}$/cm^{-1} 3400-3100 (OH), 1643 (C=N), 1613, 1501 (C=C). ^{1}H NMR (400 MHz, DMSO-d_6) δ 14.68 (1H, d, $J_{NH,CH}$ = 4.0 Hz, NH), 8.47 (1H, d, $J_{CH,NH}$ = 3.2 Hz, CH=), 6.94 (1H, dd, J = 1.2 Hz, J = 8.0 Hz, H-arom), 6.89 (1H, dd, J = 1.6 Hz, J = 8.0 Hz, H-arom), 6.57 (1H, t, J = 8.0 Hz, H-arom), 4.85 (3H, t, J = 5.2 Hz, OH), 3.73 (3H, s, CH_3), 3.61 (6H, d, J = 4.8 Hz, CH_2). ^{13}C NMR (100 MHz, DMSO-d_6): 164.6 (C=N), 158.8, 150.1, 124.7, 117.6, 115.3, 114.8 (C-arom), 66.9 (C-N), 61.6 (3C, CH_2), 56.2 (CH_3). Anal. calcd. for $C_{12}H_{17}NO_5$ (255.27): C, 56.46; H, 6.71; N, 5.49. Found: C, 56.19; H, 6.79; N, 5.39.

(*Z*)-6-({[1,3-Dihydroxy-2-(hydroxymethyl)propan-2-yl]amino}methylene)-2-hydroxycyclohexa-2,4-dienone (52): (3.54 g, 89%); m.p. 144-145 ºC; IR (KBr) $\bar{\nu}_{max}$/cm^{-1} 3500-3100 (OH), 1640 (C=N), 1524, 1467 (C=C). ^{1}H NMR (400 MHz, DMSO-d_6) δ 14.42 (1H, bs, OH-arom), 8.42 (1H, s, CH=N), 6.78 (1H, dd, J = 8.0 Hz, J = 1.6 Hz, H-arom), 6.70 (1H, dd, J = 8.0 Hz, J = 1.6 Hz, H-arom), 6.36 (1H, t, J = 8.0 Hz, H-arom), 4.99 (3H, bs, OH), 3.64 (6H, s, CH_2). ^{13}C NMR (100 MHz, DMSO-d_6): 164.3 (C=N), 162.3, 148.6, 123.0, 115.3, 115.3, 114.0 (C-arom), 66.3 (C-N), 61.3 (3C, CH_2). Anal. calcd. for $C_{11}H_{15}NO_5$ (241.24): C, 54.77; H, 6.27; N, 5.81. Found: C, 54.89; H, 6.36; N, 5.68.

(*Z*)-6-({[1,3-Dihydroxy-2-(hydroxymethyl)propan-2-yl]amino}methylene)-5-methoxycyclohexa-2,4-dienone (53): (3.83 g, 91%); m.p. 176-177 ºC; IR (KBr) $\bar{\nu}_{max}$/cm^{-1} 3400-3100 (OH), 1631 (C=O), 1615 (C=C). ^{1}H NMR (400 MHz, DMSO-d_6) δ 15.22 (1H, d, $J_{NH,CH}$ = 6.4 Hz, NH), 8.76 (1H, d, $J_{CH,NH}$ = 6.4 Hz, CH=), 7.17 (1H, t, J = 8.0 Hz, H-arom), 6.23 (1H, d, J = 8.4 Hz, H-arom), 6.12 (1H, d, J = 8.0 Hz, H-

arom), 4.92 (3H, t, J = 5.2 Hz, OH), 3.78 (3H, s, OCH_3), 3.59 (6H, d, J = 5.2 Hz, CH_2). ^{13}C NMR (100 MHz, DMSO-d_6): 170.8 (C=O), 160.2 (C-arom), 159.3 (*C*H=C), 135.2, 113.2, 107.3, 96.4 (C-arom), 66.5 (C-N), 61.6 (3C, CH_2), 55.9 (OCH_3). Anal. calcd. for $C_{12}H_{17}NO_5$ (255.27): C, 56.46, H, 6.71, N, 5.49. Found: C, 56.44; H, 6.64, N, 5.44.

(*Z*)-6-({[1,3-Dihydroxy-2-(hydroxymethyl)propan-2-yl]amino}methylene)-3-hydroxy-5-methylcyclohexa-2,4-dienone (54): (0.76 g, 18%); m.p. 190-191 ºC; IR (KBr) $\bar{\nu}_{max}$/cm^{-1} 3500-3300 (OH), 1594 (C=O), 1567 (C=C). ^1H NMR (400 MHz, DMSO-d_6) δ 14.90 (1H, d, $J_{NH,CH}$ = 7.6 Hz, NH), 9.75 (1H, s, OH-arom), 8.39 (1H, d, $J_{CH,NH}$ = 7.6 Hz, CH=), 5.88 (1H, d, J = 2.0 Hz, H-arom), 5.77 (1H, d, J = 2.0 Hz, H-arom), 4.89 (3H, s, OH), 3.58 (6H, d, J = 4.0 Hz, CH_2), 2.22 (3H, s, CH_3). ^{13}C NMR (100 MHz, DMSO-d_6): 174.4 (C=O), 163.0 (C-arom), 158.4 (*C*H=C), 141.2, 109.0, 107.4, 102.2 (C-arom), 64.8 (C-N), 61.1 (3C, CH_2), 18.4 (CH_3). Anal. calcd. for $C_{12}H_{17}NO_5$ (255.27): C, 56.46, H, 6.71, N, 5.49. Found: C, 56.21, H, 6.85, N, 5.55.

(*Z*)-6-({[1,3-Dihydroxy-2-(hydroxymethyl)propan-2-yl]amino}methylene)-3,5-dimethoxycyclohexa-2,4-dienone (55): (3.62 g, 77%); m.p. 208-209 ºC; IR (KBr) $\bar{\nu}_{max}$/cm^{-1} 3300-3100 (OH), 1633 (C=O), 1610 (C=C). ^1H NMR (400 MHz, DMSO-d_6) δ 14.03 (1H, d, J = 12.0 Hz, NH), 8.47 (1H, d, J = 11.6 Hz, CH=), 5.57 (1H, d, J = 1.6 Hz, H-arom), 5.49 (1H, d, J = 1.6 Hz, H-arom), 5.05 (3H, t, J = 5.0 Hz, OH), 3.73 (3H, s, OCH_3), 3.68 (3H, s, OCH_3), 3.56 (6H, d, J = 5.2 Hz, CH_2). ^{13}C NMR (100 MHz, DMSO-d_6): 179.0 (C=O), 167.3, 161.4 (C-arom), 155.8 (*C*H=C), 102.1, 96.3, 86.3 (C-arom), 64.6 (C-N), 61.3 (3C, CH_2), 55.8, 55.4 (OCH_3). Anal. calcd. for $C_{13}H_{19}NO_6$ (285.29): C, 54.73, H, 6.71, N, 4.91. Found: C, 54.40; H, 6.76, N, 5.03.

(*Z*)-6-({[1,3-Dihydroxy-2-(hydroxymethyl)propan-2-yl]amino}methylene)-2,3-dihydroxycyclohexa-2,4-dienone (56): (2.63 g, 62%); m.p. 192-193 ºC; IR (KBr) $\bar{\nu}_{max}$/cm^{-1} 3450-3100 (OH), 1634 (C=N), 1554, 1512, 1466 (C=C). ^1H NMR (400 MHz, DMSO-d_6) δ 13.90 (1H, s, OH), 8.17 (1H, s, CH=N), 6.60 (1H, d, J = 9.2 Hz, H-arom), 6.00 (1H, d, J = 8.8 Hz, H-arom), 5.03 (3H, bs, OH), 3.61 (6H, s, CH_2). ^{13}C NMR (100 MHz, DMSO-d_6): 166.8 (C=O), 162.2 (*C*H=C), 147.9, 134.4, 124.3, 109.3, 106.4 (C-arom), 65.0 (C-N), 61.3 (3C, CH_2). Anal. calcd. for $C_{11}H_{15}NO_6$ (257.24): C, 51.36, H, 5.88, N, 5.44. Found: C, 51.25; H, 6.18, N, 5.38.

(*Z*)-6-({[1,3-Dihydroxy-2-(hydroxymethyl)propan-2-yl]amino}methylene)-2,4-difluorocyclohexa-2,4-dienone (57): (3.19 g, 74%); m.p. 169-170 ºC; IR (KBr) $\bar{\nu}_{max}$/cm^{-1} 3400-3200 (OH), 1645 (C=N), 1552, 1521, 1468 (C=C). ^1H NMR (400 MHz, DMSO-d_6) δ 14.83 (1H, s, OH), 8.50 (1H, s, CH=N), 7.26 (1H, m, H-arom), 7.09 (1H, m, H-arom), 5.03 (3H, s, OH), 3.62 (6H, d, J = 3.6 Hz, CH_2). ^{13}C NMR (100 MHz, DMSO-d_6): 164.1 (t, J = 3.0 Hz, C=N), 157.8 (d, J = 14.5 Hz), 153.0 (dd, J = 12.1 Hz, J = 245.6 Hz), 149.8 (dd, J = 10.7 Hz, J = 229.6 Hz), 116.0 (dd, J = 7.2 Hz, J = 10.0 Hz), 112.0 (dd, J = 4.1 Hz, J = 21.7 Hz), 109.1 (dd, J = 21.6 Hz, J = 28.7 Hz) (C-arom), 67.0 (C-N), 61.1 (3C, CH_2). Anal. calcd. for $C_{11}H_{13}F_2NO_4$ (261.22): C, 50.58, H, 5.02, N, 5.36. Found: C, 50.34; H, 5.00, N, 5.19.

(*Z*)-6-({[1,3-Dihydroxy-2-(hydroxymethyl)propan-2-yl]amino}methylene)-2,4-dichlorocyclohexa-2,4-dienone (58): (4.76 g, 98%); m.p. 218-220 ºC; IR (KBr) $\bar{\nu}_{max}$/cm^{-1} 3500-3100 (OH), 1642 (C=O),

1597, 1509 (C=C). ^{1}H NMR (400 MHz, DMSO-d_6) δ 14.80 (1H, d, $J_{NH,CH}$ = 11.6 Hz, NH), 8.52 (1H, d, $J_{CH,NH}$ = 11.6 Hz, CH=), 7.51 (1H, d, J = 2.8 Hz, H-arom), 7.45 (1H, d, J = 2.8 Hz, H-arom), 5.16 (3H, t, J = 5.2 Hz, OH), 3.63 (6H, d, J = 5.2 Hz, CH_2). ^{13}C NMR (100 MHz, DMSO-d_6): 168.3 (C=O), 164.6 (*C*H=C), 133.9, 131.7, 126.9, 115.8, 114.4 (C-arom), 66.6 (C-N), 60.8 (3C, CH_2). Anal. calcd. for $C_{11}H_{13}Cl_2NO_4$ (294.13): C, 44.92, H, 4.45, N, 4.76. Found: C, 44.96; H, 4.46, N, 4.76.

(*Z*)-6-({[1,3-Dihydroxy-2-(hydroxymethyl)propan-2-yl]amino}methylene)-2,4-dibromocyclohexa-2,4-dienone (59): (5.75 g, 91%); m.p. 236-237 ºC; IR (KBr) $\bar{\nu}_{max}$/cm^{-1} 3400-3100 (OH), 1640 (C=O), 1585 (C=C). ^{1}H NMR (400 MHz, DMSO-d_6) δ 14.77 (1H, d, $J_{NH,CH}$ = 11.6 Hz, NH), 8.49 (1H, d, $J_{CH,NH}$ = 12.0 Hz, CH=), 7.73 (1H, d, J = 2.8 Hz, H-arom), 7.61 (1H, d, J = 2.4 Hz, H-arom), 5.16 (3H, t, J = 5.0 Hz, OH), 3.63 (6H, d, J = 5.2 Hz, CH_2). ^{13}C NMR (100 MHz, DMSO-d_6): 169.1 (C=O), 164.6 (*C*H=C), 139.1, 135.7, 118.7, 116.4, 101.3 (C-arom), 66.6 (C-N), 60.8 (3C, CH_2). Anal. calcd. for $C_{11}H_{13}Br_2NO_4$ (383.03): C, 34.49, H, 3.42, N, 3.66. Found: C, 34.55; H, 3.35, N, 3.46.

(*Z*)-6-({[1,3-Dihydroxy-2-(hydroxymethyl)propan-2-yl]amino}methylene)-2,5-dinitrocyclohexa-2,4-dienone (60): (3.95 g, 76%); m.p. 221-223 ºC; IR (KBr) $\bar{\nu}_{max}$/cm^{-1} 3600-3100 (OH), 1645 (C=O), 1620 (C=C). ^{1}H NMR (400 MHz, DMSO-d_6) δ 13.84 (1H, d, $J_{NH,CH}$ = 14.4 Hz, NH), 8.94 (1H, d, $J_{CH,NH}$ = 14.8 Hz, CH=), 8.90 (1H, d, J = 3.2 Hz, H-arom), 8.76 (1H, d, J = 3.2 Hz, H-arom), 5.39 (3H, t, J = 5.2 Hz, OH), 3.68 (6H, d, J = 5.2 Hz, CH_2). ^{13}C NMR (100 MHz, DMSO-d_6): 170.5 (C=O), 167.4 (*C*H=C), 141.3, 137.9, 130.3, 127.4, 117.8 (C-arom), 67.9 (C-N), 60.2 (3C, CH_2). Anal. calcd. for $C_{11}H_{13}N_3O_8$ (315.24): C, 41.91, H, 4.16, N, 13.33. Found: C, 41.82; H, 4.18, N, 13.29.

(*Z*)-6-({[1,3-Dihydroxy-2-(hydroxymethyl)propan-2-yl]amino}methylene)-2-methoxy-4-nitrocyclohexa-2,4-dienone (61): (3.72 g, 75%); m.p. 221-222ºC; IR (KBr) $\bar{\nu}_{max}$/cm^{-1} 3500-3100 (OH), 1641 (C=O), 1608 (C=C). ^{1}H NMR (400 MHz, DMSO-d_6) δ 13.83 (1H, d, $J_{NH,CH}$ = 14.0 Hz, NH), 8.67 (1H, d, $J_{CH,NH}$ = 14.0 Hz, CH=), 8.27 (1H, d, J = 2.0 Hz, H-arom), 7.37 (1H, d, J = 2.0 Hz, H-arom), 5.25 (3H, s, OH), 3.77 (3H, s, CH_3), 3.65 (6H, d, J = 3.6 Hz, CH_2). ^{13}C NMR (100 MHz, DMSO-d_6): 173.7 (C=O), 166.2 (*C*H=C), 152.5, 132.2, 127.1, 111.7, 105.9 (C-arom), 66.7 (C-N), 60.6 (3C, CH_2), 56.0 (CH_3). Anal. calcd. for $C_{12}H_{16}N_2O_7$ (300.26): C, 48.00, H, 5.37, N, 9.33. Found: C, 47.81; H, 5.44, N, 9.26.

(*Z*)-6-({[1,3-Dihydroxy-2-(hydroxymethyl)propan-2-yl]amino}methylene)-4-bromo-2-methoxycyclohexa-2,4-dienone (62): (3.14 g, 57%); m.p. 195-186ºC; IR (KBr) $\bar{\nu}_{max}$/cm^{-1} 3400-3100 (OH), 1644 (C=N), 1598, 1504, 1459 (C=C). ^{1}H NMR (400 MHz, DMSO-d_6) δ 14.56 (1H, d, $J_{NH,CH}$ = 7.6 Hz, NH), 8.39 (1H, d, $J_{CH,NH}$ = 7.6 Hz, CH=), 7.14 (1H, d, J = 2.4 Hz, H-arom), 6.87 (1H, d, J = 2.4 Hz, H-arom), 4.95 (3H, s, OH), 3.73 (1H, s, CH_2), 3.61 (6H, d, J = 3.2 Hz, CH_2). ^{13}C NMR (100 MHz, DMSO-d_6): 163.5 (C=N), 162.6, 152.3, 126.3, 116.8, 116.7, 103.5 (C-arom), 66.5 (C-N), 61.3 (3C, CH_2), 56.3 (CH_3). Anal. calcd. for $C_{12}H_{16}BrNO_5$ (334.16): C, 43.13; H, 4.83; N, 4.19. Found: C, 43.08; H, 4.80; N, 4.17.

(*Z*)-6-({[1,3-Dihydroxy-2-(hydroxymethyl)propan-2-yl]amino}methylene)-2,4-dibromo-3-methoxycyclohexa-2,4-dienone (63): Following the general synthetic procedure from 0.67 g (5.5 mmol)

of α,α,α-tris (hydroxymethyl)methylamine (1.98 g, 87%); m.p. 225-226 ºC; IR (KBr) $\bar{\nu}_{max}$/cm^{-1} 3400-3100 (OH), 1641 (C=O), 1589, 1506 (C=C). ^{1}H NMR (400 MHz, DMSO-d_6) δ 14.41 (1H, d, $J_{NH,CH}$ = 12.8 Hz, NH), 8.46 (1H, d, $J_{CH,NH}$ = 12.8 Hz, CH=), 7.69 (1H, s, H-arom), 5.17 (3H, t, J = 5.2 Hz, OH), 3.79 (3H, s, OCH_3), 3.62 (6H, d, J = 5.2 Hz, CH_2). ^{13}C NMR (100 MHz, DMSO-d_6): 172.0 (C=O), 163.9 (*C*H=C), 159.5, 136.7, 113.7, 112.3, 98.7 (C-arom), 66.2 (C-N), 60.8 (3C, CH_2), 60.5 (OCH_3). Anal. calcd. for $C_{12}H_{15}Br_2NO_5$ (413.06): C, 34.89, H, 3.66, N, 3.39. Found: C, 34.98; H, 3.59, N, 3.39.

(*Z*)-1-({[1,3-dihydroxy-2-(hydroxymethyl)propan-2-yl]amino}methylene)naphthalen-2(1*H*)-one (65): (3.18 g, 70%); m.p. 160-162 ºC; IR (KBr) $\bar{\nu}_{max}$/cm^{-1} 3300-3100 (OH), 1636 (C=O), 1543, 1491 (C=C); ^{1}H-NMR (400 MHz, DMSO-d_6) δ 14.02 (1H, d, $J_{NH,CH}$ = 12.4 Hz, NH), 8.88 (1H, d, $J_{CH,NH}$ =12.6 Hz, CH), 7.93 (1H, d, J = 8.3 Hz, H-arom), 7.67 (1H, d, J = 9.3 Hz, H-arom), 7.59 (1H, d, J = 7.6 Hz, H-arom), 7.40 (1H, t, J = 7.4 Hz, H-arom), 7.15 (1H, t, J = 7.4 Hz, H-arom), 6.63 (1H, d, J = 9.4 Hz, H-arom), 5.12 (3H, t, J = 5.0 Hz, OH), 3.66 (6H, d, J = 4.9 Hz, CH_2). ^{13}C-NMR (100 MHz, DMSO-d_6): 179.8 (C=O), 156.2 (*C*H=C), 137.8, 135.3, 129.4, 128.4, 127.1, 125.4, 122.3, 118.5, 105.7 (C-arom), 65.0 (C-N), 61.3 (3C, CH_2). Anal. calcd. for $C_{15}H_{17}NO_4$ (275.30): C, 65.44, H, 6.22, N, 5.09. Found: C, 65.26; H, 6.21, N, 5.02.

AUTHOR INFORMATION

Corresponding Authors. *E-mails: rmarvaz@unex.es, palacios@unex.es.

ACKNOWLEDGEMENTS

This work was supported by the Junta de Extremadura and Fondo Europeo de Desarrollo Regional (Grant IB16167 and GR18015). The Research & Technological Innovation and Supercomputing Center of Extremadura (CénitS) is gratefully acknowledged for permitting the use of the supercomputer LUSITANIA II.

DEDICATION

This paper is dedicated to the memory of María Dolores Méndez.

REFERENCES

(1) a) Jeffrey, G. A. In *An Introduction to Hydrogen Bonding*; Truhlar, D. G., Ed.; Oxford University Press: New York; 1997; b) Jeffrey, G. A.; Saenger, W. *Hydrogen Bonding in Biological Structures*; Springer-Verlag: Berlin, 1991; c) Desiraju, G. R.; Steiner, T. *The weak hydrogen bond in structural chemistry and biology*, Oxford University Press, New York, 1999; d) Scheiner, S. *Hydrogen Bonding*, Oxford University Press, New York, 1997; e) Scheiner, S. *Intermolecular Interactions-From Van der Waals to Strongly Bound Complexes*; Wiley: New York, 1997.

(2) a) Desiraju, G. R. In *Crystal Engineering: The Design of Organic Solids*; Elsevier: Amsterdam, The Netherlands, 1989; b) Gerlt, J. A.; Kreevoy, M. M.; Cleland, W. W.; Frey, P. A. Understanding enzymic catalysis: the importance of short, strong hydrogen bonds. *Chem. Biol*. **1997**, *4*, 259-267; c) Perrin, C. L.; Nielson, J. B. "Strong" Hydrogen Bonds in Chemistry and Biology. *Annu.*

Rev. Phys. Chem. **1997**, *48*, 511-544; d) Desiraju, G. R. Hydrogen Bridges in Crystal Engineering: Interactions without Borders. *Acc. Chem. Res*. **2002**, *35*, 565-573; e) Meyer, E. A.; Castellano, R. K.; Diederich, F. Interactions with Aromatic Rings in Chemical and Biological Recognition. *Angew. Chem., Int. Ed*. **2003**, *42*, 1210-1250; f) Sobczyk, L.; Grabowski, S. J.; Krygowski, T. M. Interrelation between H-Bond and Pi-Electron Delocalization. *Chem. Rev*. **2005**, *105*, 3513-3560; g) Krygowski, T. M.; Szatylowicz, H. Interrelation between the Substituent Effects, π-Electron Delocalization and H-Bonding. *Trends Org. Chem*. **2006**, *11*, 37-53.

(3) For a review on tautomeric equilibria, see: Raczynska, E. D.; Kosinska, W.; Osmialowski, B.; Gawinecki, R. Tautomeric Equilibria in Relation to Pi-Electron Delocalization. *Chem. Rev*. **2005**, *105*, 3561-3612.

(4) For reviews, see: a) Steiner, T. The Hydrogen Bond in the Solid State. *Angew. Chem., Int. Ed*. **2002**, *41*, 49-76; b) Rozas, I. On the Nature of Hydrogen Bonds: an Overview on Computational Studies and a Word About Patterns. *Phys. Chem. Chem. Phys*. **2007**, *9*, 2782-2790; c) Grabowski, S. J. Theoretical studies of strong hydrogen bonds. *Annu. Rep. Prog. Chem., Sect. C: Phys. Chem*. **2006**, *102*, 131-165.

(5) Gilli, P.; Bertolasi, V.; Ferretti, V.; Gilli, G. Evidence for Resonance-assisted Hydrogen Bonding. 4. Covalent Nature of the Strong Homonuclear Hydrogen Bond. Study of the O-H--O System by Crystal Structure Correlation Methods. *J. Am. Chem. Soc*. **1994**, *116*, 909-915.

(6) a) Gilli, G.; Bellucci, F.; Ferretti, V.; Bertolasi, V. Evidence for Resonance-assisted Hydrogen Bonding from Crystal-structure Correlations on the Enol Form of the β-Diketone Fragment. *J. Am. Chem. Soc*. **1989**, *111*, 1023-1028; b) Bertolasi, V.; Gilli, P.; Ferretti, V.; Gilli, G. Evidence for Resonance-assisted Hydrogen Bonding. 2. Intercorrelation between Crystal Structure and Spectroscopic Parameters in Eight Intramolecularly Hydrogen Bonded 1,3-Diaryl-1,3-propanedione Enols. *J. Am. Chem. Soc.* **1991**, *113*, 4917-4925; c) Gilli, P.; Bertolasi, V.; In *The Chemistry of Enols*; Rappoport, Z. Ed.; Wiley, Chichester, 1990; p 713 (Chapter 13).

(7) a) Bertolasi, V.; Gilli, P.; Ferretti, V.; Gilli, G. Resonance-Assisted O-H ··· O Hydrogen Bonding: Its Role in the Crystalline Self-Recognition of β-Diketone Enols and its Structural and IR Characterization. *Chem. Eur. J*. **1996**, *2*, 925-934; b) Gilli, G.; Bertolasi, V.; Ferretti, V.; Gilli, P. Resonance-Assisted Hydrogen Bonding. III. Formation of Intermolecular Hydrogen-Bonded Chains in Crystals of β-Diketone Enols and its Relevance to Molecular Association. *Acta Crystallogr*. **1993**, *B49*, 564-576; c) Gilli, P.; Ferretti, V.; Bertolasi, V.; Gilli, G. In *Advances in Molecular Structure Research*; Hargittai, I., Hargittai, M., Eds.; JAI Press Inc.: Greenwich, CT, 1996; Vol. 2, p 67; d) Gilli, P.; Ferretti, V.; Gilli, G. In *Fundamental Principles of Molecular Modeling*; Gans, W., Amann, A., Boeyens, J. C. A., Eds.; Plenum Press: New York, 1996, pp 119-141; e) Gilli, P.; Bertolasi, V.; Preto, L.; Lyčka, A.; Gilli, G. The Nature of Solid-State N−H···O/O−H···N Tautomeric Competition in Resonant Systems. Intramolecular Proton Transfer in Low-Barrier Hydrogen Bonds Formed by the ···O=C−C=N−NH··· ⇄ ···HO−C=C−N=N··· Ketohydrazone−Azoenol System. A Variable-Temperature X-ray Crystallographic and DFT Computational Study. *J. Am. Chem. Soc*. **2002**, *124*, 13554-13567; f) Gilli, P.; Bertolasi, V.; Ferretti, V.; Gilli, G. Evidence for Intramolecular N−H···O Resonance-Assisted Hydrogen Bonding in β-Enaminones and Related Heterodienes. A Combined Crystal-Structural, IR and NMR Spectroscopic, and Quantum-Mechanical Investigation. *J. Am. Chem. Soc*. **2000**, *122*, 10405-10417; g) Bertolasi, V.; Ferretti, V.; Gilli, P.; Gilli, G.; Issa, Y. M.; Sherif, O. E. Intramolecular N–H ··· O Hydrogen Bonding Assisted by Resonance. Part 2. Intercorrelation between Structural and Spectroscopic Parameters for Five 1,3-Diketone Arylhydrazones Derived from Dibenzoylmethane. *J. Chem. Soc., Perkin Trans. 2* **1993**, 2223-2228; h) Bertolasi, V.; Nanni, L.; Gilli, G.; Ferretti, V.; Gilli, P.; Issa, Y. M.; Sherif, O. E. Intramolecular N-H...O=C Hydrogen-Bonding Assisted by Resonance. Inyercorrelation Between Structural and Spectroscopic Data for 6 Beta-Diketo-Arylhydrazones Derived from Benzoylacetone or Acetylacetone. *New. J. Chem*. **1994**, *18*, 251-261; i) Bertolasi, V.; Gilli, P.; Ferretti, V.; Gilli, G.; Vaughan, K. Interplay between Steric and Electronic Factors in Determining the Strength of Intramolecular Resonance-Assisted NH···O Hydrogen Bond in a Series of β-Ketoarylhydrazones. *New J. Chem*. **1999**, *23*, 1261-1267.

(8) a) Alkorta, I.; Elguero, J.; Mó, O.; Yañez, M.; del Bene, J. E. Do Coupling Constants and Chemical Shifts Provide Evidence for the Existence of Resonance-Assisted Hydrogen Bonds? *Mol. Phys*. **2004**, *102*, 2563-2574; b) Alkorta, I.; Elguero, J.; Mó, O.; Yáñez, M.; Del Bene, J. E. Are Resonance-Assisted Hydrogen Bonds 'Resonance Assisted'? A Theoretical NMR Study. *Chem. Phys. Lett.* **2005**, *411*, 411-415; c) Sanz, P.; Mó, O.; Yañez, M.; Elguero, J. Non-Resonance-Assisted Hydrogen Bonding in

Hydroxymethylene and Aminomethylene Cyclobutanones and Cyclobutenones and their Nitrogen Counterparts. *Chem. Phys. Chem*. **2007**, *8*, 1950-1958; d) Sanz, P.; Mó, O.; Yañez, M.; Elguero. J. Resonance-Assisted Hydrogen Bonds: A Critical Examination. Structure and Stability of the Enols of β-Diketones and β-Enaminones. *J. Phys. Chem. A* **2007**, *11*, 3585-3591; e) Sanz, P.; Mó, O.; Yañez, M.; Elguero, J. Bonding in Tropolone, 2-Aminotropone, and Aminotroponimine: No Evidence of Resonance-Assisted Hydrogen-Bond Effects. *Chem. Eur. J*. **2008**, *14*, 4225-4232.

(9) a) Dobosz, R.; Gawinecki, R. DFT Studies on Tautomeric Preferences: Proton Transfer in 1,5-bis(Pyridin-2-yl)- and 1,5-bis(Quinolin-2-yl)pentane-2,4-diones. *J. Mol. Struct. (Theochem)* **2010**, *940*, 119-123; b) Filarowski, A.; Majerz, I. AIM Analysis of Intramolecular Hydrogen Bonding in *O*-Hydroxy Aryl Schiff Bases. *J. Phys. Chem. A* **2008**, *112*, 3119-3126; c) Houjou, H.; Motoyama, T.; Banno, S.; Yoshikawa, I.; Araki, K. Experimental and Theoretical Studies on Constitutional Isomers of 2,6-Dihydroxynaphthalene Carbaldehydes. Effects of Resonance-Assisted Hydrogen Bonding on the Electronic Absorption Spectra. *J. Org. Chem*. **2009**, *74*, 520-529; d) Lenain, P.; Mandado, M.; Mosquera, R. A.; Bultinck, P. *Interplay between Hydrogen-Bond Formation and Multicenter π-Electron Delocalization: Intramolecular Hydrogen Bonds***.** *J. Phys. Chem. A* **2008**, *112*, 10689-10696; e) Palusiak, M.; Simon, S.; Solà, M. Interplay between Intramolecular Resonance-Assisted Hydrogen Bonding and Local Aromaticity. II. 1,3-Dihydroxyaryl-2-aldehydes. *J. Org. Chem.* **2009**, *74*, 2059-2066; f) Kluba, M.; Lipkowski, P.; Filarowski, A. Theoretical investigation of tautomeric equilibrium in *ortho*-hydroxy phenyl Schiff bases. *Chem. Phys. Lett*. **2008**, *463*, 426-430; g) Filarowski, A.; Kochel, A.; Kluba, M.; Kamounah, F. S. Structural and Aromatic Aspects of Tautomeric Equilibrium in Hydroxy Aryl Schiff Bases. *J. Phys. Org. Chem*. **2008**, *21*, 939-944; h) Mariam, Y. H.; Musin, R. N. Transition from Moderate to Strong Hydrogen Bonds: Its Identification and Physical Bases in the Case of O−H···O Intramolecular Hydrogen Bonds. *J. Phys. Chem. A* **2008**, *112*, 134-145; i) Palusiak, M.; Simon, S.; Solà, M. The Proton Transfer Reaction in Malonaldehyde Derivatives: Substituent Effects and Quasi-aromaticity of the Proton Bridge. *Chem. Phys*. **2007**, *342*, 43-54; j) Palusiak, M.; Krygowski, T. M. Application of AIM Parameters at Ring Critical Points for Estimation of π-Electron Delocalization in Six-Membered Aromatic and Quasi-Aromatic Rings. *Chem. Eur. J*. **2007**, *13*, 7996-8006; k) Woodford, J. N. Density Functional Theory and Atoms-in-Molecules Investigation of Intramolecular Hydrogen Bonding in Derivatives of Malonaldehyde and Implications for Resonance-Assisted Hydrogen Bonding. *J. Phys. Chem. A* **2007**, *111*, 8519-8530; l) Gawinecki, R.; Kuczek, A.; Kolehmainen, E.; Ośmiazowski, B.; Krygowski, T. M.; Kauppinen, R. Influence of Bond Fixation in Benzo-Annulated *N*-Salicylideneanilines and Their *ortho*-C(=O)X Derivatives (X = CH_3, NH_2, OCH_3) on Tautomeric Equilibria in Solution. *J. Org. Chem*. **2007**, *72*, 5598-5607; m) Krygowski, T. M.; Zachara, J. E.; Ośmiazowski, B.; Gawinecki, R. Topology-Driven Physicochemical Properties of π-Electron Systems. 1. Does the Clar Rule Work in Cyclic π-Electron Systems with the Intramolecular Hydrogen or Lithium Bond? *J. Org. Chem*. **2006**, *71*, 7678-7682; n) Palusiak, M.; Simon, S.; Solà, M. Interplay between Intramolecular Resonance-Assisted Hydrogen Bonding and Aromaticity in *o*-Hydroxyaryl Aldehydes. *J. Org. Chem*. **2006**, *71*, 5241-5248; o) Fonseca Guerra, C.; Bickelhaupt, F. M. Charge Transfer and Environment Effects Responsible for Characteristics of DNA Base Pairing. *Angew. Chem., Int. Ed*. **1999**, *38*, 2942-2945; p) Fonseca Guerra, C.; Bickelhaupt, F. M.; Snijders, J. G.; Baerends, E. J. The Nature of the Hydrogen Bond in DNA Base Pairs: the Role of Charge Transfer and Resonance Assistance. *Chem. Eur. J*. **1999**, *5*, 3581-3594.

(10) Krygowski, T. M.; Szatylowicz, H.; Stasyuk, O. A.; Dominikowska, J.; Palusiak, M. Aromaticity from the Viewpoint of Molecular Geometry: Application to Planar Systems. *Chem. Rev*. **2014**, *114*, 6383-6422 and references therein.

(11) Lloyd, D.; Marshall, D. R. *Quasi-Aromatic Compounds Examples of Regenerative, or Meneidic Systems*. In *Aromaticity, Pseudo-Aromaticity, Anti-Aromaticity, Proceedings of an International Symposium, Jerusalem, 31.03-3.04 1970*; Bergmann, E. D., Pullman, B., Eds.; The Israel Academy of Sciences and Humanities: Jerusalem, **1971**.

(12) Zubatyuk, R. I.; Shishkin, O. V.; Gorb, L.; Leszczynski, J. Homonuclear versus Heteronuclear Resonance-assisted Hydrogen Bonds: Tautomerism, Aromaticity, and Intramolecular Hydrogen Bonding in Heterocyclic Systems with Different Exocyclic Proton Donor/Acceptor. *J. Phys. Chem. A* **2009**, *113*, 2943–2952.

(13) Romero-Fernández, M. P.; Ávalos, M.; Babiano, R.; Cintas, P.; Jiménez, J. L.; Light, M. E.; Palacios, J. C. Pseudo-cyclic Structures of Mono- and di-Azaderivatives of Malondialdehydes. Synthesis and Conformational disentanglement by Computational Analyses. *Org. Biomol. Chem*. **2014**, *12*, 8997–9010.

(14) Rodríguez-Córdoba, W.; Zugazagoitia, J. S.; Collado-Fregoso, E.; Peon, J. Excited State Intramolecular Proton Transfer in Schiff Bases. Decay of the Locally Excited Enol State Observed by Femtosecond Resolved Fluorescence. *J. Phys. Chem. A*, **2007**, *111*, 6241-6247.

(15) Blagus, A.; Cinčić, D.; Friščić, T.; Kaitner, B.; Stilinović, V. Schiff Bases Derived from Hydroxyaryl Aldehydes: Molecular and Crystal Structure, Tautomerism, Quinoid Effect, Coordination Compounds. *Maced. J. Chem. Chem. Eng*. **2010**, *29*, 117-138.

(16) a) Paredes-García, V.; Venegas-Yazigi, D.; Lough, A. J.; Latorre, R. Potassium *N*-(6-oxocyclohexa-1,3-dien-5-ylidenemethyl)-glycinate. *Act. Cryst*. **2000**, *C56*, e283; b) Dominiak, P. M.; Grech, E.; Barr, G.; Teat, S.; Mallinson, P.; Wozniak, K. Neutral and Ionic Hydrogen Bonding in Schiff Bases. *Chem. Eur. J*. **2003**, *9*, 963-970; c) Ozeryanskii, V. A.; Pozharskii, A. F.; Schiff, W.; Kamiénski, B.; Sawka-Dobrowolska, W.; Sobczyk, L.; Grech, E. Novel Polyfunctional Tautomeric Systems Containing Salicylideneamino and Proton Sponge Moieties. *Eur. J. Org. Chem*. **2006**, 782-790; d) Chumakov, Y. M.; Tsapkov, V. I.; Starikova, Z. A.; Vorontsov, I. I.; Korlyukov, A. A.; Antosyak, B. Y.; Perrin, M. The Structure and Antimycotic Activity of Condensation Products of Some Aminoalcohols with Salicylaldehyde and its Derivatives. *J. Mol. Struct*., **2003**, *647*, 269-274; e) Ogawa, K.; Kasahara, Y.; Ohtani, Y.; Harada, J. Crystal Structure Change for the Thermochromy of *N*-Salicylideneanilines. The First Observation by X-ray Diffraction. *J. Am. Chem. Soc*. **1998**, *120*, 7107-7108; f) Makal, A.; Schilf, W.; Kamienski, B.; Szady-Chelmieniecka, A.; Grech, E.; Wozniak, K. Hydrogen Bonding in Schiff Bases-NMR, Structural and Experimental Charge Density Studies. *Dalton Trans*. **2011**, *40*, 421-430.

(17) a) Ensali, C. C.; Albayrak, Ç.; Odabasoglu, M.; Endönmez, A. 2-[(2-Hydroxy-4-nitrophenyl)aminomethylene]cyclohexa-3,5-dien-1(2*H*)-one. *Acta Cryst*. **2003**, *C59*, 601-602 ; b) Kia, R; Esmazilbeig, A.; Harkema, S. Intramolecular Hydrogen Bonding and Tautomerism in 1-[(2-Hydroxyphenylamino)methylene]-2-(1*H*)-5-phenylazosalicylalenone. *Acta Cryst.* **2004**, *A60*, s267.

(18) a) Yüce, S.; Özek, A.; Albayrak, Ç.; Odabasoglu, M.; Büyükgüngör, O. A Redetermination of 1-{4-[(2-Hydroxybenzylidene)-amino]phenyl}ethanone. *Acta Cryst.* **2004**, *E60*, 718-719; b) Rekhlova, O. Y.; Furmanova, N. G.; Chanturiya&Chikhladze, G. F. Crystal and Molecular Structure of Salicylideneaminoacetophenone. *Kristallografiya*, **1991**, *36*, 117-120; c) Pappalardo, A.; Amato, M. E.; Ballistreri, F. P.; Notti, A.; Tomaselli, G. A.; Toscano, R. M.; Sfrazzetto, G. T. Synthesis and Topology of [2+2]Calix[4]resorcarene-Based Chiral Cavitand-Salen Macrocycles. *Tetrahedron Lett.* **2012**, *53*, 7150-7153.

(19) a) Krygowski, T. M.; Wozniak, K.; Anulewicz, R.; Pawlak, D.; Kolodziejski, W. Through-Resonance Assisted Ionic Hydrogen Bonding in 5-Nitro-*N*-salicylideneethylamine. *J. Phys. Chem. A* **1977**, *101*, 9399-9404; b) Elmani, A.; Elerman, Y.; Svoboda, I.; 5-Chloro-*N*-(2-hydroxy-5-methylphenyl)salicylaldimine. *Acta Cryst.* **2001**, *C57*, 485-486.

(20) Schilf, W.; Kamiénski, B.; Szady-Chelmieniecka, A.; Grech, E. The ^{15}N and ^{13}C Solid State NMR Study of Intramolecular Hydrogen Bond in Some Schiff Bases. *J. Mol. Struct*. **2004**, *700*, 105-108.

(21) a) Ogawa, K.; Harada, J. Aggregation Controlled Proton Tautomerization in Salicylideneanilines *J. Mol. Struct*. **2003**, *647*, 211-216; b) For a review see: Vladimir I. Minkin, A. V. Tsukanov, A. D. Dubonosov, V. A. Bren. Tautomeric Schiff Bases: Iono-, Solvato-, Thermo- and Photochromism. *J. Mol. Struct*. **2011**, *998*, 179–191.

(22) a) Martínez, R. F.; Ávalos, M.; Babiano, R.; Cintas, P.; Jiménez, J. L.; Light, M. E.; Palacios, J. C. Tautomerism in Schiff Bases. The Cases of 2-Hydroxy-1-naphthaldehyde and 1-Hydroxy-2-naphthaldehyde Investigated in Solution and the Solid State. *Org. Biomol. Chem*. **2011**, *9*, 8268-8275; b) Martínez, R. F.; Ávalos, M.; Babiano, R.; Cintas, P.; Jiménez, J. L.; Light, M. E.; Palacios, J. C. Schiff Bases from TRIS and *ortho*-Hydroxyarenecarbaldehydes: Structures and Tautomeric Equilibria in the Solid State and in Solution. *Eur. J. Org. Chem*. **2011**, 3137–3145.

(23) Yüce, S.; Özek, A.; Albayrak, Ç.; Odabasoglu, M.; Büyükgüngör, O. 3-(4-Acetylphenyliminomethyl)-1,2-dihydroxybenzene. *Acta Cryst*. **2004**, *E60*, 810-812.

(24) a) Koşar, B; Büyükgüngör, O.; Albayrak, Ç.; Odabaşoğlu, M. 3-Hydroxy-6-[(4-hydroxyphenylamino)methylene]cyclohexa-2,4-dienone and 2-Hydroxy-6-[(4-hydroxyphenylamino)methylene]cyclohexa-2,4-dienone. *Acta Cryst*. **2004**, *C60*, 458-460; b) Kosar, B.; Albayrak, Ç.; Odabasoglu, M.; Büyükgüngör, O. 2-Hydroxy-6-[(2-hydroxyphenylamino)methylene]cyclohexa-2,4-

dienone. *Acta Cryst*. **2004**, *E61*, 1097-1099; c) Şahin, O.; Büyükgüngör, O.; Albayrak, Ç.; Odabasoglu, M. 2-Hydroxy-6-[(2-methoxyphenyl)aminomethylene]cyclohexa-2,4-dienone. *Acta Cryst*. **2005**, *E61*, 1579-1581.

(25) a) Yeap, G.-Y.; Ha, S.-T.; Ishizawa, N.; Suda, K.; Boey, P.-L.; Kamil, W. A. Synthesis, Crystal Structure and Spectroscopic Study of *para* Substituted 2-Hydroxy-3-methoxybenzalideneanilines. *J. Mol. Struct*. **2003**, *658*, 87-99; b) Ünver, H.; Kendi, E.; Güven, K.; Durlu, T. N. Synthesis, Spectroscopic Studies, Crystal Structure and Conformation Analysis of *N*-(2-Fluoro-3-methoxy)-salicylaldimine. *Z. Naturforsch.* **2002**, *57b*, 685-690; c) Şahin, O.; Büyükgüngör, O.; Albayrak, Ç.; Odabaşoğlu, M. (*E*)-2-Methoxy-6-[(2-trifluoromethylphenylimino)methyl]phenol. *Acta Cryst*. **2005**, *E61*, 1288-1290; d) Koşar, B.; Albayrak, Ç.; Odabaşoglu, M.; Büyükgüngör, O. (*E*)-2-Ethoxy-6-[(4-nitrophenyl)iminomethyl]phenol. *Acta Cryst.* **2005**, *E61*, 2109-2111; e) Khoo, L. E.; Hu, H. J.; Hazell, A. 4-Chloro-2-[2-(dimethylamino)ethylaminomethyl]phenol and 2-[2-(dimethylamino)ethylaminomethyl]-6-methoxyphenol. *Acta Cryst*. **1999**, *C55*, 245-248; f) Gali, N.; Matkovic-Calogovic, D.; Cimerman, Z. Structure and Spectroscopic Characteristics of *N*,*N*′-*bis*(2-Hydroxy-3-methoxyphenylmethylidene)-2,6-pyridinediamine. *Structural Chemistry* **2000**, *11*, 361-365.

(26) Ersanli, C. C.; Albayrak, Ç.; Odabasoglu, M.; Thöne, C.; Erdönmez, A. 4-[(2-Chlorophenyl)diazenyl]-6-methoxy-2-{[tris(hydroxymethyl)methyl]aminomethylene}cyclohexa-3,5-dien-1(2H)-one. *Acta Cryst*. **2004**, *C60*, o133-o135.

(27) Çazir, Ö.; Elerman, Y.; Elmali, A. Crystal Structure of *N*,*N*′-Bis(4-hydroxysalicylidene)-1,2-phenylenediimine, Methanol Solvate. *Anal. Sci*. **2002**, *18*, 377-378.

(28) a) Akine, S.; Taniguchi, T.; Nabeshima, T. Synthesis and Crystal Structure of a Novel Triangular Macrocyclic Molecule, tris(H_2saloph), and its Water Complex. *Tetrahedron Lett*. **2001**, *42*, 8861-8864; b) Gallart, A. J.; MacLachlan, M. J. Ion-Induced Tubular Assembly of Conjugated Schiff-Base Macrocycles. *Angew. Chem. Int. Ed*. **2003**, *42*, 5307-5310; c) Chong, J. H.; Sauer, M.; Patrick, B. O.; MacLachlan, M. J. Highly Stable Keto-Enamine Salicylideneanilines. *Org. Lett*. **2003**, *5*, 3823-3826; d) Gallart, A. J.; Yun, M.; Sauer, M.; Yeung, C. S.; MacLachlan, M. J. Tautomerization in Naphthalenediimines: A Keto-Enamine Schiff Base Macrocycle. *Org. Lett*. **2005**, *7*, 4827-4830; e) Sauer, M.; Yeung, C.; Chong, J. H.; Patrick, B. O.; MacLachlan, M. J. *N*-Salicylideneanilines: Tautomers for Formation of Hydrogen-Bonded Capsules, Clefts, and Chains. *J. Org. Chem*. **2006**, *71*, 775-778; f) Shopsowitz, K. E.; Edwards, D.; Gallant, A. J.; MacLachlan, M. J. Highly Substituted Schiff Base Macrocycles via Hexasubstituted Benzene: A Convenient Double Duff Formylation of Catechol Derivatives. *Tetrahedron* **2009**, *65*, 8113-8119.

(29) Grajda, M; Wierzbicki, M.; Cmoch, P.; Szumna, A. Inherently Chiral Iminoresorcinarenes through Regioselective Unidirectional Tautomerization. *J. Org. Chem*. **2013**, *78*, 11597-11601.

(30) Mehr, S. H. M.; Fukuyama, K.; Bishop, S.; Lelj, F.; MacLachlan, M. J. Deuteration of Aromatic Rings under Very Mild Conditions through Keto-Enamine Tautomeric Amplification. *J. Org. Chem*. **2015**, *80*, 5144-5150.

(31) a) Fuh, A. Y. G.; Chen, Y. D.; Liu, C. K.; Cheng, K. T. Azo Dye Adsorption Effect Induced by Elliptically Polarized Light in Azo Dye-Doped Liquid Crystals. *Dyes Pigm.* **2012**, *92*, 949-953; b) Lee, W.; Yuk, S. B.; Choi, J.; Jung, D. H.; Choi, S. H.; Park, J.; Kim, J. P. Synthesis and Characterization of Solubility Enhanced Metal-Free Phthalocyanines for Liquid Crystal Display Black Matrix of Low Dielectric Constant. *Dyes Pigm*. **2012**, *92*, 942-948.

(32) a) Menati, S.; Azadbakht, A.; Azadbakht, R.; Taeb, A.; Kakanejadifard, A. Synthesis, Characterization, and Electrochemical Study of Some Novel, Azo-Containing Schiff Bases and their Ni(II) Complexes. *Dyes Pigm.* **2013**, *98*, 499-506; b) Zhang, P.; Shi, B. B.; Wei, T. B.; Zhang, Y. M.; Lin, Q.; Yao, H.; You, X. M. A Naphtholic Schiff Base for Highly Selective Sensing of Cyanide via Different Channels in Aqueous Solution. *Dyes Pigm.* **2013**, *99*, 857-862; c) Ibrahim, M. M.; Ali, H. M.; Abdullah, M. A.; Hassandarvish, P. Acute Toxicity and Gastroprotective Effect of the Schiff Base Ligand ^{1}H-Indole-3-ethylene-5-nitrosalicylaldimine and its Nickel (II) Complex on Ethanol Induced Gastric Lesions in Rats. *Molecules* **2012**, *17*, 12449-12459; d) Xie, Y. Z.; Shan, G. G.; Li, P.; Zhou, Z. Y.; Su, Z. M. A novel class of Zn(II) Schiff base complexes with aggregation-induced emission enhancement (AIEE) properties: Synthesis, characterization and photophysical/electrochemical properties. *Dyes Pigm.* **2013**, *96*, 467-474; e) Ahmadi, R. A.; Amani, S. *Molecules* **2012**, *17*, 6434-6448; f) Tao, T.; Xu, F.; Chen, X. C.; Liu, Q. Q.; Huang, W.; You, X. Z. Comparisons Between Azo Dyes and Schiff Bases Having the Same Benzothiazole/Phenol Skeleton: Syntheses, Crystal Structures and Spectroscopic Properties. *Dyes Pigm.* **2012**, *92*, 916-922; g) Zabulica, A.; Balan, M.; Belei, D.; Sava, M.; Simionescu, B. C.;

Marin, L. Novel Luminescent Phenothiazine-Based Schiff Bases with Tuned Morphology. Synthesis, Structure, Photophysical and Thermotropic Characterization. *Dyes Pigm.* **2013**, *96*, 686-698; h) Ceyhan, G.; Tümer, M.; Köse, M.; McKee, V.; Akar, S. Structural Characterization, Luminescence and Electrochemical Properties of the Schiff Base Ligands. *J. Lumin.* **2012**, *132*, 2917-2928.

(33) a) Seyedi, S. M.; Sandaroos, R.; Zohuri, G. H. Novel Cobalt(II) Complexes of Amino Acids–Schiff Bases Catalyzed Aerobic Oxidation of Various Alcohols to Ketones and Aldehyde. *Chin. Chem. Lett.* **2010**, *21*, 1303-1306; b) Yin, L.; Jia, X.; Li, X. S. Simply Air: Vanadium-Catalyzed Oxidative Kinetic Resolution of Methyl *o*-Chloromandelate by Ambient Air. *Chin. Chem. Lett*. **2010**, *21*, 774-777; c) Yang, Y. L.; Wan, N. N.; Wang, W. P.; Xie, Z. F.; Wang, J. D. Synthesis of bis(Indolyl)methanes Catalyzed by Schiff Base–Cu(II) Complex. *Chin. Chem. Lett.* **2011**, *22*, 1071-1074.

(34) a) Al-Shaalan, N. H. Synthesis, Characterization and Biological Activities of Cu(II), Co(II), Mn(II), Fe(II), and UO_2(VI) Complexes with a New Schiff Base Hydrazone: *O*-Hydroxyacetophenone-7-chloro-4-quinoline Hydrazone. *Molecules* **2011**, *16*, 8629-8645; b) Alwan, S. M. Synthesis and Preliminary Antimicrobial Activities of New Arylideneamino-1,3,4-thiadiazole-(thio/dithio)-acetamido Cephalosporanic Acids. *Molecules* **2012**, *17*, 1025-1038; c) Mohammed, I. A.; Hamidi, R. M. Synthesis of New Liquid Crystalline Diglycidyl Ethers. *Molecules* **2012**, *17*, 645-656; d) Badrey, M. G.; Gomha, S. M. 3-Amino-8-hydroxy-4-imino-6-methyl-5-phenyl-4,5-dihydro-3*H*-chromeno[2,3-d]pyrimidine: An Effecient Key Precursor for Novel Synthesis of Some Interesting Triazines and Triazepines as Potential Anti-Tumor Agents. *Molecules* **2012**, *17*, 11538-11553.

(35) a) Ceyhan, G.; Köse, M.; Tümer, M.; Demirtaş, İ.; Yağlioğlu, A. Ş.; McKee, V. Structural Characterization of Some Schiff Base Compounds: Investigation of their Electrochemical, Photoluminescence, Thermal and Anticancer Activity Properties. *J. Lumin.* **2013**, *143*, 623-634; b) Taha, Z. A.; Ajlouni, A. M.; Momani, W. A. Structural, Luminescence and Biological Studies of Trivalent Lanthanide Complexes with *N*,*N*′-bis(2-Hydroxynaphthylmethylidene)-1,3-propanediamine Schiff Base Ligand. *J. Lumin.* **2012**, *132*, 2832-2841; c) Fani, N.; Bordbar, A. K.; Ghayeb, Y. Spectroscopic, Docking and Molecular Dynamics Simulation Studies on the Interaction of Two Schiff Base Complexes with Human Serum Albumin. *J. Lumin.* **2013**, *141*, 166-172; d) Ion, B. F.; Bushnell, E. A. C.; Luna, P. D.; Gauld, J. W. A Molecular Dynamics (MD) and Quantum Mechanics/Molecular Mechanics (QM/MM) Study on Ornithine Cyclodeaminase (OCD): A Tale of Two Iminiums. *Int. J. Mol. Sci.* **2012**, *13*, 12994-13011; e) Kumar, S.; Koh, J. Physiochemical, Optical and Biological Activity of Chitosan-Chromone Derivative for Biomedical Applications. *Int. J. Mol. Sci.* **2012**, *13*, 6102-6116; f) For a review on the antimicrobial activities of Schiff bases, see: Da Silva, C. M.; Da Silva, D. L.; Modolo, L. V.; Alves, R. B.; De Resende, M. A.; Martins, C. V. B.; De Fátima, Â. Schiff Bases: A Short Review of Their Antimicrobial Activities. *J. Adv. Res*. **2011**, *2*, 1-8.

(36) Akhaja, T. N.; Raval, J. P. Design, Synthesis, *in vitro* Evaluation of Tetrahydropyrimidine–isatin Hybrids as Potential Antibacterial, Antifungal and Anti-tubercular Agents. *Chin. Chem. Lett*. **2012**, *23*, 446-449.

(37) Hansen, P. E.; Rozwadowski, Z.; Dziembowska, T. NMR Studies of Hydroxy Schiff Bases. *Curr. Org. Chem.* **2009**, *13,* 194-215.

(38) Akaba, R.; Sakuragi, H.; Tokumaru. K. Substituent Effects on Azomethine Proton Chemical Shifts and ^{13}C–H Coupling Constants in *N*-Benzylideneanilines. Generality of Inverse Substituent Effects on the Azomethine Proton Chemical Shifts. *Bull. Chem. Soc. Jpn*. **1985**, *58*, 1711-1716.

(39) Kishore, K.; Sathyanarayana, D.N.; Bhanu, V.A. ^{13}C and ^{1}H NMR Study of *N*-5′-Methylsalicylideneanilines. *Magn. Reson. Chem*. **1987**, *25*, 471-473.

(40) a) Chumakov, Y. M.; Antosyak, B. Ya.; Mazus, M. D.; Tsapkov, V. I.; Samus, N. M. Crystal Structures of *N*-(Salicylidene)-Tris(hydroxymethyl)methylamine and *N*-(5-Chlorosalicylidene)-Tris(hydroxymethyl)methylamine. *Cryst. Rep.* **2000**, *45*, 945-950; b) Asgedom, G.; Sreedhara, A.; Kivikoski, J.; Valkonen, J.; Kolehmainen, E.; Rao, C. P. Alkoxo Bound Monooxo- and Dioxovanadium(V) Complexes: Synthesis, Characterization, X-ray Crystal Structures, and Solution Reactivity Studies. *Inorg. Chem*. **1996**, *35*, 5674-5683; c) Cungen, Z.; Peizi, Z.; Dan, W.; Kaibei, Y. Evidence of Proton Transfer from the Hydroxy O Atom to the Imine N Atom. Crystal Structure of N-Salicylideneamine-1-Tris(Hydroxymethyl)Methane. *J. Chem. Res.* **2000**, 402-403; d) Odabasoglu, M.; Albayrak, Ç.; Büyükgüngör, O.; Lönnecke, P. 2-{[Tris(hydroxymethyl)methyl]aminomethylene}cyclohexa-3,5-

dien-1(2*H*)-one and its 6-hydroxy and 6-methoxy derivatives. *Acta Cryst*. **2003**, *C59*, 616-619; e) Chumakov, M. Y. M.; Tsapkov, V. I.; Bocelli, G.; Antosyak, B. Ya.; Gulya, A. P. Crystal Structures of 6-[(2-Hydroxy-1,1-bis-hydroxymethyl-ethylamino)-methylene]-4-nitro-cyclohexa-2,4-dienone hydrate and 6-[(2-Hydroxy-1,1-bis-hydroxymethyl-ethylamino)-methylene]-4-bromo-cyclohexa-2,4-dienone. *J. Struct. Chem*. **2006**, *47*, 346-351; f) Odababaşoğlu, M.; Albayrak, Ç.; Özkanza, R.; Aykan, F. Z.; Lonecke, P. Some Polyhydroxy Azo-Azomethine Derivatives of Salicylaldehyde: Synthesis, Characterization, Spectroscopic, Molecular Structure and Antimicrobial Activity Studies. *J. Mol. Struct*. **2007**, *840*, 71-89; g) Yüce, S.; Albayrak, Ç.; Odabaşoğlu, M.; Büyükgüngör, O. (*Z*)-6-{[1,3-Dihydroxy-2-(hydroxymethyl)propan-2-yliminio]methyl}-2-ethoxyphenolate, (*Z*)-6-{[1,3-dihydroxy-2-(hydroxymethyl)propan-2-yliminio]methyl}-4-nitratocyclohexa-2,4-dienone mono-hydrate and (*R*,*E*)-2-[(1-hydroxybutan-2-ylimino)methyl]phenol. *Acta Cryst*. **2006**, *C62*, o389-o393; h) Ng, S. W. Low-Temperature Redetermination of 4-Chloro-2-[tris-(hydroxymethyl)methyliminomethyl]phenol as Zwitterionic 4-Chloro-2-[tris(hydroxymethyl)methyliminiomethyl]phenolate. *Acta Cryst*. **2008**, *E64*, o2455; i) Koşar, B.; Albayrak, Ç.; Odabaşoğlu, M.; Büyükgüngör, O. 4-[(3-Chlorophenyl)diazenyl]-6-methoxy-2-{[tris(hydroxymethyl)methyl]aminomethylene}cyclohexa-3,5-dien-1(2H)-one. *Acta Cryst*. **2004a**, *E60*, o190-o192; j) Ersanli, C. C.; Albayrak, Ç.; Odabaşoğlu, M.; Büyükgüngör, O. (*Z*)-6-{[1,3-Dihydroxy-2-(hydroxymethyl)propan-2-ylamino]methylene}-2-methoxy-4-[(*E*)-*o*-tolyldiazenyl]cyclohexa-2,4-dienone. *Acta Cryst*. **2006**, *C62*, o483-o485.

(41) a) Albayrak, Ç.; Odabasoglu, M.; Büyükgüngör, O.; Lönnecke, P. 5-(2-Chlorophenyldiazenyl)salicylaldehyde and 4-(2-chlorophenyldiazenyl)-2-{[tris(hydroxymethyl)methyl]aminomethylene}cyclohexa-3,5-dien-1(2*H*)-one. *Acta Cryst*. **2004**, *C60*, o318-o320; b) Ersanli, C. C.; Albayrak, Ç.; Odabasoglu, M.; Kazak, C. (Z)-6-{[1,3-Dihydroxy-2-(hydroxymethyl)propan-2-ylamino]methylene}-2-methoxy-4-{(E)-[3-(trifluormethyl)phenyl]diazenyl}cyclohexa-2,4-dienone. *Acta Cryst*. **2005**, *E61*, o4051-o4053; c) Odabasoğlu, M.; Albayrak, Ç.; Büyükgüngör, O.; Goesmann, H. 4-[(3-Chlorophenyl)diazenyl]-2-{[tris(hydroxymethyl)-methyl]aminomethylene}cyclohexa-3,5-dien-1(2H)-one. *Acta Cryst*. **2003**, *C59*, 0234-0236; d) Ersanli, C. C.; Albayrak, Ç.; Odabasoğlu, M.; Büyükgüngör, O. (Z)-4-[(E)-(4-Butylphenyl)diazenyl]-6-{[1,3-dihydroxy-2-(hydroxymethyl)propan-2-ylamino]methylene}-2-methoxycyclohexa-2,4-dienone. *Acta Cryst*. **2005**, *E61*, o4139-o4141; e) Özek, A.; Albayrak, Ç.; Odabasoglu, M.; Büyükgüngör, O. (*Z*)-4-(2,6-Dichlorophenyldiazenyl)-6-{[1,3-dihydroxy-2-(hydroxymethyl)propan-2-ylamino]methylene}-2-methoxycyclohexa-2,4-dienone and the 3-Methoxyphenyldiazenyl and 4-Methoxyphenyldiazenyl Analogues. *Acta Cryst*. **2006**, *C62*, o173-o177; f) Şahin, O.; Albayrak, Ç.; Odabasoğlu, M.; Büyükgüngör, O. (Z)-6-{[1,3-Dihydroxy-2-(hydroxymethyl)propan-2-ylamino]methylene}-4-[(E)-(4-ethylphenyl)diazenyl]cyclohexa-2,4-dienone. *Acta Cryst*. **2005**, *E61*, o2076-o2078.

(42) Schiff bases derived from TRIS and 4-methoxy-, 6-methoxy, 3-fluoro-, 4-fluoro-, 6-fluoro-, 3,5-difluoro- and 3,6-difluorosalycilaldehydes have all enaminic structure in the solid state as shown by X-ray data: Palacios, J. C. *et al.*, unpublished results.

(43) Alarcón, S. H.; Olivieri, A. C.; Sanz, D.; Claramunt, R. M.; Elguero, J. Substituent and Solvent Effects on the Proton Transfer Equilibrium in Anils and Azo Derivatives of Naphthol. Multinuclear NMR Study and Theoretical Calculations. *J. Mol. Struct*. **2004**, *705*, 1-9.

(44) Nazir, H.; Yildiz, M.; Yilmaz, H.; Tahir, M. N.; Ülkü, D. Intramolecular Hydrogen Bonding and Tautomerism in Schiff Bases. Structure of *N*-(2-pyridil)-2-oxo-1-naphthylidenemethylamine. *J. Mol. Struc*. **2000**, *524*, 241-250.

(45) a) Alarcón, S. H.; Olivieri, A. C.; González-Sierra, M. ^{13}C NMR Spectroscopic and AM1 Study of the Intramolecular Proton Transfer in Anils of Salicylaldehyde and 2-Hydroxynaphthalene-1-carbaldehyde. *J. Chem. Soc. Perkin Trans. 2* **1994**, 1067-1070; b) Alarcón, S. H.; Olivieri, A. C.; Cravero, R. M.; Labadie, G.; González-Sierra, M. Ground- and Excited-State Prototropic Tautomerism in Anils of Aromatic α-Hydroxy Aldehydes Studied by Electronic Absorption, Fluorescence and ^{1}H and ^{13}C NMR Spectroscopies and Semi-Empirical Calculations. *J. Phys. Org. Chem.* **1995**, *8*, 713-720; c) Katritzky, A.; Ghiviriga, I.; Leeming, P.; Soti, F. Hydrogen Bonding and Tautomerism in Anils of Salicylaldehydes and Related Compounds. A Study of Deuterium Isotope Effects on ^{13}C Chemical Shifts. *Magn. Reson. Chem.* **1996**, *34*, 518-526; d) Rozwadowski, Z.; Majewski, E.; Dziembowska, T.; Hansen, P. E. Deuterium isotope effects on ^{13}C chemical shifts of intramolecularly hydrogen-bonded Schiff bases. *J. Chem. Soc. Perkin Trans. 2* **1999**, 2809-2817.

(46) a) Dziembowska, T.; Rozwadowski, Z.; Filarowski, A.; Hansen, P. E. NMR Study of Proton Transfer Equilibrium in Schiff Bases Derived from 2-Hydroxy-1-naphthaldehyde and 1-Hydroxy-2-acetonaphthone. Deuterium Isotope Effects on ^{13}C and ^{15}N

Chemical Shifts. *Magn. Reson. Chem.* **2001**, *39*, S67-S80; b) Karakaş, A.; Elmali, A.; Ünver, H.; Svoboda, I. Nonlinear Optical Properties of Some Derivatives of Salicylaldimine-Based Ligands. *J. Mol. Struct*. **2004**, *702*, 103-110; c) Filarowski, A.; Koll, A.; Rospenk, M.; Król-Starzomska, I.; Hansen, P. E. Tautomerism of Sterically Hindered Schiff Bases. Deuterium Isotope Effects on ^{13}C Chemical Shifts. *J. Phys. Chem. A* **2005**, *109*, 4464-4473; d) Rozwadowski, Z.; Amroziak, K.; Szypa, M.; Jagodzińska, E.; Spychaj, S.; Schilf, W.; Kamieński, B. The ^{15}N and ^{13}C NMR Study of Schiff Bases of Amino Acids and their Lithium Salts in Solid State and DMSO Solution. *J. Mol. Struct.* **2005**, *734*, 137-142.

(47) a) Schilf, W.; Kamiénski, B.; Kolodziej, B.; Grech, E. The NMR Study of Hydrogen Bond Formation in Some Tris(((salicylidene)amino)ethyl)amine Derivatives in Solution and in the Solid State. *J. Mol. Struct*. **2004**, *708*, 33-38; b) Berger, S.; Braun, S.; Kalinowski, H.-O. *NMR Spectroscopy of the Non-Metallic Elements*; John Wiley & Sons Ltd.: Chichester; 1996; c) Schilf, W.; Bloxsidge, J. P.; Jones, J. R.; Lu, S.-Y. Investigations of Intramolecular Hydrogen Bonding in Three Types of Schiff Bases by ^{2}H and ^{3}H NMR Isotope Effects. *Magn. Reson. Chem.* **2004**, *42*, 556-560; d) Schilf, W.; Kamieński, B.; Szady-Chelmieniecka, A.; Grech, E. The Intramolecular Hydrogen Bonds in Some Schiff Bases Derived from Cyclopropyl-, Cyclobutyl- and Cyclopentylamine. *J. Mol. Struct.* **2005**, *743*, 237-241; e) Schilf, W.; Kamieński, B.; Szady-Chelmieniecka, A.; Grech, E.; Makal, A.; Woźniak, K. NMR and X-Ray Studies of 2,6-Bis(alkylimino)phenol Schiff Bases. *J. Mol. Struct.* **2007**, *844-845*, 94-101.

(48) a) Kamieński, B.; Schilf, W.; Dziembowska, T.; Rozwadoski, Z.; Szady-Chelmieniecka, A. The ^{15}N and ^{13}C Solid State NMR Study of Intramolecular Hydrogen Bond in Some Schiff's Bases. *Solid State NMR.* **2000**, *16*, 285-289; b) Schilf, W.; Kamieński, B.; Dziembowska, T.; Rozwadoski, Z.; Szady-Chelmieniecka, A. ^{15}N NMR Study of the Intramolecular Hydrogen Bond in *N*-Salicylidene-alkylamines. *J. Mol. Struct.* **2000**, *552*, 33-37.

(49) a) Gilli, P.; Pretto, L.; Gilli. G. PA/pK_a Equalization and the Prediction of the Hydrogen-Bond Strength: A Synergism of Classical Thermodynamics and Structural Crystallography. *J. Mol. Struct*. **2007**, *844-845*, 328 ; b) Gilli, P.; Bertolasi, V.; Pretto, L.; Gilli, G. Outline of a Transition-State Hydrogen-Bond Theory. *J. Mol. Struct*. **2006**, *790*, 40-49; c) Gilli, G.; Gilli, P. Towards a Unified Hydrogen-Bond Theory. *J. Mol. Struct*. **2000**, *552*, 1-15.

(50) a) Tabei, K.; Saitou, E. The Nuclear Magnetic Resonance and Infrared Spectra of Aromatic Azomethines. *Bull. Chem. Soc. Japn*. **1969**, *42*, 1440-1443; b) Inamoto, N.; Kushida, K.; Masuda, S.; Ohta, H.; Satoh, S.; Tamura, Y.; Tokumaru, K.; Tori, K.; Yoshida, M. Novel Substituent Effects in ^{1}H and ^{13}C NMR Spectra of 4-and 4'-Substituted *N*-Benzylideneanilines. *Tetrahedron Lett*. **1974**, *41*, 3617-3620; c) Akaba, R.; Sakuragi, H.; Tokumaru, K. A New Aspect on the Origin of an Anomalous Substituent Effect on the Azomethine Proton Chemical Shifts in 4-Substituted *N*-Benzylideneanilines. *Bull. Chem. Soc. Japn.* **1985**, *58*, 301-303; d) Akaba, R.; Sakuragi, H.; Tokumaru, K. Multiple Substituent Effects on ^{13}C Chemical Shifts of *N*-Benzylideneanilines. Evidence for Substituent–Substituent Interactions and Their Implications of Conformational Changes with Substituents. *Bull. Chem. Soc. Japn.* **1985**, *58*, 1186-1195; e) Akaba, R.; Sakuragi, H.; Tokumaru, K. Substituent Effects on Azomethine Proton Chemical Shifts and ^{13}C–H Coupling Constants in *N*-Benzylideneanilines. Generality of Inverse Substituent Effects on the Azomethine Proton Chemical Shifts. *Bull. Chem. Soc. Japn.* **1985**, *58*, 1711-1716 ; f) Kawasaki, A. Effect of Substituents on the ^{13}C Chemical Shifts of the Azomethine Carbon Atom of *N*-Benzylideneanilines and 2-*N*-Arylimino-2-*p*-nitrophenylethanenitriles. *J. Chem. Soc. Perkin Trans. 2* **1990**, 223-228; g) Jovanovic, B. Ž.; Mišic-Vukovic, M.; Marinkovic, A. D.; Vajs, V. Effect of Substituents on the ^{13}C Chemical Shifts of the Azomethine Carbon Atom of *N*-(Phenyl substituted)pyridine-4-aldimines. *J. Mol. Struct.* **1999**, *482-483*, 375-378, h) Jovanovic, B. Ž.; Mišic-Vukovic, M.; Marinkovic, A. D.; Vajs, V. Effect of substituents on the ^{13}C Chemical Shifts of the Azomethine Carbon Atom of *N*-(phenyl substituted)pyridine-3- and -2-aldimines. *J. Mol. Struct.* **2002**, *642*, 113-118; i) Jovanovic, B. Ž.; Marinkovic, A. D.; Assaleh, F. H.; Csanádi, J. Effect of Substituents on the ^{13}C Chemical Shifts of the Azomethine Carbon Atom of *N*-(Substituted phenylmethylene)-3- and -4-aminobenzoic Acids. *J. Mol. Struct.* **2005**, *744-747*, 411-416.

(51) Ortegón-Reyna, D.; Garcías-Morales, C.; Padilla-Martínez, I.; García-Báez, E.; Aríza-Castolo, A.; Peraza-Campos, A.; Martínez-Martínez, F. NMR Structural Study of the Prototropic Equilibrium in Solution of Schiff Bases as Model Compounds. *Molecules* **2014**, *19*, 459-481.

(52) a) Krygowski, T. M.; Stępień, B.; Anulewicz-Ostrowska, R.; Diziembowska, T. π-Electron Delocalisation in the Spacer of the O-H…N Bridge in Schiff Bases. Crystal and Molecular Structure of 3,5-Dimethoxy-2-[(phenylimino)methyl]phenol and 4-Methoxy-2-[(phenylimino)methyl]phenol. *Tetrahedron* **1999**, *55*, 5457-5464.

(53) a) The values of σ have been taken from: Hansch, C.; Leo, A.; Taft, R. W. A Survey of Hammett Substituent Constants and Resonance and Field Parameters. *Chem. Rev*. **1991**, *91*, 165-195; b) March, J. *Advanced Organic Chemistry*; Wiley-Interscience: New York; 1992, p. 280; c) Carey, F. A.; Sundberg, R. J. *Advanced Organic Chemistry*; Plenum Press: New York; 1990, p. 201.

(54) Barlin, G. B.; Perrin, D. D. Prediction of the Strengths of Organic Acids. *Q. Rev. Chem. Soc.* **1966**, *20*, 75-101.

(55) a) Riddle, J. A.; Bollinger, J. C.; Lee, D. Escape from a Nonporous Solid: Mechanically Coupled Biconcave Molecules. *Angew. Chem. Int. Ed. Engl.* **2005**, *44*, 6689-6693; b) Yelamaggad, C. V.; Achalkumar, A. S.; Rao, D. S. S.; Prasad, S. K. Self-Assembly of C_{3h} and C_s Symmetric Keto-enamine Forms of Tris(*N*-salicylideneanilines) into Columnar Phases of Discotic Liquid Crystals. *J. Am. Chem. Soc.* **2004**, *126*, 6506-6507; c) Jiang, X.; Bollinger, J. C.; Lee, D. Two-Dimensional Electronic Conjugation: Cooperative Folding and Fluorescence Switching. *J. Am. Chem. Soc.* **2006**, *128*, 11732-11733; d) Riddle, J. A.; Lathrop, S. P.; Bollinger, J. C.; Lee, D. Schiff Base Route to Stackable *Pseudo*-Triphenylenes: Stereoelectronic Control of Assembly and Luminescence. *J. Am. Chem. Soc.* **2006**, *128*, 10986-10987; e) Zhu, Y.; Long, H.; Zhang, W. Imine-Linked Porous Polymer Frameworks with High Small Gas (H_2, CO_2, CH_4, C_2H_2) Uptake and CO_2/N_2 Selectivity. *Chem. Mater*. **2013**, *25*, 1630-1635; f) Lim, Y.-K.; Wallace, S.; Bollinger, J. C.; Chen, X.; Lee, D. Triferrocenes Built on a C_3-Symmetric Ligand Platform: Entry to Redox-Active *pseudo*-Triphenylenes via Chelation-Driven Stereoselection of Triple Schiff Bases. *Inorg. Chem*. **2007**, *46*, 1694-1703; g) Yelamaggad, C. V.; Achalkumar, A. S.; Rao, D. S. S.; Prasad, S. K. A New Class of Discotic Mesogens Derived from Tris(*N*-salicylideneaniline)s Existing in C_{3h} and C_s Keto-Enamine Forms. *J. Org. Chem.* **2007**, *72*, 8308-8318; h) Yelamaggad, C. V.; Achalkumar, A. S.; Rao, D. S. S.; Prasad, S. K. Luminescent, Liquid Crystalline Tris(*N*-salicylideneaniline)s: Synthesis and Characterization. *J. Org. Chem.* **2009**, *74*, 3168-3171; i) Feldscher, B.; Stammler, A.; Bögge, H.; Glaser, T. Synthesis and Characterization of a Trinuclear Cu^{II}_3 Complex Bridged by An Extended Phloroglucinol-Ligand: Implications for a Rational Enhancement of Ferromagnetic Interactions. *Dalton Trans.* **2010**, *39*, 11675-11685; j) Yelamaggad, C. V.; Achalkumar, A. S. Tris(*N*-salicylideneanilines) [TSANs] Exhibiting a Room Temperature Columnar Mesophase: Synthesis and Characterization. *Tetrahedron Lett.* **2006**, *47*, 7071-7075, k) Vieweger, M.; Jiang, X.; Lim, Y.-K.; Jo, J.; Lee, D.; Dragnea, B. Conformationally Dynamic π-Conjugation: Probing Structure–Property Relationships of Fluorescent Tris(*N*-salicylideneaniline)s. *J. Phys. Chem. A* **2011**, *115*, 13298-13308; l) Chandra, S.; Kundu, T.; Kandambeth, S.; BabaRao, R.; Marathe, Y.; Kunjir, S. M.; Banerjee, R. Phosphoric Acid Loaded Azo (−N═N−) Based Covalent Organic Framework for Proton Conduction. *J. Am. Chem. Soc.* **2014**, *136*, 6570-6573.

(56) a) Guieu, S.; Crane, A. K.; MacLachlan, M. J. Campestarenes: Novel Shape-Persistent Schiff base Macrocycles with 5-Fold Symmetry. *Chem. Commun*. **2011**, *47*, 1169-1171; b) Guieu, S.; White, N. G.; Lelj, F.; MacLachlan, M. J. The Rich Tautomeric Behavior of Campestarenes. *Chem. Eur. J*. **2016**, *22*, 17657-17672; c) Nam, S.; Ware, D. C.; Brothers, P. J. Campestarenes: new building blocks with 5-fold symmetry. *Org. Biomol. Chem*. **2018**, *16*, 6460-6469.

(57) a) Echevarria, A.; Nascimento, M.; Gerônimo, V.; Miller, J.; Giesbrecht, A. NMR Spectroscopy, Hammett Correlations and Biological Activity of Some Schiff Bases Derived from Piperonal. *J. Braz. Chem. Soc.* **1999**, *10*, 60-64; b) Neuvonen, K.; Fülöp, F.; Neuvonen, H.; Koch, A.; Kleinpeter, E.; Pihlaja, K. Substituent Influences on the Stability of the Ring and Chain Tautomers in 1,3-*O*,*N*-Heterocyclic Systems: Characterization by ^{13}C NMR Chemical Shifts, PM3 Charge Densities, and Isodesmic Reactions. *J. Org. Chem.* **2001**, *66*, 4132-4140; c) Neuvonen, K.; Fülöp, F.; Neuvonen, H.; Koch, A.; Kleinpeter, E.; Pihlaja, K. Comparison of the Electronic Structures of Imine and Hydrazone Side-Chain Functionalities with the Aid of ^{13}C and ^{15}N NMR Chemical Shifts and PM3 Calculations. The Influence of C=N-Substitution on the Sensitivity to Aromatic Substitution. *J. Org. Chem.* **2003**, *68*, 2151-2160; d) Zhurko, A.G.; Aleksandriiskii, V. V.; Burmistrov, V. A. Conformational State of Benzilidene Aniline Derivatives from *ab initio* Calculation and NMR Spectroscopy Data. *J. Struct. Chem.* **2006**, *47*, 622-628.

(58) Schilf, W. Intramolecular hydrogen bond investigations in some Schiff bases using C-C and N-C coupling constants. *J. Mol. Struct*. **2004**, *689*, 245-249.

(59) a) Dudek, G. O.; Dudek, E. P. Spectroscopic Studies of Keto-Enol Equilibria. VII. Nitrogen-15 Substituted Schiff Bases. *J. Am. Chem. Soc*. **1964**, *86*, 4283-4287; b) Dudek, G. O.; Dudek, E. P. Spectroscopic Study of Keto–Enol Tautomerization in Phenol Derivatives. *Chem. Comm*. **1965**, 464-466; c) Dudek, G. O.; Dudek, E. P. Spectroscopic Studies of Keto-Enol Equilibria. IX. N^{15}-Substituted Anilides. *J. Am. Chem. Soc.* **1966**, *88*, 2407-2412.

(60) Stepien, B. T.; Cyrański, M. K.; Krygowski, T. M. Aromaticity Strongly Affected by Substituents in Fulvene and Heptafulvene as a New Method of Estimating the Resonance Effect. *Chem. Phys. Lett.* **2001**, *350*, 537-542.

(61) Alarcón, S. H.; Pagani, D.; Bacigalupo J.; Olivieri, A. C. Spectroscopic and Semi-empirical MO Study of Substituent Effects on the Intramolecular Proton Transfer in Anils of 2-Hydroxybenzaldehydes. *J. Mol. Struct*. **1999**, *475*, 233-240.

(62) Romero-Fernández, M. P.; Ávalos, M.; Babiano, R.; Cintas, P.; Jiménez, J. L.; Palacios, J. C. Rethinking Aromaticity in H-Bonded Systems. Caveats for Transition Structures Involving Hydrogen Transfer and π-Delocalization. *J. Phys. Chem. A* **2015**, *119*, 525-534.

(63) Matamoros, E.; Cintas, P.; Palacios, J. C. Tautomerism and Stereodynamics in Schiff Bases from Gossypol and Hemigossypol with *N*-Aminoheterocycles. *Org. Biomol. Chem*. **2019**, *17*, 6229-6250.

(64) Marcus, R. A. Theoretical Relations among Rate Constants, Barriers, and Brönsted Slopes of Chemical Reactions. *J. Phys. Chem*. **1968**, *72*, 891-899.

(65) Schaefer, T. A Relationship between Hydroxyl Proton Chemical Shifts and Torsional Frequencies in Some Ortho-Substituted Phenol Derivatives. *J. Phys. Chem.* **1975**, *79*, 1888-1890.

(66) Emsley, J. Very Strong Hydrogen Bonding. *Chem. Soc. Rev*. **1980**, *9*, 91-124.

(67) Parthasarathi, R.; Subramanian, V. Characterization of Hydrogen Bonding: From van der Waals Interactions to Covalency. In *Hydrogen Bonding-New Insights*; Grabowski, S. J., Ed.; Springer: Berlin; 2006, Ch. 1, pp. 2-50.

(68) Hansen, P. E.; Koch, A.; Kleinpeter, E. Ring Current and Anisotropy Effects on OH Chemical Shifts in Resonance-Assisted Intramolecular H-Bonds. *Tetrahedron Lett*. **2018**, *59*, 2288-2292.

(69) Musin, R. N.; Mariam, Y. H. An Integrated Approach to the Study of Intramolecular Hydrogen Bonds in Malonaldehyde Enol Derivatives and Naphthazarin: Trend in Energetic versus Geometrical Consequences. *J. Phys. Org. Chem*. **2006**, *19*, 425-444.

(70) a) Bird, C. W. A New Aromaticity Index and its Application to Five-Membered Ring Heterocycle. *Tetrahedron* **1985**, *41*, 1409-1414; b) Bird, C. W. The Application of a new Aromaticity Index to Six-Membered Ring Heterocycle. *Tetrahedron* **1986**, *42*, 89-92; c) Bird, C. W. Heteroaromaticity. 8. The Influence of *N*-Oxide Formation on Heterocyclic Aromaticity. *Tetrahedron* **1993**, *49*, 8441-8448; d) Kotelevskii, S. I. ; Prezhdo, O. V. Aromaticity indices revisited: refinement and application to certain five-membered ring heterocycles. *Tetrahedron* **2001**, *57*, 5715-29; e) Pozharskii, A. F. *Theoretical Principles of Heterocyclic Chemistry*; Khimia: Moscow, 1985; p. 22; f) Pozharskii, A. F. Heteroaromaticity (review). *Chem. Heterocycl. Compd.* **1985**, *21*, 717-749; g) Mezei, M.; Beveridge, D. L. Free Energy Simulations. *Anal. N. Y. Acad. Sci.* **1986**, *482*, 1-23; h) Raczynska, E. D.; Duczmal, K.; Hallmann, M. Tautomeric Equilibria and π-Electron Delocalization for the Substrate (Pyruvate) and Inhibitor (Oxamate) of Lactate Dehydrogenase-DFT Studies. *Polish J. Chem.* **2007**, *81*, 1655-1666; i) Raczynska, E. D.; Hallmann, M.; Duczmal, K. Consequences of Covalent and Non-covalent Interactions on Conformational Preferences and π-Electron Delocalization for the Substrate (Pyruvate) and Inhibitor (Oxamate) of Lactate Dehydrogenase - DFT Studies. *Polish J. Chem.* **2008**, *82*, 1077-1090; j) Raczynska, E. D.; Hallmann, M.; Kolczynska, K.; Stepniewski, T. On the Harmonic Oscillator Model of Electron Delocalization (HOMED) Index and its Application to Heteroatomic π-Electron System. *Symmetry* **2010**, *2*, 1485-1509; k) Frizzo, C. P.; Martins, M. A. P. Aromaticity in Heterocycles: New HOMA Index Parametrization. *Struct. Chem.* **2012**, *23*, 375-380.

(71) a) Kruszewski, J.; Krygowski, T. M. Definition of Aromaticity Basing on the Harmonic Oscillator Model. *Tetrahedron Lett.* **1972**, *13*, 3839-3842; b) Krygowski, T. M. Crystallographic Studies of Inter- and Intramolecular Interactions Reflected in Aromatic Character of π-Electron Systems. *J. Chem. Inf. Comput. Sci.* **1993**, *33*, 70-78.

(72) a) Schleyer, P. v. R. Introduction: Aromaticity. *Chem. Rev*. **2001**, *101*, 1115-1118.; b) Krygowski, T. M.; Cyrański, M. K. Structural Aspects of Aromaticity. *Chem. Rev*. **2001**, *101*, 1385-1420; c) Matito, E.; Duran, M.; Solà, M. The Aromatic Fluctuation Index (FLU): A New Aromaticity Index Based on Electron Delocalization. *J. Chem. Phys*. **2005**, *122*, 014109 (1-8).

(73) Rusinska-Roszak, D. Energy of Intramolecular Hydrogen Bonding in *ortho*-Hydroxybenzaldehydes, Phenones and Quinones. Transfer of Aromaticity from *ipso*-Benzene Ring to the Enol System(s). *Molecules* **2017**, *22*, 481-500.

(74) Zhao, Y.; Truhlar, D. G. The M06 suite of density functionals for main group thermochemistry, thermochemical kinetics, noncovalent interactions, excited states, and transition elements: two new functionals and systematic testing of four M06-class functionals and 12 other functionals. *Theor. Chem. Acc*. **2008**, *120*, 215-241.

(75) a) McLean, A. D.; Chandler, G. S. Contracted Gaussian basis sets for molecular calculations. I. Second row atoms, Z=11–18. *J. Chem. Phys*., **1980**, *72*, 5639-5648; b) Raghavachari, K.; Binkley, J. S.; Seeger, R.; Pople, J. A. Self-consistent molecular orbital methods. XX. A basis set for correlated wave functions *J. Chem. Phys*. **1980**, *72*, 650-654.

(76) Gaussian 09, Revision A.1. Frisch, M. J.; Trucks, G. W.; Schlegel, H. B.; Scuseria, G. E.; Robb, M. A.; Cheeseman, J. R.; Scalmani, G.; Barone, V.; Mennucci, B.; Petersson, G. A.; Nakatsuji, H.; Caricato, M.; Li, X.; Hratchian, H. P.; Izmaylov, A. F.; Bloino, J.; Zheng, G.; Sonnenberg, J. L.; Hada, M.; Ehara, M.; Toyota, K.; Fukuda, R.; Hasegawa, J.; Ishida, M.; Nakajima, T.; Honda, Y.; Kitao, O.; Nakai, H.; Vreven, T.; Montgomery, J. A., Jr.; Peralta, J. E.; Ogliaro, F.; Bearpark, M.; Heyd, J. J.; Brothers, E.; Kudin, K. N.; Staroverov, V. N.; Kobayashi, R.; Normand, J.; Raghavachari, K.; Rendell, A.; Burant, J. C.; Iyengar, S. S.; Tomasi, J.; Cossi, M.; Rega, N.; Millam, J. M.; Klene, M.; Knox, J. E.; Cross, J. B.; Bakken, V.; Adamo, C.; Jaramillo, J.; Gomperts, R.; Stratmann, R. E.; Yazyev, O.; Austin, A. J.; Cammi, R.; Pomelli, C.; Ochterski, J. W.; Martin, R. L.; Morokuma, K.; Zakrzewski, V. G.; Voth, G. A.; Salvador, P.; Dannenberg, J. J.; Dapprich, S.; Daniels, A. D.; Farkas, Ö.; Foresman, J. B.; Ortiz, J. V.; Cioslowski, J.; Fox, D. J. Gaussian, Inc., Wallingford CT, **2009**.

(77) Zhao, Y.; Truhlar, D. G. Density Functionals with Broad Applicability in Chemistry. *Acc. Chem. Res*. **2008**, *41*, 157-167.

(78) Marenich, A. V.; Cramer, C. J.; Truhlar, D. G. Universal Solvation Model Based on Solute Electron Density and on a Continuum Model of the Solvent Defined by the Bulk Dielectric Constant and Atomic Surface Tensions *J. Phys. Chem. B* **2009**, *113*, 6378-6396.

(79) Tomasi, J.; Mennucci, B.; Cancès, E. The IEF version ofthe PCM solvation method: an overview of a newmethod addressed to study molecular solutes at the QM ab initio level. *J. Mol. Struct.* **1999**, *464*, 211-226.

(80) Liotard, D. A.; Hawkins, G. D.; Lynch, G. C.; Cramer, C. J.; Truhlar, D. G. Improved methods for semiempirical solvation models. *J. Comput. Chem.* **1995**, *16*, 422-440.

(81) a) Pavia, M. R.; Cohen, M. P.; Dilley, G. J.; Dubuc, G. R; Durgin, T. L.; Forman, F. W.; Hediger, M. E.; Milot, G.; Powers, T. S.; Sucholeiki, I.; Zhou, S.; Hangauer, D. G. The design and synthesis of substituted biphenyl libraries. *Bioorg. Med. Chem*. **1996**, *4*, 659-666; b) Visser, H. L. Ueber die Halogensubstitutionsprodukte des Salicins und seiner Derivate. *Arch. Pharm*. **1897**, *235*, 544-560.

(82) a) Hinterding, K.; Knebel, A.; Herrlich, P.; Waldmann, H. Synthesis and biological evaluation of aeroplysinin analogues: a new class of receptor tyrosine kinase inhibitors. *Biorg. Med. Chem*. **1998**, *6*, 1153-1162; b) Córdoba, R.; Csakÿ, A. G.; Plumet, J. Tetrabutylammonium cyanide catalyzes the addition of TMSCN to aldehydes and ketones. *ARKIVOC* **2004**, *IV*, 94-99; c) Akakura, H.; Sasakura, K.; Ueno, T.; Urano, Y.; Terai, T.; Hanaoka, K.; Tsuboi, T.; Nagano, T. Development of Luciferin Analogues Bearing an Amino Group and Their Application as BRET Donors. *Chem. Asian J*. **2010**, *5*, 2053-2061; d) Bhusal, R. P; Cho, P. Y.; Kim, S.-A.; Park, H.; Kim, H. S. Synthesis of Green Emitting Coumarin Bioconjugate for the Selective Determination of Flu Antigen. *Bull. Korean Chem. Soc*. **2011**, *32*, 1461-1462.

(83) Casiraghi, G.; Casnati, G.; Pochini, A. Ç.; Ungaro, R. Template catalysis via non-transition metal complexes. New highly selective syntheses on phenol systems. *Pure & Appl. Chem.* **1983**, *55*, 1677-1688.